THE GEOLOGY OF POST-CHUNIESPOORT DEPOSITS IN THE VERWOERDBURG AREA SOUTH OF PRETORIA WITH SPECIFIC REFERENCE TO ENGINEERING PROPERTIES OF THE RED SOILS

by

CHARLES BRIAN WILKINS

Submitted in fulfilment of the requirements for the degree

MAGISTER SCIENTIAE

in the Faculty of Science
University of Pretoria

PRETORIA

October 1985

THIS THESIS REPRESENTS THE ORIGINAL WORK
OF THE AUTHOR EXCEPT WHERE SPECIFIC
ACKNOWLEDGEMENT IS MADE TO
THE WORK OF OTHERS

OCTOBER 1985

ABSTRACT

Dolomitic rocks of the Chuniespoort Group south of Pretoria contain karstic depressions filled with younger sediments. Constructions underlain by these sediments were recently damaged which necessitated a sedimentological and engineering geological investigation of this material and a study of the bedrock geology. An area in Verwoerdburg was selected for this study.

The bedrock comprises chert-poor dolomite, and its weathering product wad, of the Lyttleton Formation, overlain by chert-rich dolomite, chert breccia and chert residuum of the Eccles Formation. The succession dips at 20° towards the east. A syenite dyke is intruded parallel to the strike of the dolomites. Groundwater solution exploited lithological and structural weaknesses in the dolomites, producing a karst topography of sinkholes, bogazis and dolines.

Ten outliers of consolidated sediments within the study area contain basal fluvioglacial diamictites, probably belonging to the Dwyka Formation. Overlying lacustrine mudstones, shales and fluvial sandstones, most likely belonging to the Ecca Group, reflect sedimentation in gradually shallowing karst depressions.

A second depositional episode, probably in Late Tertiary to Middle Quaternary times, introduced quartz silt to the study area under loessic conditions. Later sedimentary reworking mixed this silt with local weathering products and filled 16 karst features to a depth greater than 9m. A younger, thin and erratically distributed sandy silt layer was then deposited in the study area.

Post-depositional weathering processes have modified the reworked loessic deposits, producing a red clayey silt with a collapsible grain structure. Under conditions of natural moisture content and loading, the clayey silt has an open grain structure but a relatively high strength and low erodibility because of the development of clay bridges between soil grains. However, a

subsequent rapid increase in moisture content while the soil is under load, causes the clay bridges to break and collapse settlement to occur.

An increase in subsurface water content usually results from leakage of water-bearing pipes or poor surface drainage. By monitoring all water-borne facilities and adhering to certain constructional procedures, the threat of soil collapse can be lessened. The red soils will then offer more favourable founding conditions than the surrounding dolomitic material.

SAMEVATTING

Dolomiete van die Chuniespoortgroep, wat suid van Pretoria geleë is, toon karststrukture wat met jonger sedimente gevul is. Onlangse skade aan strukture wat op hierdie sedimente opgerig is, het 'n sedimentologiese en ingenieursgeologiese ondersoek van die vulmateriaal, asook 'n geologiese studie van die vloergesteentes, genoodsaak.

Die vloergesteentes bestaan uit chertarme dolomiet, en sy verweringsproduk mangaanaarde, van die Lytteltonformasie, wat bedek word deur chertryke dolomiet, chert breksies en chertresidu van die Ecclesformasie. Die opeenvolging het 'n ooswaartse helling van 20°. 'n Siënietgang het parallel met die strekking van die dolomiet ingedring. 'n Karsttopografie van sinkgate, 'bogazis' en dolines het ontstaan as gevolg van voorkeur erosie deur grondwater langs litologies en struktureel swakker plekke in die dolomiet.

Binne die studiegebied is 10 loslappe van gekonsolideerde sedimente, met basale fluvioglasiale diamiktiete wat heel moontlik aan die Dwykaformasie behoort. Die daaropvolgende lakustrine modderstene, skalies en fluviale sandstene, wat moontlik aan die Eccagroep behoort, verteenwoordig afsetting binne vlakker-wordende karstdepressies.

'n Tweede fase van afsetting, moontlik gedurende die Laat Tersiêre tot Middel Kwaternêre tydperk, het 'n loesagtige kwarts-slik tot die studiegebied ingevoer. Sedimentêre herwerking het die slik met lokale verweringsprodukte vermeng en 16 karststrukture is tot dieper as 9m opgevul. Daarna is 'n jonger, dun en oneweredig-verspreide sanderige sliklaag in die studiegebied afgeset.

Na afsetting het verweringsprosesse die herwerkte loesagtige afsettings verander en 'n rooi klei-agtige slik met 'n potensieel swigbare korrelstruktuur geproduseer. Onder normale toestande van voginhoud en belading, besit die klei-agtige slik 'n oop korrelstruktuur en is redelik sterk en moelik erodeerbaar as

gevolg van kleibrûe tussen die korrels. 'n Vinnige verhoging van die voginhoud, tesame met belading, sal veroorsaak dat die kleibrûe breek en ineenstorting van die korrelstruktuur sal plaasvind met 'n daaropvolgende versakking.

Die verhoging van die voginhoud vind gewoonlik plaas as gevolg van lekkasies van waterpype of swak oppervlakdreineering. Die gevaar van grondswigting kan verminder word deur alle waterleidingfasiliteite te monitor en om aan sekere strukturele prosedures te voldoen. Onder sulke omstandighede sal die rooigronde selfs 'n beter fondasie bied as die dolomitiese materiaal.

CONTENTS

LIST OF APPENDICES

LIST OF FIGURES

PAGE

I. INTRODUCTION

1. STUDY AIMS

Dolomite of the Chuniespoort Group is soluble to acidic groundwater, resulting in karst features such as sinkholes and dolines developing in these rocks to form a karst topography. This surface topography is often covered by an overburden comprising a weathering residuum of chert rubble or wad, or transported sediments and red soils. Engineering geological investigations, which are normally carried out prior to development in areas underlain by dolomite, concentrate on the dolomitic bedrock and residuum as these materials are considered the greatest threat to surface stability. The younger sediments have traditionally been assumed to offer more stable and safer ground conditions.

Recently, however, buildings in Verwoerdburg underlain by more than 70m of these post-Chuniespoort deposits suffered damage due to cracking of exterior walls and concrete floors. The Engineering Geology Division of the Geological Survey therefore required a thorough investigation of these sediments. This study was undertaken to determine the general geology of a chosen portion of the Verwoerdburg area and to examine the post-Chuniespoort cover in greater detail. This includes the distribution, lithology and origin of the karst-fill materials. Finally, the engineering properties of the red soils will be examined and an assessment of the risk of developing on the soils will be attempted. Precautionary measures necessary for building on these soils will be recommended.

2. LOCATION OF THE STUDY AREA

The study area is situated in the township of Verwoerdburg, 8km south of Pretoria and is approximately 9km^2 in size (Figure 1). Most of the area is undeveloped and covered by grass and trees and few good rock outcrops occur. Two disused clay quarries in the south and numerous borrow-pits in the north and east contain the best geological exposures.

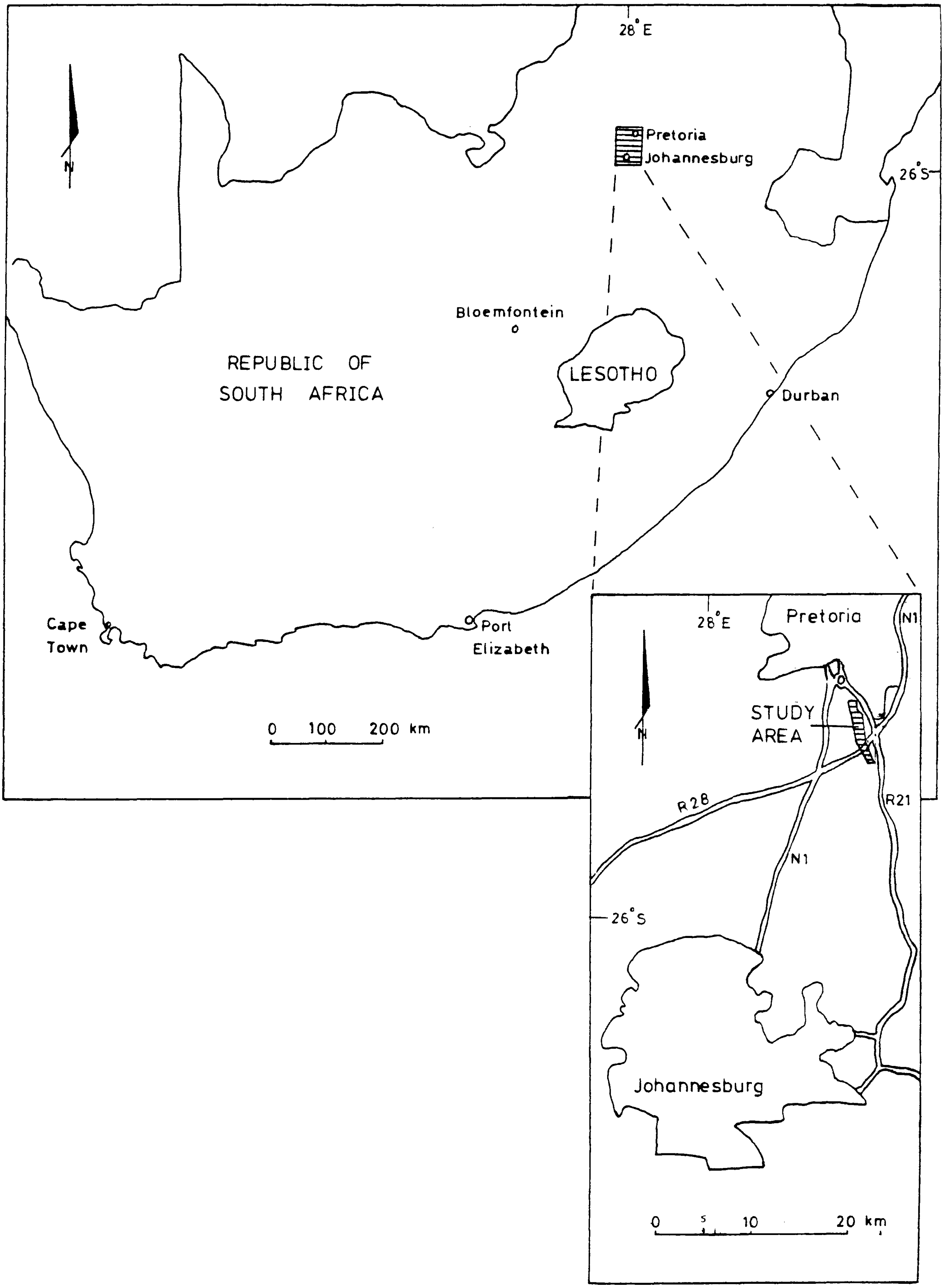

Figure 1. Locality map of the study area.

The area investigated is gently undulating and slopes from 1500m above mean sea level in the centre to 1475m in the north and south. Surface runoff is towards the Apies River in the north and the Sesmylspruit to the south and west.

3. PREVIOUS WORK

Since the study area was first developed in the 1940's, 77 reports and letter reports written by the Engineering Geology Division of the Geological Survey, various consulting geotechnical engineers and engineering geologists have been produced. Access to this information is, however, restricted and these reports are referred to only by the author's name, publication date and the report number. These sources deal with the suitability of specific zones for development and the causes of surface subsidence and damage to buildings. They concentrate on the dolomitic bedrock and residuum,as ground instability was generally found to be related to karstic processes. A total of 489 pneumatic percussion boreholes, 25 diamond-drill boreholes, 180 small diameter and 12 large diameter augerholes were drilled and 48 testpits dug within the study area during these investigations.

Unstable surface conditions associated with post-Chuniespoort material have also been identified. Wiid (1981) and Jones (1984) describe problems in areas underlain by Karoo outliers. Knight (1958, 1961, 1963), Knight and Dehlen (1963), Mackechnie (1968), Jennings and Knight (1975), Roux (1981), Bénet (1981) and Wagener (1983) discuss aeolian soils in the Transvaal which exhibit a collapsible grain structure.

A residual gravity survey of most of the study area was carried out by the Geological Survey in 1971. In addition, a thermal infra-red line scanning survey of the dolomitic region south of Pretoria was carried out (Minnett and Withers, 1980).

The Chuniespoort Group has been studied by a number of authors. The general lithology is described by Jansen (1977) and Brink (1979, 1981). The formation of sinkholes and a karst topography is discussed by Brink and Partridge (1965), Foose (1968), Marker (1971, 1980), Martini and Kavalieris (1976) and Partridge (1981).

Kleywegt and Enslin (1973), Marker (1974 a), Jansen (1977), Brink (1979), Wiid (1981) and Jones (1984) discuss Karoo outliers in the Chuniespoort Group dolomites. Karoo Sequence clay deposits of the Transvaal are described by Bennetts and Pieterse (1963), Bennetts (1965), Coetzee (1968), Skawran (1971), Hammerbeck (1972), Bredell (1974, 1978), Schmidt (1976) and Jansen (1977). Cave deposits and hominid remains in the dolomites have been studied by Brain (1958), Marker (1974 b), Vrba (1975), Beaumont et. al. (1978) and Stiles and Partridge (1979).

4. GENERAL GEOLOGY

The study area is underlain by dolomitic rocks of the Chuniespoort Group, Transvaal Sequence (Figure 2). These sediments are between 2100 and 2300 million years old and are subdivided into four formations with distinguishing chert contents (South African Committee for Stratigraphy, 1980, p. 192). Chert-poor dolomites of the Lyttelton Formation occur in the west of the study area and are overlain to the east by chert-rich dolomites and chert breccia of the Eccles Formation.

The dolomites dip at approximately 20° to the east and conformably overlie the Black Reef Formation southwest of the area investigated (Figure 3). The Black Reef sediments rest unconformably on the Halfway House Granite further to the southwest. East of the study area, the Pretoria Group unconformably overlies the Chuniespoort Group. A syenite dyke of post-Transvaal age is located in the east of the study area. This dyke is vertical and trends roughly north-south, parallel to the strike of the dolomites.

The dolomites in the study area are unconformably overlain by thick deposits of the Karoo Sequence. These outliers are between 190 and 280 million years old (South African Committee for Stratigraphy, 1980, p. 548) and comprise diamictite, various types of mudstone,

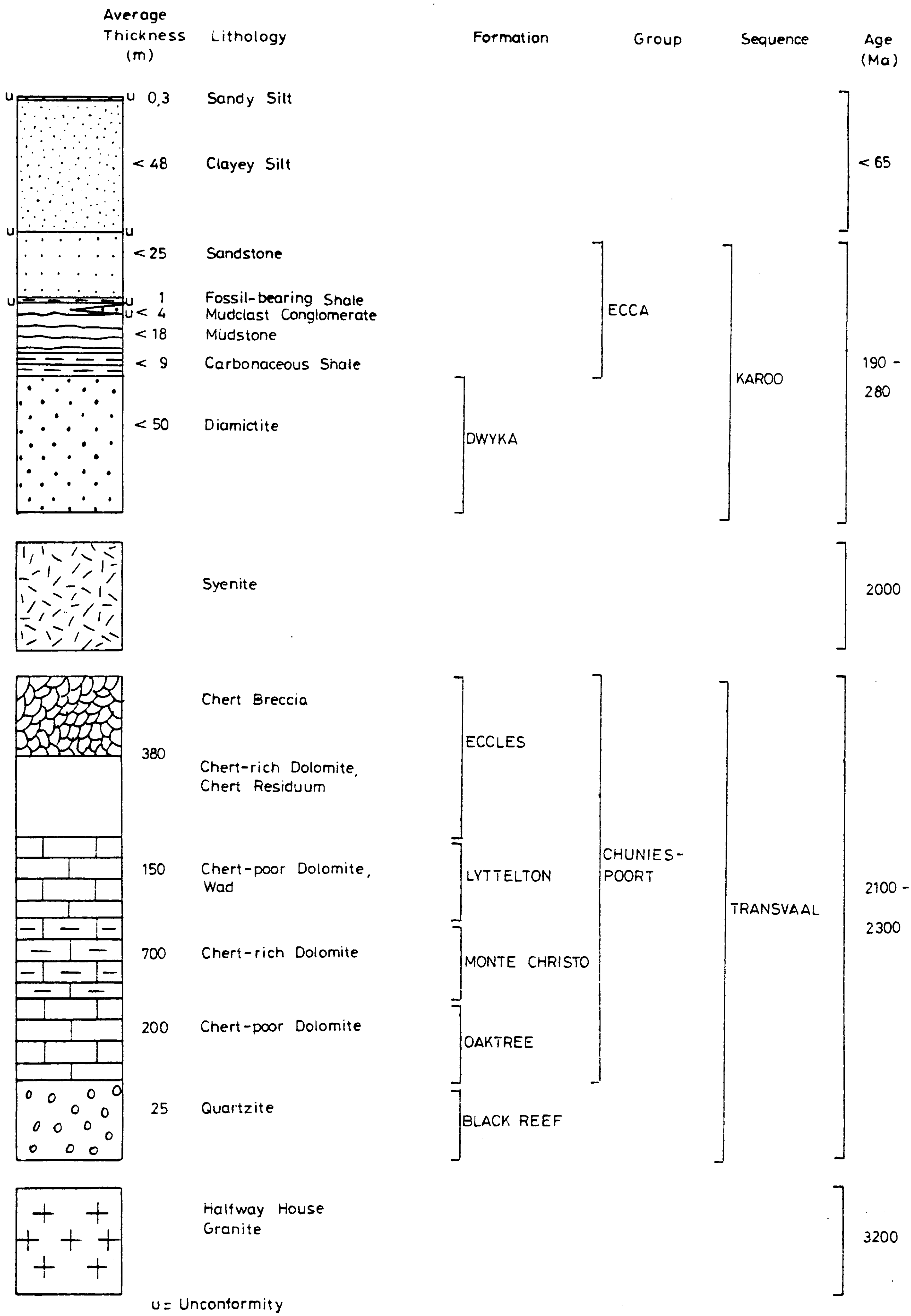

Figure 2. Stratigraphic succession of the study area (Modified after South African Committee for Stratigraphy, 1980).

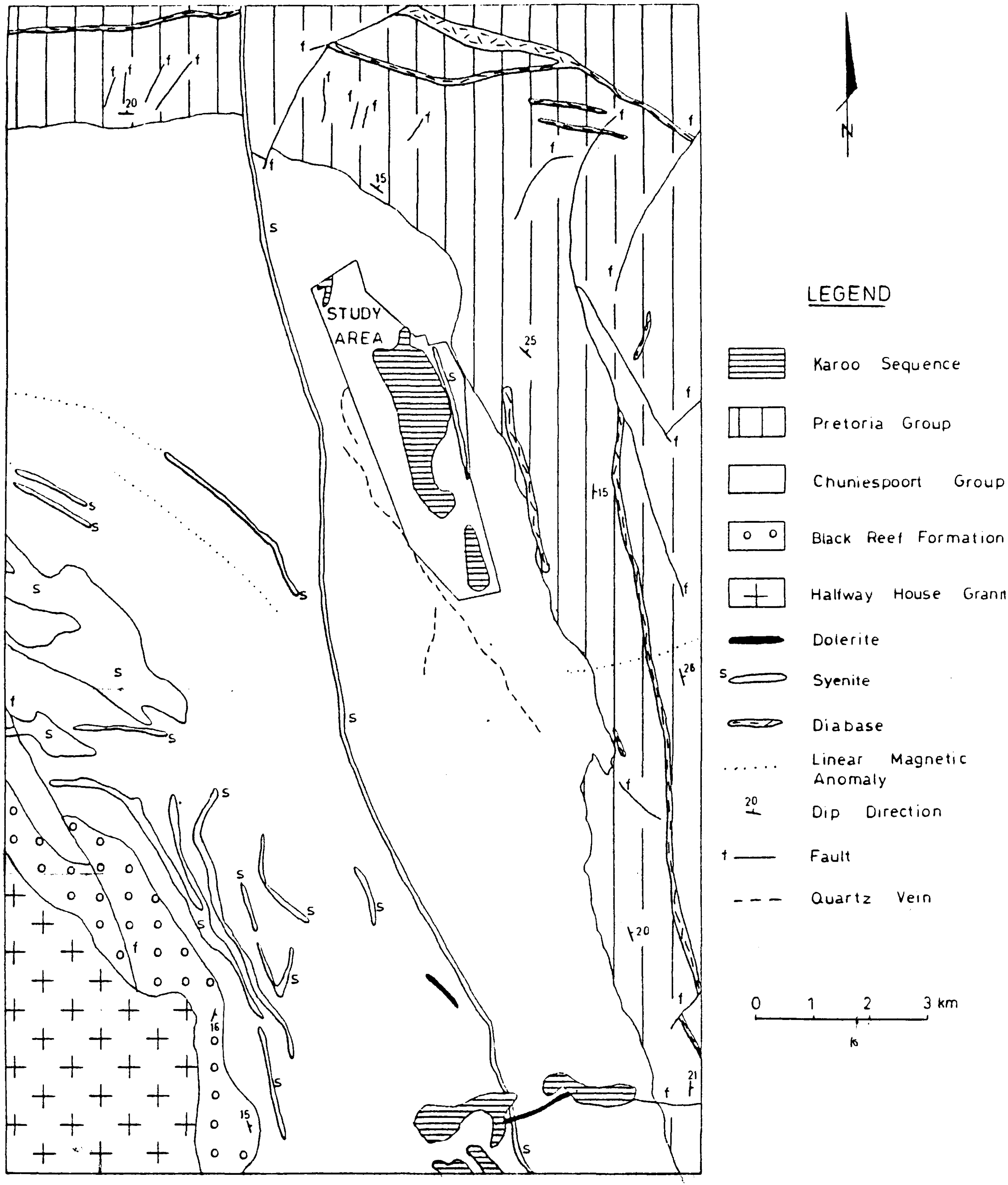

Figure 3. General geology of the study area (Modified after Sheet 2528CC, Geological Survey, 1973).

conglomerate and sandstone. These sediments accumulated in karst features in the dolomites and were therefore protected from later erosion.

A cover of red soils, younger than 65 million years (South African Committee for Stratigraphy, 1980, p. 628 - 629), occurs throughout most of the study area. This soil varies greatly in thickness and sedimentological properties and is mainly preserved in karst depressions.

5. METHODS OF INVESTIGATION

A geological map of the study area was drawn using existing borehole data, the 1:50 000 geology sheet (Sheet 2528 CC, Geological Survey, 1973) and by field mapping. This geological map, the residual gravity map (Sheet Ghp 3426, Geological Survey, 1971) and the thermal infra-red line scanning images (Minnett and Withers , 1980) were then studied to determine the dolomitic bedrock topography and the geometry of the overlying sediments. Zones where information was lacking were identified and a drilling program was initiated. One hundred and forty 30m deep pneumatic percussion boreholes and 78 small diameter augerholes were sunk. Some 60m and 90m deep percussion boreholes were also drilled to determine the watertable depth, cause of certain gravity anomalies, geometry of the syenite intrusion and the stratigraphy of the outliers.

The geological investigation revealed 16 depressions filled with more than 9m of red soil and 10 Karoo outliers. Systematic sampling of this area was then carried out to establish the sedimentological properties of the material. Each soil-filled structure was numbered and, where possible, disturbed samples were taken at 4,5, 10, 20 and 30m by augerhole drilling (Figure 4). These depths were selected so that test results could be compared horizontally and vertically within a depression and with those from other soil pockets. A total of 75 disturbed soil specimens of 15kg each were collected. Six samples of Karoo Sequence sandstone and 2 of the soil covering the Halfway House Granite and

Figure 4. Distribution of the sample sites within the study area.

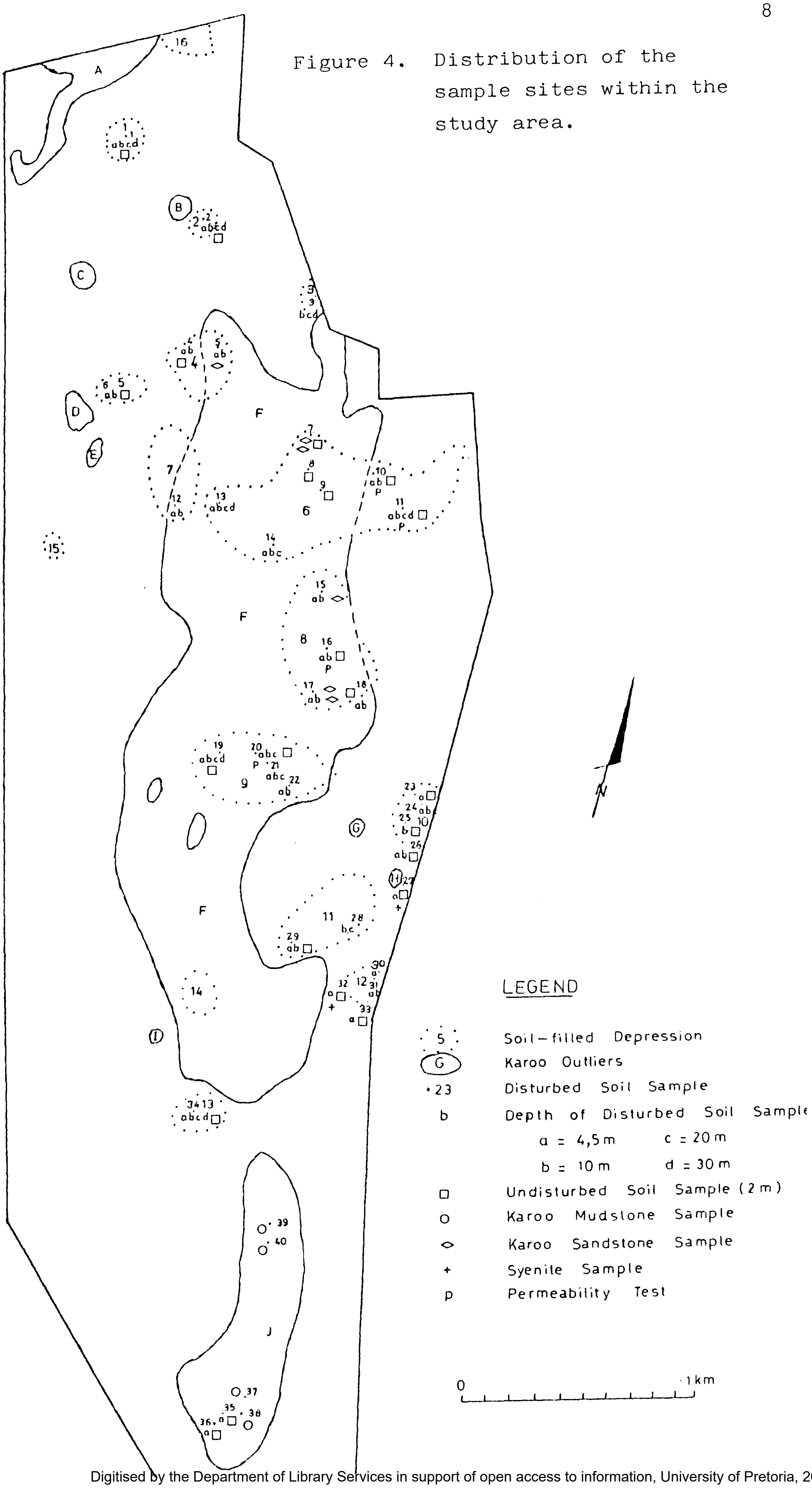

the Black Reef Formation 10km southwest of the study area were recovered for sedimentological analysis. Four Karoo Sequence mudstone and 2 syenite samples were also collected.

The sedimentological properties of the red soil were determined by examining the grain size distribution and composition of the samples and the morphology of individual grains. A portion of each disturbed soil specimen was initially sieved using 8 sieve sizes between 2,75 ϕ (0,15mm) and -4,0 ϕ (14,0mm). The silt and clay fractions were graded using a hydrometer. The grain size distribution for each sample and the average for every soil-filled depression was then calculated (Appendix 1). The graphic method described by Folk and Ward (1957) was used to analyse the average grain size distribution of the soils and the Karoo Sequence sandstone.

Compositional data was obtained by various methods. For the coarse sand and gravel fractions, grains of different composition were separated by hand with the aid of a binocular microscope. The various populations were then weighed and the modal composition calculated (Appendix 2). A visual estimation of the fine sand and silt composition was made using a binocular microscope and a scanning electron microscope respectively. The composition of the clay, heavy minerals and the bulk composition of the red soils was determined by X-ray diffraction. The method described by Carver (1971) was followed for the heavy mineral separation. The composition of the syenite and the Karoo Sequence mudstone was established by X-ray diffraction and chemical analysis.

The morphology of individual soil grains was compared with the standard visual estimation diagrams of Sneed and Folk (1958) and Pettijohn et. al. (1972) (Appedix 3). Colour and freshness of the grains was also examined. The Karoo sandstone samples and the granitic soil found southwest of the study area were compared to the red soils (Appendix 3). The binocular microscope was used for the sand and gravel fractions and the scanning electron microscope for the silt grains. After preparation by the method suggested by Krinsley and Doornkamp (1973, p. 7), the quartz grain surface textures in the silt and fine sand fraction of the red soils were examined under the scanning electron microscope.

To establish the engineering properties of the red soils , 23 undisturbed samples from 11 soil-filled depressions (Figure 4) were collected at a depth of 2m, using a mechanical excavator. Each specimen weighed approximately 20kg and was wrapped in mutton cloth and sealed in wax to retain the natural moisture content. The collapse potential of the soils was determined from the undisturbed samples using a modified version of the Collapse Potential Test outlined by Jennings and Knight (1975). An applied load of 80 kN/m^2 was used instead of 200 kN/m^2 as fairly light structures such as residential houses are the main type of constructions expected within the study area. Shear strength was calculated from shear box test results. A portion of the disturbed samples was used to establish the Atterberg Limits, following the standard laboratory procedure of Smith (1978, p. 8-9). Constant head field permeability tests were carried out in three of the soil-filled depressions (Figure 4) using the method of Cedergren (1967).

II. BEDROCK GEOLOGY

1. BEDROCK LITHOLOGY

The bedrock underlying the study area consists of dolomites of the Chuniespoort Group, Transvaal Sequence and a syenite dyke (Figure 5). The Lyttelton Formation occurs in a narrow zone striking north-south in the west of the study area and comprises chert-poor dolomite overlain by up to 35m of wad. No outcrops of chert-poor dolomite are therefore present and the occurrence of this rock type was established by drilling. The wad is a moist, dark brownish-black clay.

Chert-rich dolomite, chert breccia and chert residuum of the Eccles Formation is found in the central and eastern portion of the study area and stratigraphically overlies the Lyttelton Formation (Figure 5). A pinnacle of chert-rich dolomite crops out in the large sinkhole situated in the east of the study area (Figure This pinnacle displays prominent inter-layering of chert and dolomite and also exhibits stromatolitic structures (Figure 7).

Chert breccia occurs in the north, east and southeast of the study area (Figure 5) where it forms topographic ridges. In outcrop, the breccia is massive and consists of angular chert fragments, up to 100mm in length, within a quartz cement. The chert fragments occasionally display layering and are blue or green when fresh but become white, with a sugary texture,when weathered.

Large portions of the study area are underlain by chert-rich residuum which reaches a maximum thickness in excess of 50m. This unconsolidated sediment appears as a dark, reddish-brown clay containing wad,abundant chert fragments and large floaters of chert. The material becomes brownish-black with an increase in the proportion of wad.

A vertical syenite dyke is situated in the east of the study area

Figure 5. Geological map of the study area.

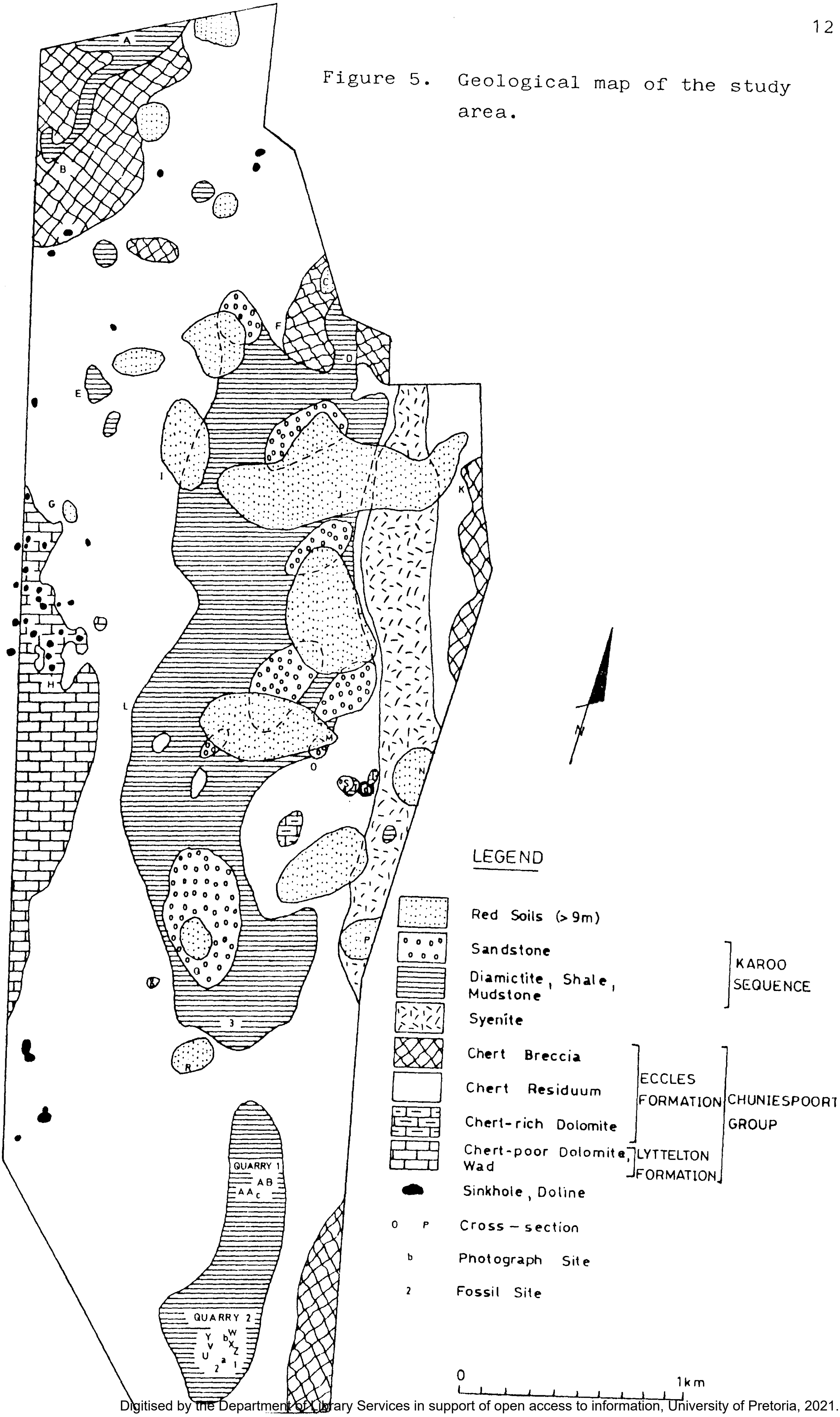

50 m

Figure 6. Large sinkhole in the east of the study area, view looking eastwards. Note the dolomite pinnacle to the left of the vehicle (Position d, Figure 5).

5 m

Figure 7. Close-up view of the chert-rich dolomite pinnacle in Figure 6, illustrating stromatolitic structures.

(Figure 5) and trends roughly north-south, parallel to the strike of the Chuniespoort Group. The intrusion crops out in the south but is deeper than 30m below the surface in the north, where it is covered by red soils. X-ray diffraction analysis indicates that the syenite is weathered, being composed of 50% feldspar, 35% pyroxene and 15% kaolinite, chlorite and sericite.

2. KARST TOPOGRAPHY

Borehole logs and the residual gravity survey indicate that a well developed karst topography exists within the study area. The Lyttelton Formation is characterised by steep gravity gradients as well as high and low anomalies (Figure 8). Cross-sections of the bedrock reveal a highly dissected and irregular topography of dolomite pinnacles separated by deep, wad-filled solution fissures or grikes (GH,Figure 9). In residual gravity profile, the pinnacles form gravity high anomalies and the grikes and zones of thick wad form relative lows. This area of dolomite and wad is characterised by surface instability. Cavities are present between the dolomite pinnacles and 21 of the 36 surface subsidences recorded within the study area since the 1940's, have occurred in this western zone of Lyttelton Formation dolomites (Figure 5). The subsidences are relatively small, with a diameter of less than 25m, are shallower than 20m and consist of sinkholes and dolines.

This area of pronounced karst development extends to the Lyttelton Quarry, 2km southwest of the study area. Marker (1974 a) describes the occurrence of exaggerated subsoil solution forms, or rund karren, in the dolomites exposed during quarrying. Major solution channels, or bogazis, up to 30m deep are also developed.

The karst topography of the Eccles Formation is more undulating and not as dissected as that formed on the Lyttelton Formation (Figure 9). The Eccles karst topography is characterised by two large bedrock valleys and relatively large palaeosinkholes and dolines filled with younger sediments (Figures 10 and 11). The major valley is 3,3km long and 0,8km wide, with gently sloping sides in the north which

Figure 8. Residual gravity map of the study area (Modified after Sheet Ghp 3426, Geological Survey, 1971).

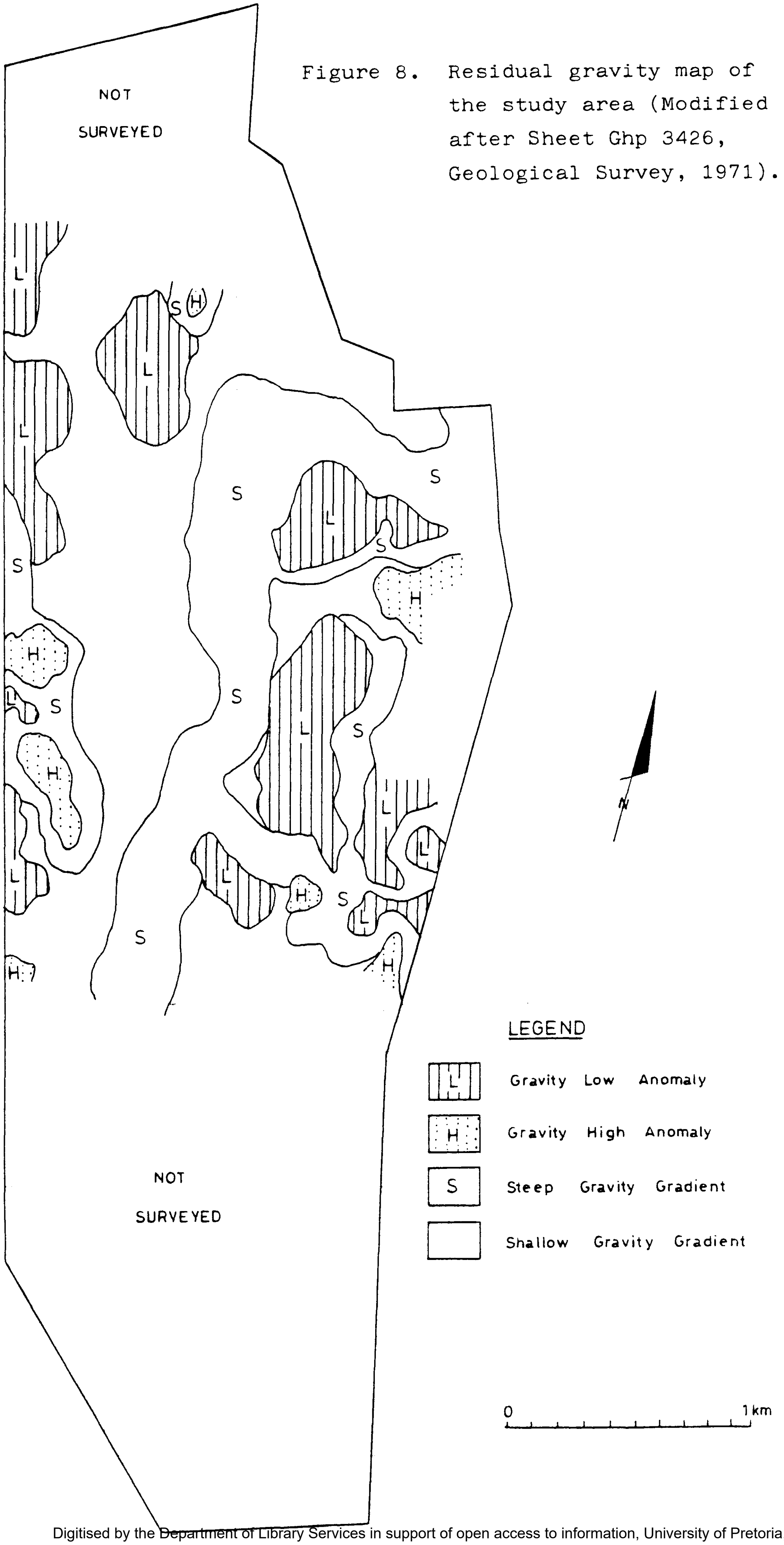

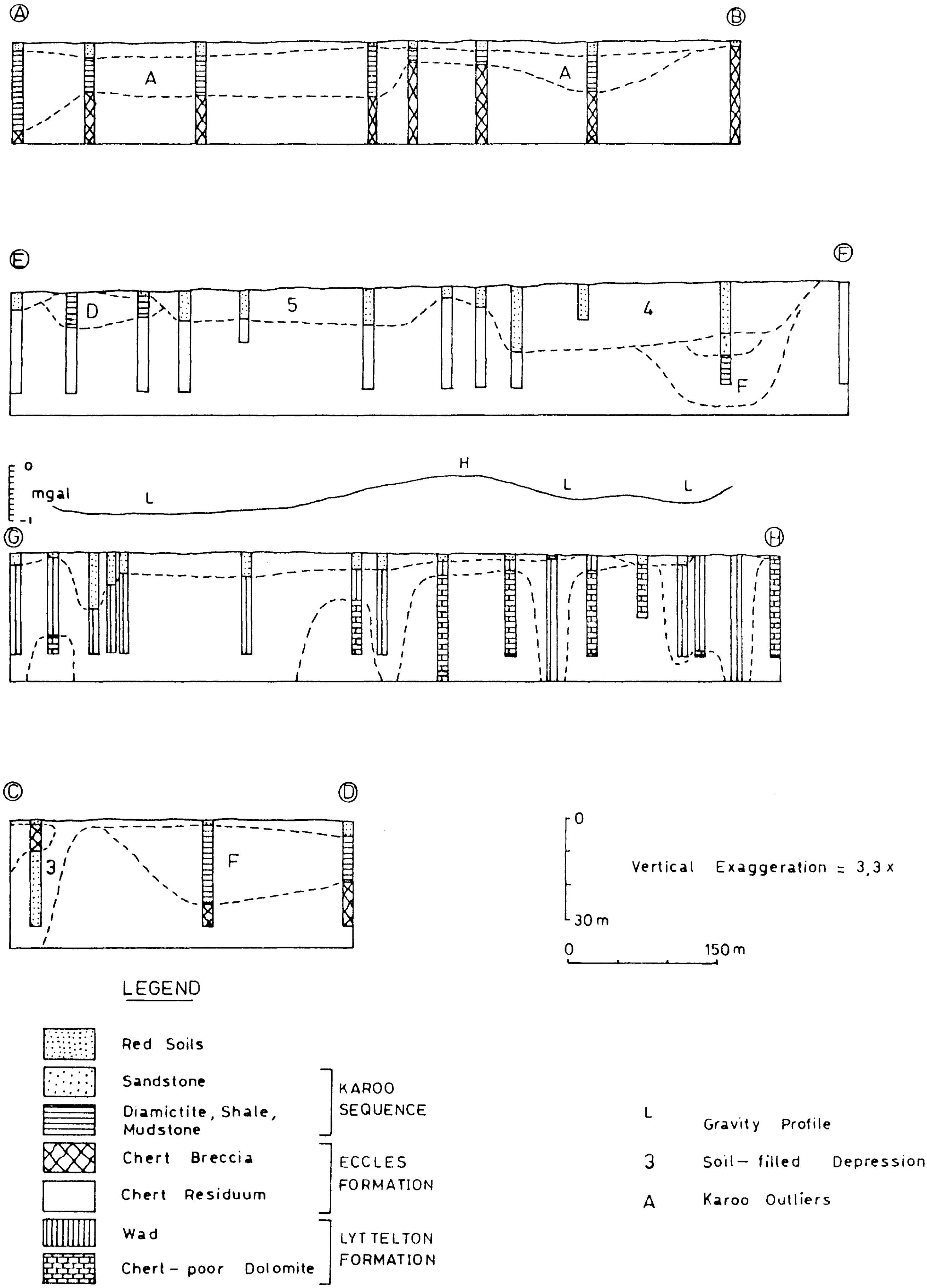

Figure 9. Cross-sections and gravity profiles of the study area showing the geology and pre-Karoo bedrock topography (See Figure 5 for profile locations).

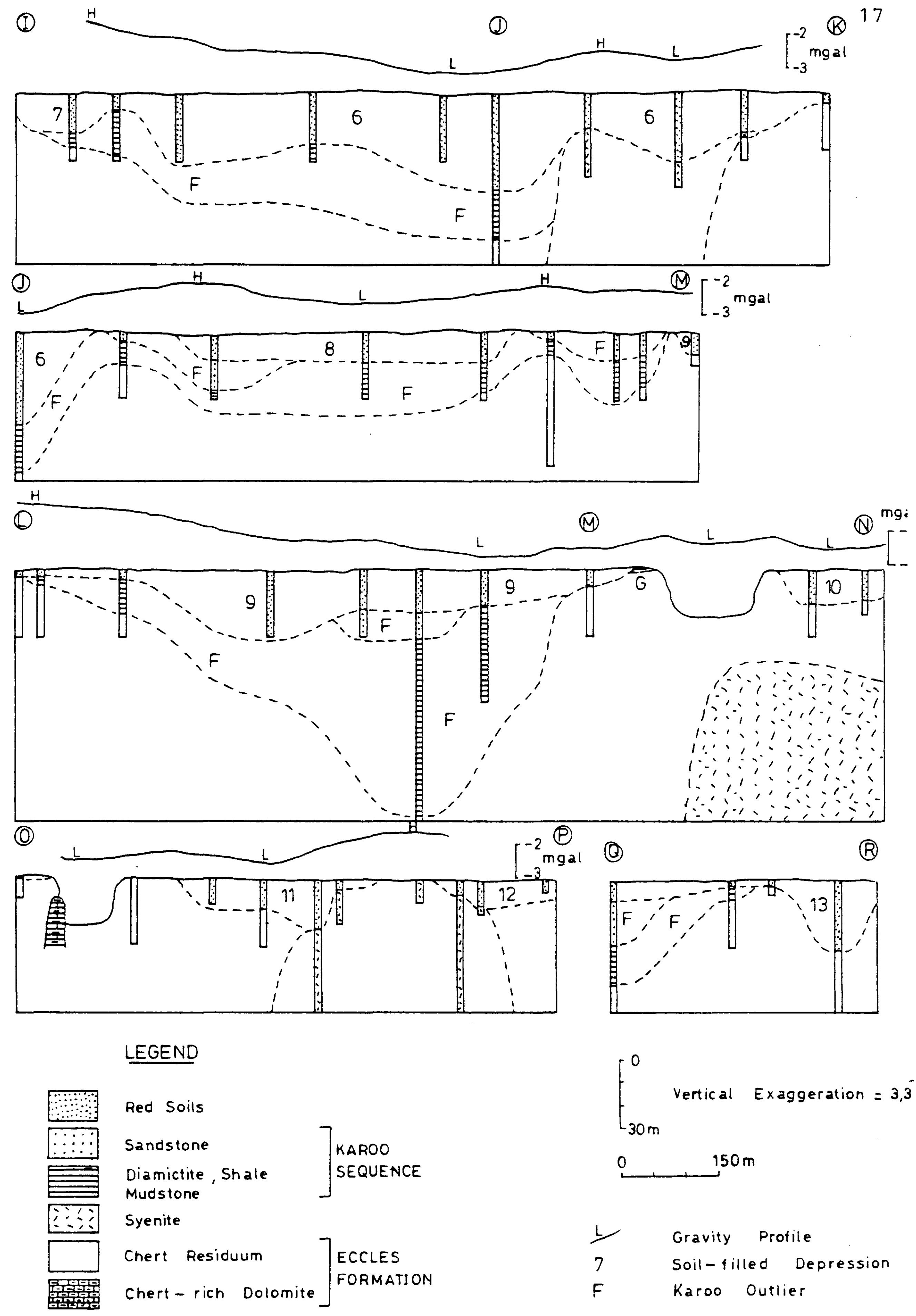

Figure 10. Cross-sections and gravity profiles of the study area showing the geology and pre-Karoo bedrock topography (See Figure 5 for profile locations).

Figure 11. Isopach map of the post-Chuniespoort deposits within the study area showing the bedrock topography.

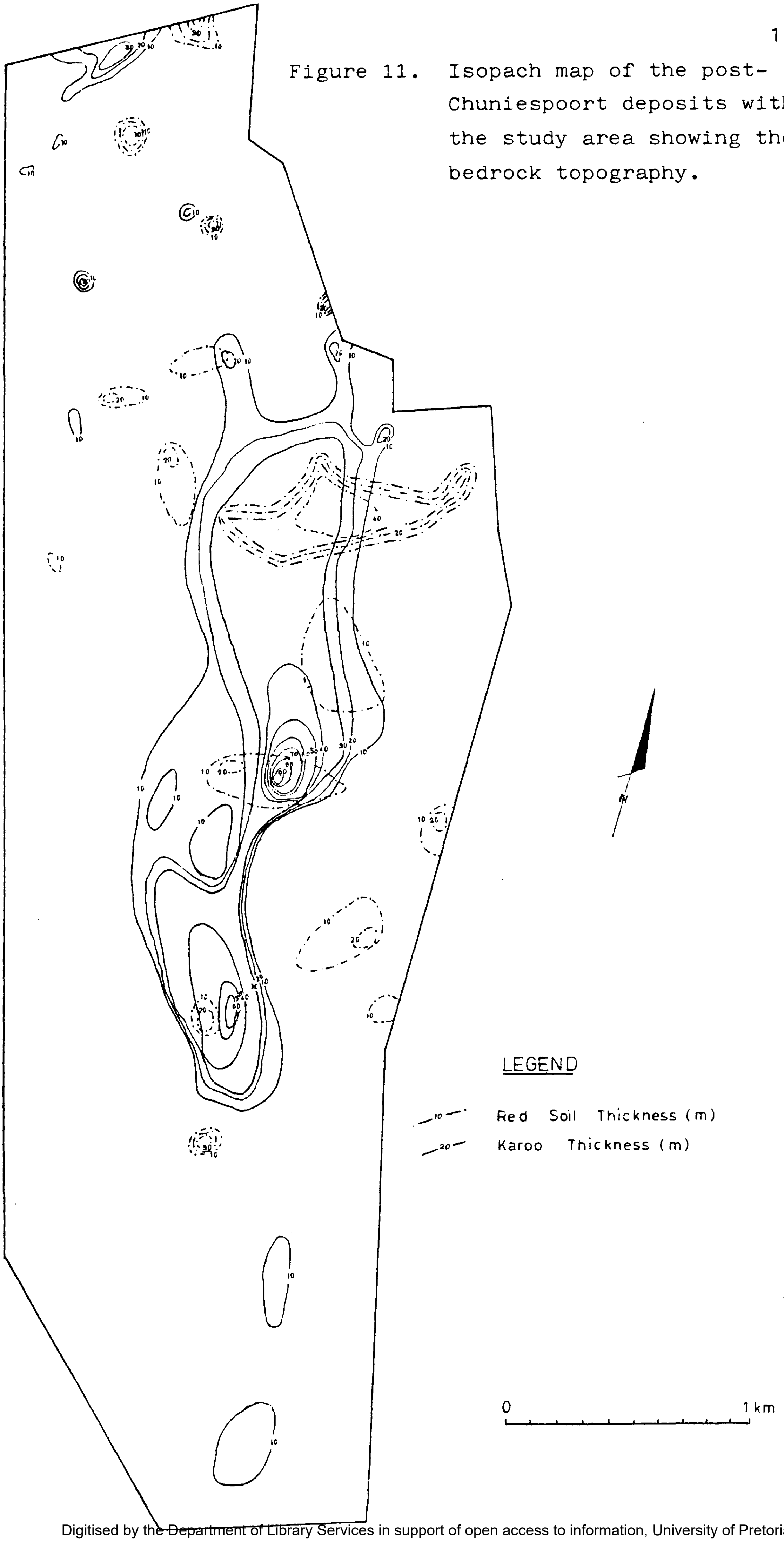

become steeper in the centre and south (Figure 11). The depth of this valley increases from 35m in the north to 90m in the centre and 60m in the south. In the extreme south, two shallow depressions of 10m depth terminate this major valley.

The valley forms a prominent gravity low anomaly in the eastern half of the study area (Figure 8). To the west, the feature is bounded by a steep gravity gradient which reflects a rapidly shallowing bedrock (Figures 8 and 10). Gravity high anomalies occur to the east and are related to syenite and chert breccia at shallow depths.

In the northwest corner of the study area, another elongated valley trends northeast - southwest and is up to 35m deep (Figure 11). Numerous large surface features up to 40m in diameter, which are roughly circular in plan, are also present. These occur either as shallow, basin-shaped dolines less than 20m in depth or narrow, deep sinkholes up to 48m in depth (Figure 11).

3. KARST DEVELOPMENT

Formation of a karst topography is influenced by geology, structure, time, hydrology, climate, biotic CO_2, topography and non-karstic processes in that region (Brink and Partridge, 1965; Jakucs, 1977; Marker, 1980). The dolomitic rocks of the Chuniespoort Group are soluble to acidic waters. Rainwater absorbs carbon dioxide in the atmosphere and the soil to produce a weak carbonic acid (Brink, 1981). This acid then leaches out calcium and magnesium bicarbonates from the dolomites.

Leaching of a manganese-rich, chert-poor dolomite produces an insoluble hydrated manganese dioxide residue known as wad (Brink, 1981). Leaching of a chert-rich dolomite results in chert-rich residue. Thick deposits of wad and chert residuum are present within the study area indicating deep weathering of the dolomites. The distribution of these materials also indicates the bedrock lithology. The chert breccia is an in situ residual deposit formed by cementation of chert debris remaining after weathering of chert-rich dolomite. The consolidated nature of this breccia suggests silicification of the interstitial material during previous erosion cycles (Jansen, 1977).

Dolomite is normally a compact and impervious rock (Brink, 1979), but in the area south of Pretoria it is highly fractured and faulted. The dip changes from easterly to northerly and large faults, quartz veins, linear magnetic anomalies and dykes are orientated approximately parallel to the regional strike of the bedrock (Figure 3). This structural framework is related to the updoming of the Halfway House Granite southwest of the study area (Jansen, 1977). Fracturing of the bedrock improves the flow of groundwater and promotes solution of the dolomites along structural weaknesses.

The distribution, shape, size and orientation of karst forms within the study area appears to be controlled by the bedrock lithology and structure. The area of intense karstification in the west only developed on chert-poor dolomite of the Lyttelton Formation. The overlying Eccles Formation contains randomly distributed sinkholes and dolines and two large valleys. The major valley trends north - south, parallel to the strike of the dolomites and the syenite dyke. These dolomites dip to the east and the dyke would therefore have acted as a barrier to groundwater movement. Dolomite solution would have been promoted on the updip side of the intrusion, thus forming the valley. However, this karstic valley could also be due to preferential bedrock solution along a major strike fault. The karst form in the northwest of the study area is orientated northeast-southwest and may be related to dip faulting in the dolomites. Similar faulting is present north of the study area (Figure 3).

Marker (1974 a) found that bedrock solution in the Lyttelton Quarry southwest of the study area occurred along structural weaknesses trending northwest - southeast. Younger Ecca grits and red soils are preserved between the dolomite pinnacles. In the

Swartkop region, 6km northwest of the study area, 10 small karst forms between 3 and 27m deep are developed parallel to a major north - south fault (Lombard and Lourens, 1983). These depressions contain sediments of the Karoo Sequence.

The karst topography within the study area is overlain by thick residual deposits and transported sediments. It is, however, evident that karst processes are still operative. The watertable is between 99 and 114m below the surface (Enslin, 1950) and karst features would have a predominent vertical orientation due to the direction of water flow above the watertable, that is, in the vadose zone (Brink and Partridge, 1965; Foose, 1968; Brink, 1979). The deep watertable may explain the great depth, up to 90m, of the large karst valley present in the study area. Several surface depressions which formed in the sediment filling this valley (Figure 5) suggest continuing karst development adjacent to the dyke. Although surface instability shows an increase during the rainy summer months (Roux, 1983, pers. comm.), the high incidence of subsidences recorded in the west of the study area appears to be related to alteration of the natural hydrology by man, in a region underlain by chert-poor dolomite and wad.

III. POST-KARST GEOLOGY

1. KARST-FILL DEPOSITS

The dolomitic bedrock within the study area is overlain by younger sediments which filled depressions in the karst topography. The cover is, therefore, very irregular in distribution and thickness, varying from thin surface deposits to sinkhole-fills greater than 100m in depth (Figure 11).

The sediments comprise consolidated material which is unconformably overlain by younger unconsolidated soils (Figures 5,9 and 10).

A. Consolidated Material

Ten outliers of consolidated sedimentary material, ranging from 50m in diameter and less than 10m deep to 3,3km in length and greater than 90m in depth, are present within the study area (Figure 11). These outliers are underlain by chert breccia and chert residuum of the Chuniespoort Group and comprise diamictite, various types of mudstone, mudclast conglomerate and sandstone (Figure 2).

Diamictite occurs at the base of the succession and is the thickest and most widespread consolidated rock type in the study area. The unit varies in thickness from 2m at the margins of the depressions to a maximum of approximately 50m in the centre of outlier F (Figure 4). A carbonaceous shale, developed only in the centre of the northern half of outlier F, overlies the diamictite. This shale has a maximum thickness of 9m.

Mudstone, up to 18m thick, occurs in the centre of the outliers examined within the study area, where it overlies the basal diamictite. A thin mudclast conglomerate with a maximum thickness of 4m unconformably overlies this mudstone (WX,Figure 12). The conglomerate occurs as 1 channel-fill and 4 fan-like lobes dipping into outlier J (Figures 13 and 14) and as a large lobe in the southern end of outlier F (Figure 4). The channel-fill conglomerate displays a basal diamictite (WX,Figure 12).

A thin fossil-bearing shale unconformably overlies older consolidated sediments (Figure 12) and Chuniespoort Group chert breccia. This shale is only developed along the southern edge of outlier F, in outlier G and in Quarry 2 (Figure 4), and is approximately 1m thick. Nine sandstone lobes unconformably overlie the outliers and dolomitic bedrock (Figure 5). This sandstone varies in thickness from a thin cover over chert residuum to a maximum of 25m over the outliers and represents the youngest stratigraphic unit of the consolidated material.

i. Diamictite

The matrix-supported diamictite consists of clasts of varying size, shape and composition set in a white, clayey sand matrix (Figure 15). The clasts mainly comprise well-rounded to angular quartzite and sandstone cobbles and boulders with lesser chert pebbles and slabs. A 30mm long euhedral quartz crystal was also found. The material is therefore polymictic and extraformational, with the clasts originating outside the depositional site (Selley, 1977, p. 105). This diamictite has a bimodal grain size distribution and is poorly sorted. The clasts appear to be oriented subparallel to the bedding and the rock has a slightly ordered fabric (Figure 15). Clast size and abundance decrease towards the centre of individual outliers and also upwards within the unit and the material grades into white, clayey sandstone.

Around the peripheries of outliers, the diamictite displays a weak bedding and dips steeply into the depressions at between 40° and 80° (Figures 13 and 14). Towards the centre of the outliers, dips shallow and the sediment becomes massive. Downwards concave

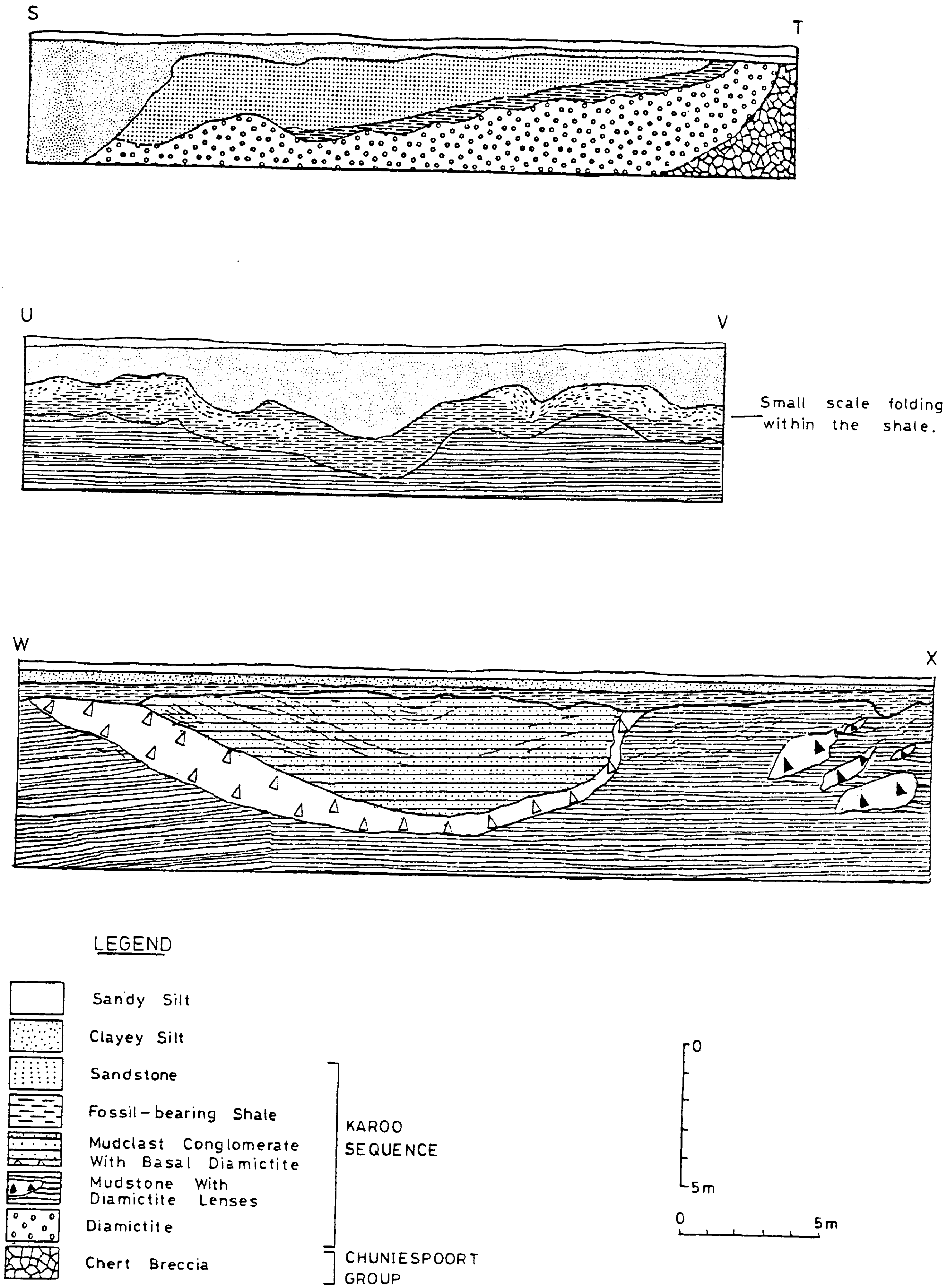

Figure 12. Cross-sections of the study area showing stratigraphic relationships of the post-Chuniespoort deposits (See Figure 5 for profile locations).

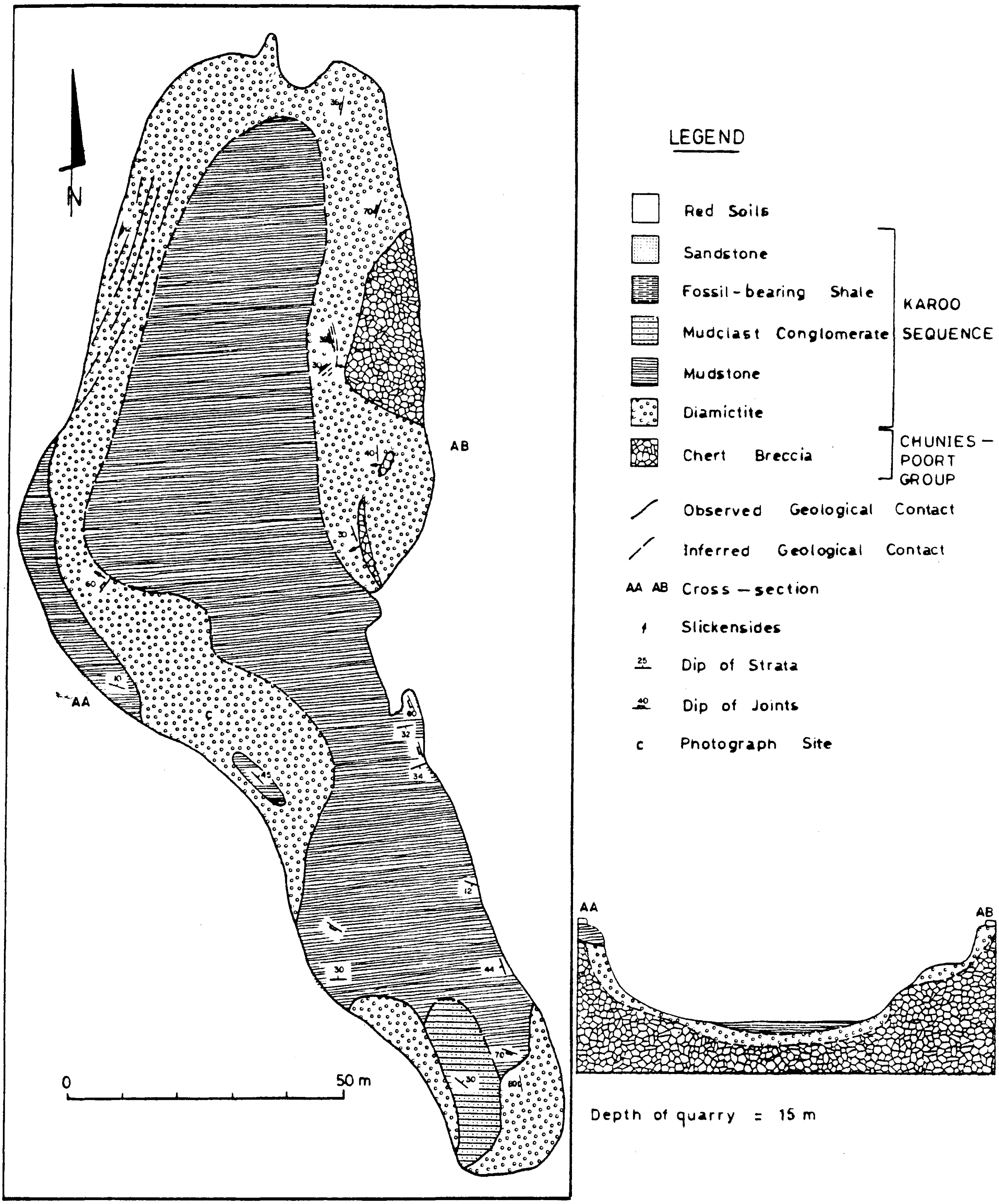

Figure 13. Geological map and cross-section of Quarry 1, Outlier J (See Figure 5 for quarry location).

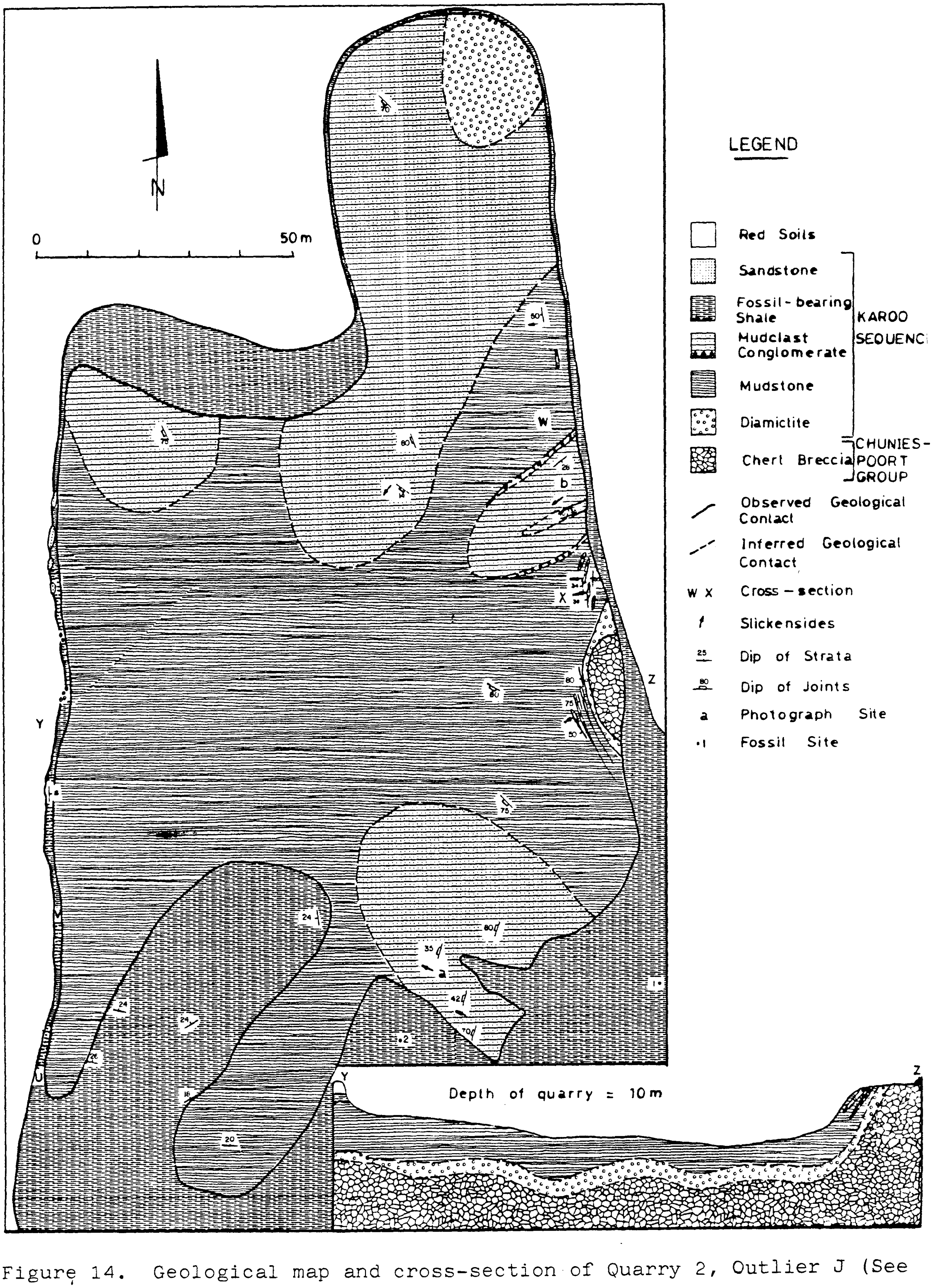

Figure 14. Geological map and cross-section of Quarry 2, Outlier J (See Figure 5 for quarry location).

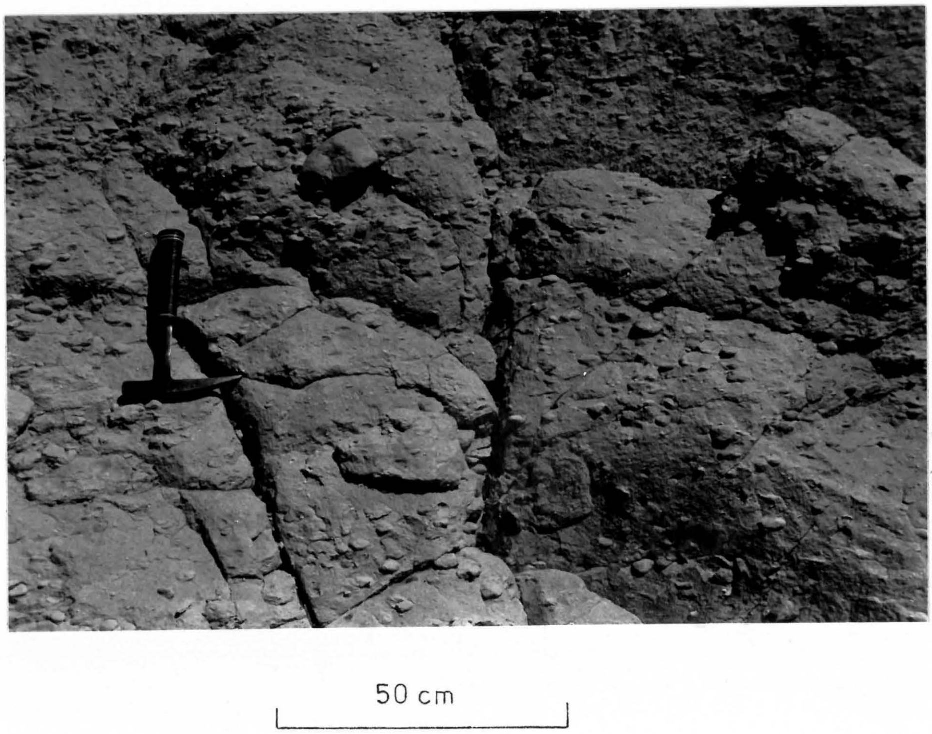

Figure 15. Diamictite displaying a large range in clast size and shape and a slightly ordered fabric (Position c, Figures 5 and 13).

joints have developed within the diamictite, subparallel with the bedding and dipping into the outliers. Slickensides are present on these joint planes and on the underlying chert breccia and trend in the same directions as the dips of the diamictite (Figures 13 and 14).

The poorly sorted nature of the material and the massive to slightly ordered fabric suggests that they are debris flow deposits (Blatt et. al., 1972, p. 161; Selley, 1977, p. 194; Collinson and Thompson, 1982, p. 118; Lowe, 1982). Such flows result from movement of unconsolidated, saturated sediment under the influence of gravity in almost any environment. The diamictite is a cohesive flow deposit in that clasts were suspended in, and supported by, the matrix (Lowe, 1982). The fine-grained matrix gives the flow a high viscosity and density, thus allowing large clasts to be transported. As the water content decreases, shear strength increases and debris flows grade into slumps and slides (Selley, 1977, p. 193). Deposition occurs when the yield stress of the matrix exceeds the maximum shear stress (Blatt et. al., 1972, p. 161). This can result from loss of water or a decrease in gradient of the surface over which the material is moving.

ii. Carbonaceous shale

This finely laminated, brownish-black shale overlies the basal diamictite unit (Figure 2). Kaey (1949) and Enslin (1950) suggest the horizon comprises remnant coal seams, but borehole samples retrieved during this investigation reveal that although carbonaceous material is present, it is not in sufficient quantities to form coal seams.

Preservation of organic matter in a sediment requires a low Eh environment to prevent oxidation of the organic compounds (Blatt et. al., 1972, p. 392). A low Eh implies the rate of influx of organic matter must exceed the quantity of oxygen available to oxidise it, and such conditions occur in a quiet water environment. Water circulation is therefore restricted and the organic matter would accumulate with silt and clay detritus, thereby forming a carbonaceous shale.

iii. Mudstone

The mudstone displays a conchoidal fracture, a flint-like appearance and is white when fresh but becomes khaki-coloured with weathering. This material is composed almost entirely of kaolinite and has a low iron content of 1,5% and a high aluminium content of 19,6%. The deposits have therefore been quarried as a source of flint and semi-flint fire-clay for the manufacture of super-duty refractory bricks (Bennetts, 1965).

The mudstone grades laterally towards the margins of the outliers and downwards within individual depressions into more silty material. This siltstone contains sand-size angular quartz and chert grains, thin lenses of diamictitic material similar to the basal diamictite unit, and rare chert breccia slabs (Figures 12 and 14). The upper portion of the mudstone is laminated and shaly.

The mudstone displays indistinct bedding and along the edges of the outliers, it dips steeply inwards at up to 80° (Figures 13 and 14). The dips shallow within the depressions to approximately 20°. The chert breccia slabs contain prominent slickensides which are orientated parallel to the dip directions of the mudstone. A steeply dipping system of joints is present and trend northwest - south-east (Figures 13 and 14).

Mudstones are derived from chemical weathering of unstable source rocks or from extreme physical attrition as, for example, found in a glacial environment (Collinson and Thompson, 1982, p. 53). The local distribution, high kaolinite content and lack of coarse-grained detritus in the mudstone of the study area suggest deposition from suspension of clay derived from a granitic or gneissic source (Selley, 1977, p. 76). The thickness, composition and largely massive nature of the mudstone indicate rather rapid deposition, with a large and constant influx of clay into a quiet, terrestrial body of water (Blatt et. al., 1972, p. 384; Selley, 1977, p.212; Collinson and Thompson, 1982,p.57). Kaolinite flakes tend to bond in an edge-to-face arrangement to form floccules (Blatt et.al. 1972,p. 394) and pure kaolinitic mudstones are therefore usually massive. The poorly sorted basal siltstone resembles a mudflow and the subordinate large clasts were transported by the high density of the fine-grained matrix (Blatt et. al., 1972, p. 161). The gradation of the mudstone into a shale at the top of the unit suggests a more episodic influx of clay and the introduction of mica and silt detritus.

iv. Mudclast conglomerate

Five fan-like lobes of this unit are less than 3m thick and comprise only conglomerate. The sixth occurrence is a 4m deep channel-fill with a 1,5m thick basal diamictite (Figures 12, 13 and 14). The conglomerate consists of kaolinite pebbles set in a kaolinitic clay matrix and is therefore oligomictic and matrix-supported. The pebbles are either individually scattered in the horizon or are concentrated in lenses up to 0,5m thick. The clasts are rounded to well-rounded with a medium to high sphericity and range from 5 to 40mm in diameter (Figure 16). The pebbles are aligned parallel to the bedding of the conglomerate and the rock thus displays an ordered, horizontal fabric (Figure 17).

The conglomerate lobes dip at approximately 30° into outlier J. Prominent joint planes are developed subparallel with the bedding and dip at between 14° and 42° into the outlier (Figures 13 and 14). The upper surface of these planes exhibit slickensides which trend in the same directions as the dips of the bedding (Figure 18). The planes are transversed by a second system of joints striking approximately north-south and dipping steeply to the west (Figure 14).

The similarity in composition of the clay pebbles and the underlying mudstone, and the erosional basal contact of the conglomerate, suggest reworking of the underlying mudstone to form a mudclast conglomerate. The large size of the pebbles indicates a local

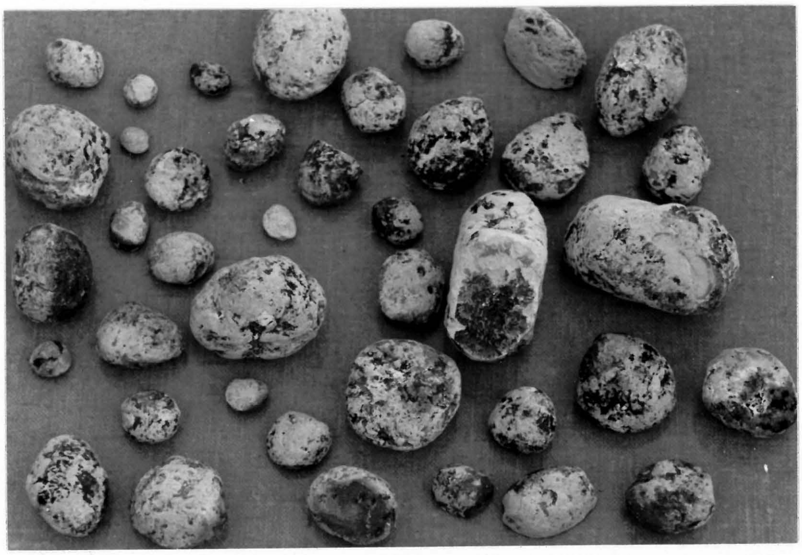

10 cm

Figure 16. A random selection of clay pebbles extracted from the mudclast conglomerate, displaying their roundness and medium to high sphericity (Collected at Position b, Figures 5 and 14).

10 cm

Figure 17. A sample of mudclast conglomerate showing the ordered, horizontal fabric (Collected at Position b, Figures 5 and 14).

Figure 18. Slickenside surface in the mudclast conglomerate (Position a, Figures 5 and 14).

source area. The conglomerate is therefore intraformational, as the pebbles originated within the depositional site (Selley, 1977, p. 105).

Bennetts (1965) describes how a mudclast conglomerate can form. Clay exposed above water dries and mud cracks develop. Slabs of clay are eroded by subsequent water movement and rounded to form clay pebbles. The pebbles are then deposited locally along with other sediment to produce a mudclast conglomerate.

v. Fossil-bearing shale

These shales are approximately 1m thick, ferruginous and black. A horizontal lamination is developed due to alternating layers of clay and silt. Mica occurs along parting planes and the shale is fissile. Flute structures, up to 8cm in length, are also present.

The sediment contains abundant, well preserved but fragmented fossil leaves (Figure 19). The leaves are identified as belonging to the genus Glossopteris from their distinctive venation structure (Kovács-Endrödy, 1983, pers. comm.). The leaves are relatively large with one leaf measuring more than 55mm in width. Although confusion exists in the exact identification and dating of the various Glossopteris species (Kovács-Endrödy, 1977, 1979, 1981), the leaves are presumed to be Permian in age. The large size of the fossils further suggests they existed in the Middle to Late Ecca period (Kovács-Endrödy, 1983, pers. comm.).

Along the eastern margin of Quarry 2, the shales are approximately horizontal. However, in the southwestern corner of the quarry, the shale dips at up to 26° into the outlier. The shale along the western edge displays prominent, small scale folding with an amplitude of 1m and a wavelength of 4m (Figure 12) and dips at 6° into the outlier (Figure 14). The shale in outlier G and F is also folded and dips at approximately 20° towards the deeper portion of the outliers.

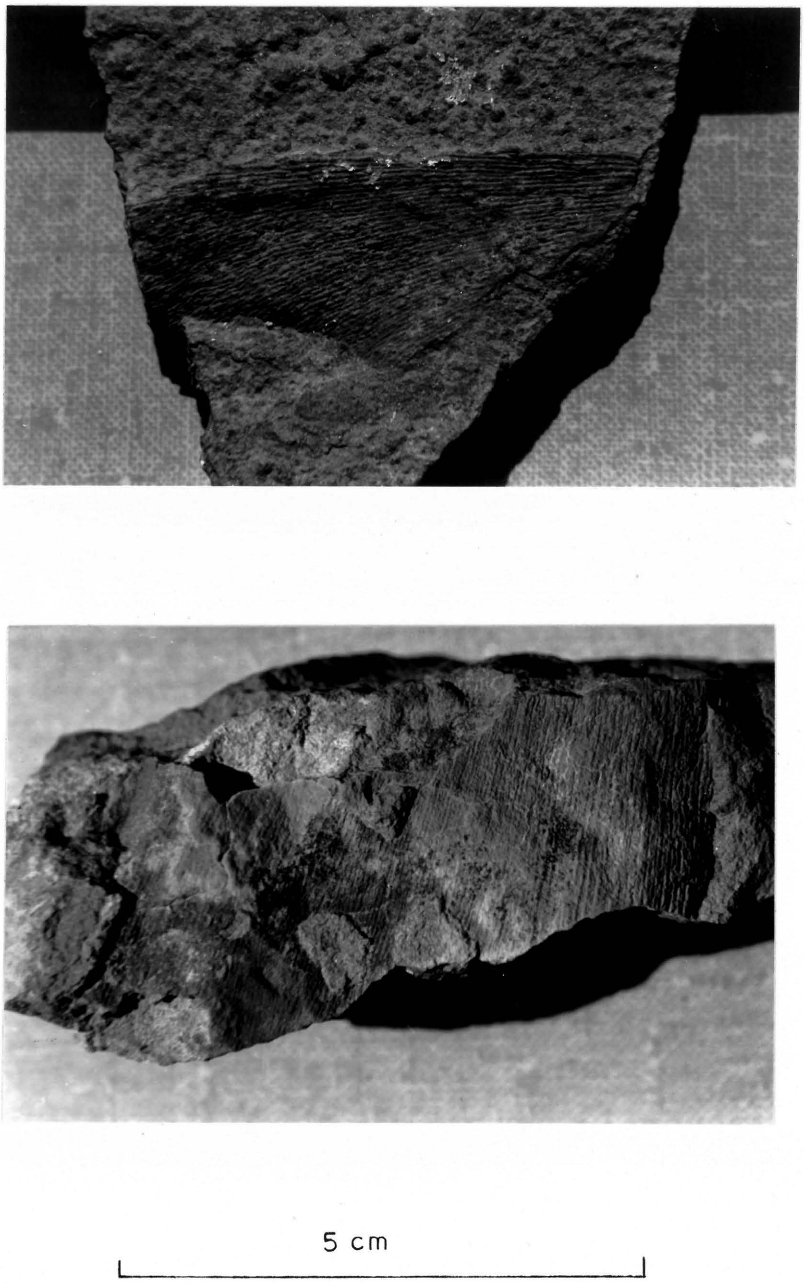

Figure 19. *Glossopteris* leaf fragments from the fossil-bearing shale (Collected at Positions 1 and 2, Figures 5 and 14).

The alternating layers of silt and clay in these shales reflect fluctuating physical or chemical conditions during sedimentation from suspension (Blatt et. al., 1972, p. 116). The prominent lamination suggests deposition in a freshwater lacustrine palaeo-environment ; little clay flocculation took place and burrowing organisms were absent. The preservation of fossil leaves implies a low Eh environment to prevent oxidation of the organic material (Blatt et. al., 1972, p. 392). This occurs in floodplain muds, lake bottoms and marshy or swampy areas. Flute structures form by the erosion of freshly deposited mud. Slight irregularities on the mud surface result in flow separation and secondary currents which scour the mud (Collinson and Thompson, 1982, p. 40). The existence of the flutes therefore implies the presence of flowing water during deposition of the shale unit.

Glossopteris plants grew in a seasonal, temperate and humid climate with short, mild winters (Kovács-Endrödy, 1979). The fragmented nature of the leaves suggests that they were transported prior to deposition, although the distance travelled must have been short for the leaves to survive.

vi. Sandstone

The sandstone is orange to red, coarse-grained and is made up of massive, normally graded beds. Individual beds unconformably overlie older beds and a thin, basal gravel lag is developed within each bed.

The sandstone has an average grain size distribution of 5% clay, 18% silt, 72% sand and 5% gravel (Appendix 1) and therefore plots as a silty sand (Figure 20a). The distribution is slightly bimodal with a very large sand fraction and a significant proportion of silt (Figures 20b and 20c). The sediment has a graphic mean grain size of 1,77 ϕ (0,29mm) and a median of 1,10 ϕ (0,47mm). The standard deviation is 2,52 ϕ and the sandstone is therefore very poorly sorted (Folk, 1968, p.46). The material has a

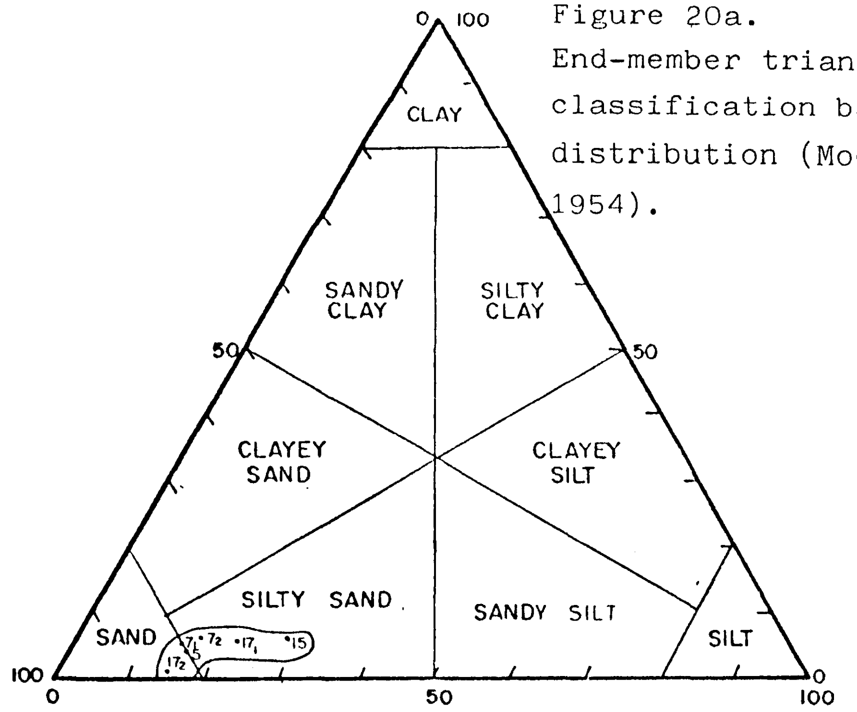

Figure 20a.
End-member triangle for sediment classification based on the grain size distribution (Modified after Shepard, 1954).

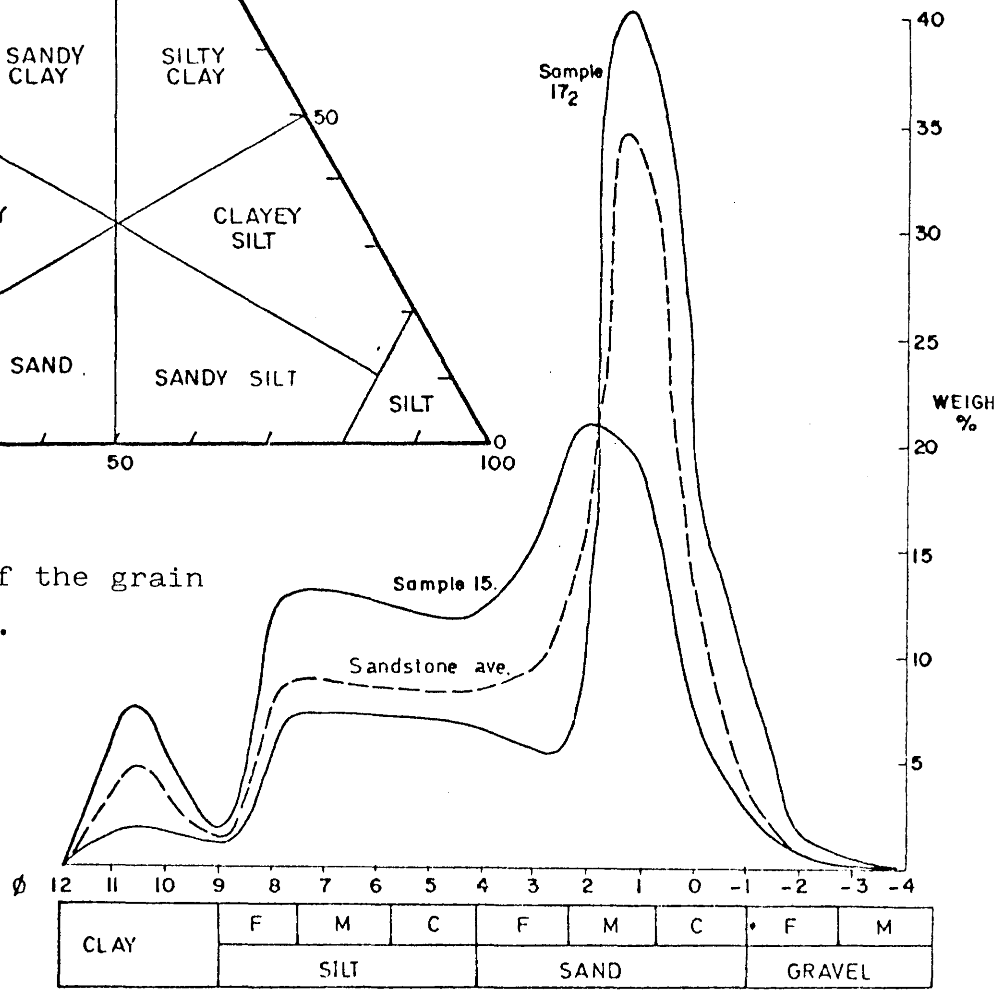

Figure 20b.
Frequency curve of the grain size distribution.

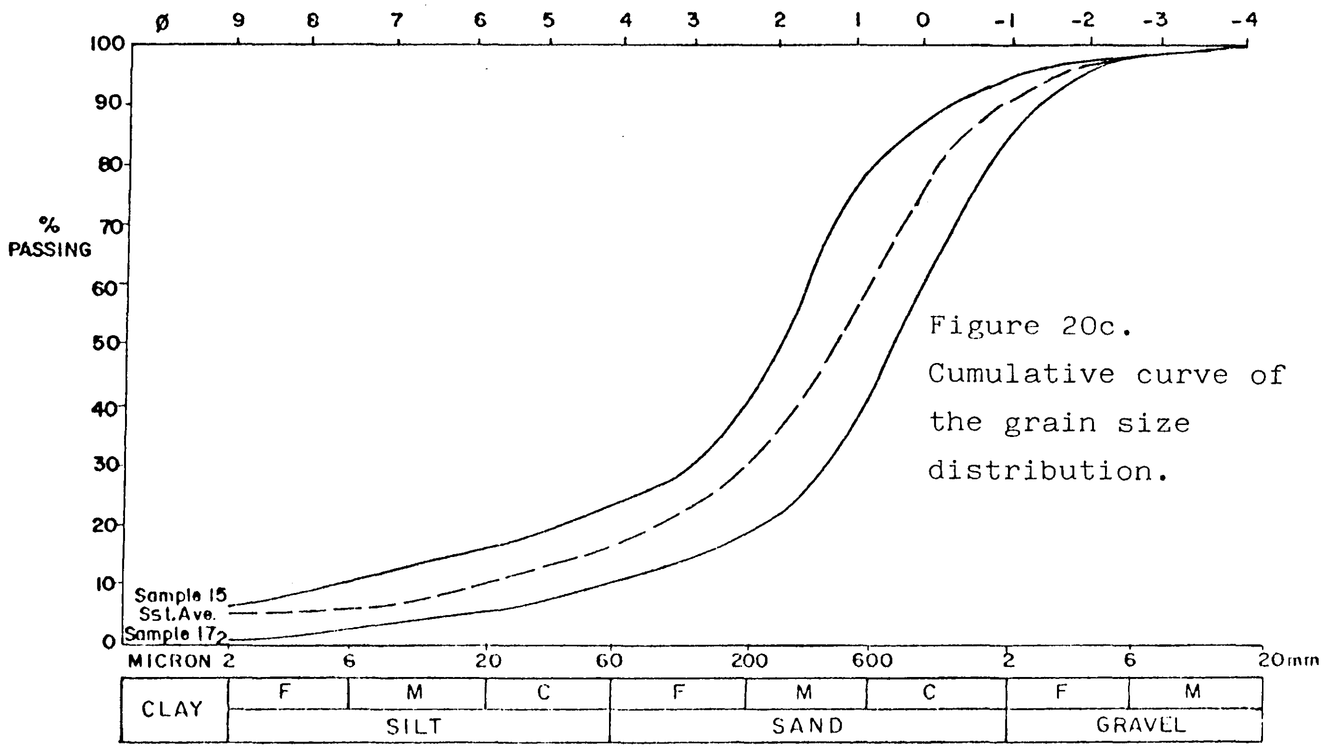

Figure 20c.
Cumulative curve of the grain size distribution.

Figure 20. Graphs of the sandstone grain size distribution. Sample 17_2 is the most coarse-grained and sample 15 is the most fine-grained.

positive skewness of 0,46, indicating an excess of fines. The kurtosis is 1,66 and the grain size distribution is thus excessively peaked or very leptokurtic (Folk, 1968, p. 48).

The sandstone has an average modal composition of 94% quartz, 5% kaolinite, 1% hematite with minor chert and goethite (Appendix 2). This sediment can therefore be classified as an orthoquartzite (Blatt et. al., 1972, p. 316). The quartz grains are subangular, colourless and unweathered with a medium sphericity and relief (Appendix 3). The small clay content, poor sorting, subangular grain shapes and high quartz composition indicates the material is texturally submature (Folk, 1968, p. 102) but mineralogically mature.

The massive sandstone beds with erosional basal contacts and normal grading suggest that deposition was cyclic and rapid (Collinson and Thompson, 1982, p. 101). Sedimentation followed the deceleration of heavily sediment-laden currents, probably in the form of surges. These submature sandstones imply a fairly nearby source of sand-size quartz grains which have undergone little reworking.

B. Unconsolidated Material

A highly irregular surface cover of unconsolidated material occurs throughout the study area (Figures 9 and 10). This cover consists of two types of red soil with different sedimentological and engineering properties. The predominant soil is a clayey silt which fills 16 depressions to between 12 and 48m in depth (Figure 11). Ten of these karstic depresssions are underlain by chert residuum, four by consolidated material and two by the syenite dyke (Figure 5). The karst forms are either narrow, deep sinkholes or basin-shaped dolines.

A thin sandy silt with an average thickness of 0,3m overlies the clayey silt. This horizon is not widely distributed and is only present in depressions 4,9 and 13, in Quarry 2 and along the margins of the large sinkhole in the east of the study area (Figures 4 and 5). The sandy silt is coarser grained, more consolidated and thus more resistant to erosion than the underlying clayey silt and characteristically protrudes in the soil profile.

i. Clayey silt

In outcrop, this soil is red to red-brown, massive and powdery. The sediment comprises quartz grains and iron oxide pisoliths in a clayey silt matrix. It differs from the chert residuum in that the soil contains few chert fragments and no large blocks or floaters of chert. The soil is also red with no wad whereas the residuum is brownish-black and wad-rich.

Grading analysis reveals that the soil has an average grain size distribution of 25% clay, 48% silt, 17% sand and 10% gravel (Appendix 1) and therefore plots as a clayey silt (Figure 21a). The distribution is bimodal to almost trimodal with large clay and silt fractions and a highly variable proportion of sand and gravel (Figures 21b and 21c). The graphic mean grain size and the median are both 5,20 ϕ (0,028mm). The standard deviation is 4,37 ϕ and the soil is therefore extremely poorly sorted (Folk, 1968, p. 46). The sediment has a negative skewness of 0,05, indicating an excess of coarse material. The kurtosis is 0,81 and the grain size distribution is thus flat-peaked or platykurtic (Folk, 1968, p. 48).

The clay consists entirely of kaolinite (Appendix 2). The silt and fine sand comprise mainly quartz grains with minor chert and iron oxides. Most of the quartz is rounded to well-rounded with a high sphericity and low relief (Appendix 3). Some quartz grains have been broken to produce subrounded fragments, angular chips and slivers. The chert is subangular with a medium relief and sphericity and is slightly weathered.

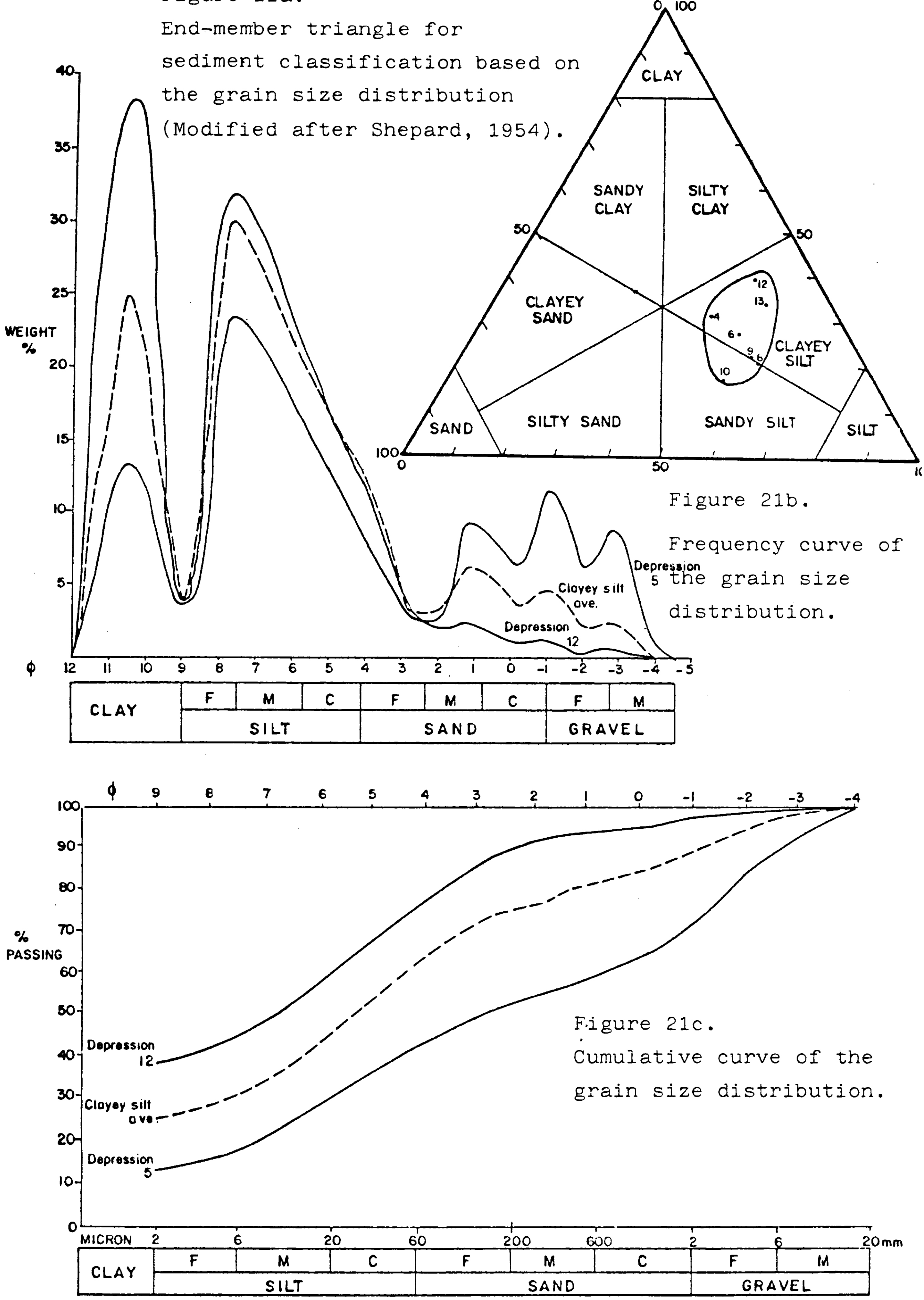

Figure 21a.
End-member triangle for sediment classification based on the grain size distribution (Modified after Shepard, 1954).

Figure 21b.
Frequency curve of the grain size distribution.

Figure 21c.
Cumulative curve of the grain size distribution.

Figure 21. Graphs of the clayey silt grain size distribution. Soil in depression 5 is the most coarse-grained and the soil in depression 12 is the most fine-grained.

The sand and gravel fractions are mainly composed of chert and iron oxide nodules with lesser amounts of quartz and minor syenite grains (Appendix 2). The chert has a low relief, medium sphericity, is angular in shape and only slightly weathered (Appendix 3). The nodules consist of quartz and chert grains cemented by hematite and minor goethite. These pisoliths have a low relief, smooth polished appearance and a metallic lustre. They have a high sphericity and are rounded and black with some corroded brown grains.

The sand - and gravel - sized quartz grains mostly have a medium relief and sphericity, and are subrounded and colourless (Appendix 3). Some subhedral to euhedral crystals and well-rounded, frosted grains are also present. The syenite grains are all weathered and display a crystalline, sugary texture.

Surface textures on quartz grains have been recognised and described by a number of authors. Research has shown that these features are either mechanically or chemically formed and their presence can be related to the original source material, diagenetic processes or to various depositional environments (Krinsley and Doornkamp, 1973, p. 9; Baker, 1976; Higgs, 1979; Manker and Ponder, 1978; Al-Saleh and Khalaf, 1982). However, some authors advocate caution in the use of quartz grain surface textures as indicators of depositional palaeoenvironments, as diagenesis can totally mask original features (Margolis and Krinsley, 1974; Subramanian, 1975; Marzolf, 1976; Ly, 1978; Manker and Ponder, 1978). Bull (1981) recommends the use of the textures as one of a number of sedimentological techniques in palaeoenvironmental reconstruction.

Quartz grain surface textures in the silt and fine sand fraction of the clayey silt show predominantly chemical features (Figure 22). Silica plastering, smooth precipitation surfaces, coated underlying structures and precipitated upturned plates are abundant. Mechanical features such as rare dish-shaped concavities and common adhering particles are also present. It is not

Figure 22. Quartz grain surface textures in the silt and fine sand fraction of the clayey silt and their possible origin (Modified after Krinsley and Doornkamp, 1973; Baker, 1976; Higgs, 1979; Manker and Ponder, 1978; Al-Saleh and Khalaf, 1982).

Quartz Grain Surface Textures		Textures Present In The Clayey Silt	Possible Origin: Source Material	Diagenesis	Environments: Glacial	Subaqueous	Loess	Aeolian	High Energy Chem.
Dish concavities	Mech.	1	0	0	0	0	0	P	0
Irregular pits		0	0	P	0	P	P	P	P
Coalescing pits		0	0	0	0	0	P	0	0
Straight cracks		0	0	0	0	P	0	0	0
Curved cracks		0	0	0	0	P	P	P	0
Striations		0	0	0	P	0	0	0	0
Mech. V's		0	0	0	0	P	0	0	0
Conchoidal fracture		0	P	0	P	P	0	0	P
Meandering ridges		0	0	0	P	0	P	P	0
Mech. upturned plates		0	P	0	P	P	P	P	P
Stepped cleav. planes		0	P	P	P	0	0	0	P
Flat cleav. face		0	P	0	P	P	0	0	0
Adhering particles		4	P	P	P	0	P	P	P
Crystal growth	Chem.	0	P	P	0	0	0	0	P
Silica plastering		4	0	P	0	0	0	0	0
Smooth precip. surface		4	0	0	0	0	P	P	0
Coated underlying struct.		4	P	P	0	0	0	0	P
Precip. upturned plates		4	P	P	0	0	P	P	0
Irreg. soln./precip. surf		0	P	P	P	P	0	P	0
Soln./cry. growth disint.		0	0	P	0	0	0	P	P
Large chem. decomp.		0	0	0	0	0	0	0	P
Soln. pits, crevasses		0	0	P	0	0	0	0	P
Scaling		0	0	P	0	0	0	0	0
Etched V's		0	0	0	0	P	0	0	P

% GRAINS SHOWING FEATURE

0	0	Absent
1	<5	Rare
2	5-25	Sparse
3	25-75	Common
4	>75	Abundant

0 Absent

P Present

possible to conclusively determine the depositional history of the soil from the observed textures. They may have been present in the source material, or could have formed in an aeolian or loessic environment or during diagenesis (Figure 22). The dish-shaped concavities do, however, suggest an aeolian influence.

The underlying geology appears to be reflected in the composition and grain size of the younger soils. Soil overlying Karoo outliers is rich in silt (Figure 23a). The material is also quartz-rich with only a small proportion of chert. Soil near the syenite has a very large kaolinite fraction, a syenite-rich silt and sand fraction and a chert-rich gravel component (Figure 23b). There is an increase in syenite and kaolinite with depth and towards the intrusion. Quartz, chert and iron oxide nodules decrease in the same directions.

Soil overlying chert residuum is gravelly and chert-rich (Figure 23c) and becomes coarser grained with depth and towards the margins of the depressions. There is also a decrease in quartz and iron oxide nodules and an increase in chert in the same directions.

The multimodal grain size distribution of the clayey silt suggests the material has experienced a complex sedimentological history (Griffiths, 1967). The grading, composition and grain textures indicate that the soil comprises 3 grain populations, each with characteristic sedimentological properties reflecting different origins. Kaolinite is usually a weathering product and the large clay content of the soil is probably post-depositional in origin. The clay either formed in situ by the breakdown of minerals with a medium to high weatheribility, such as feldspar (Knight, 1961), or was washed into the soil during erosion of adjacent rocks.

The silt and fine sand fraction is mineralogically and texturally mature (Folk, 1968, p. 102). The quartz-rich, chert-poor

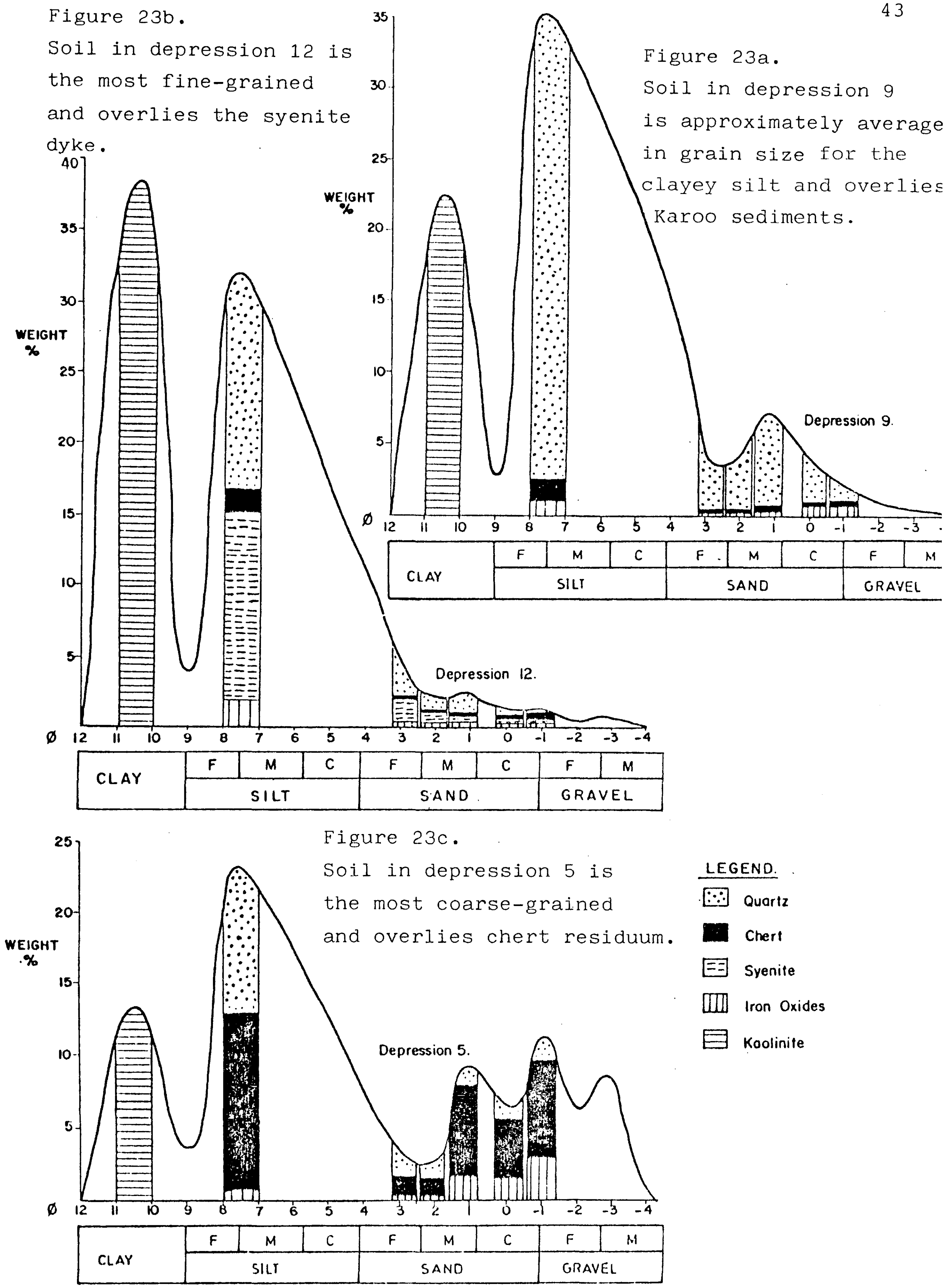

Figure 23a.
Soil in depression 9 is approximately average in grain size for the clayey silt and overlies Karoo sediments.

Figure 23b.
Soil in depression 12 is the most fine-grained and overlies the syenite dyke.

Figure 23c.
Soil in depression 5 is the most coarse-grained and overlies chert residuum.

Figure 23. Graphs depicting the influence of the underlying geology on the grain size and composition of the clayey silt.

composition of the silt implies an external source area as the dolomictic bedrock would produce a chert-rich, coarse-grained soil and Karoo sediments a polymictic, coarse-grained soil. The maturity and composition of the silt implies a polycyclic sedimentological history with cycles of weathering, erosion, transportation and deposition (Selley, 1977, p. 89). The grain size and quartz grain surface textures suggest aeolian transportation and deposition of the silt and fine sand fractions.

The coarse sand and gravel in the soil is mineralogically and texturally immature. The material was derived locally from weathering of the dolomitic bedrock and the syenite dyke. The abundant iron oxide nodules developed in situ through cementation of quartz and chert grains by hematite and goethite. These oxides probably originated from dissolution of mafic and heavy minerals in the soil and underlying dolomite by hydrolysis (Walker, 1967; Schluger, 1976). Iron dissolved in the groundwater and precipitated under oxidising conditions in colloform habits to form pisoliths (Selley, 1977, p. 56; Hubert and Reed, 1978). A thin layer of iron oxide on grain surfaces results in the red colour of the soil (Rhodes, 1968; Folk, 1976; Schluger, 1976).

ii. Sandy silt

This thin surficial layer of unconsolidated soil has a horizontal, unconformable contact with the underlying clayey silt. A basal lag of small pebbles and iron oxide nodules is developed along the unconformity. The soil is red to red-brown, massive and sandy.

The horizon has an average grain size distribution of 12% clay, 45% silt, 42% sand and 1% gravel (Appendix 1) and therefore plots as a sandy silt (Figure 24 a). The distribution is bimodal with a very large silt and sand fraction and a smaller clay fraction (Figures 24 b and 24 c). The graphic mean grain size is 4,06 ϕ (0,059mm) and the median is 3,40 ϕ(0,096mm). The standard deviation is 3,15 ϕ and the soil is therefore very

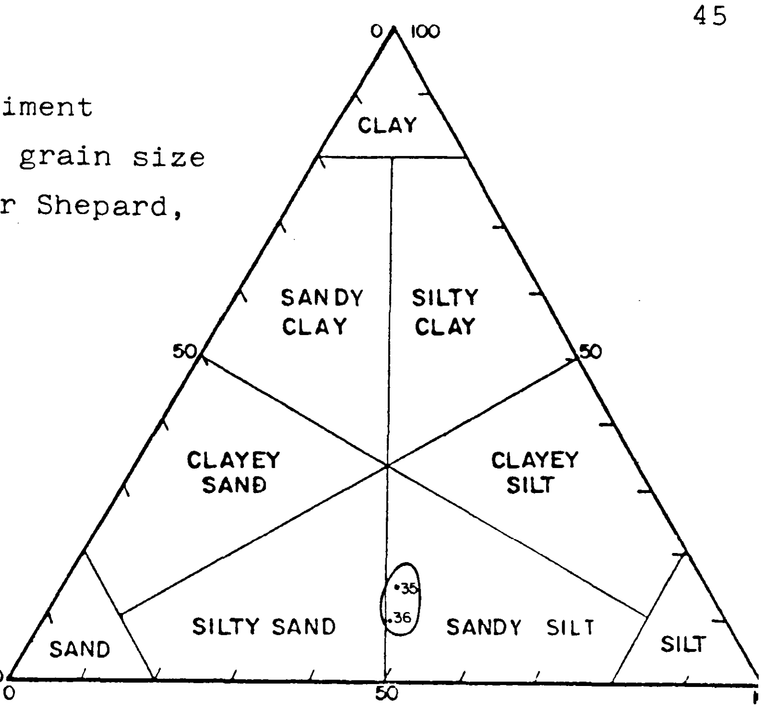

Figure 24a.
End-member triangle for sediment classification based on the grain size distribution (Modified after Shepard, 1954).

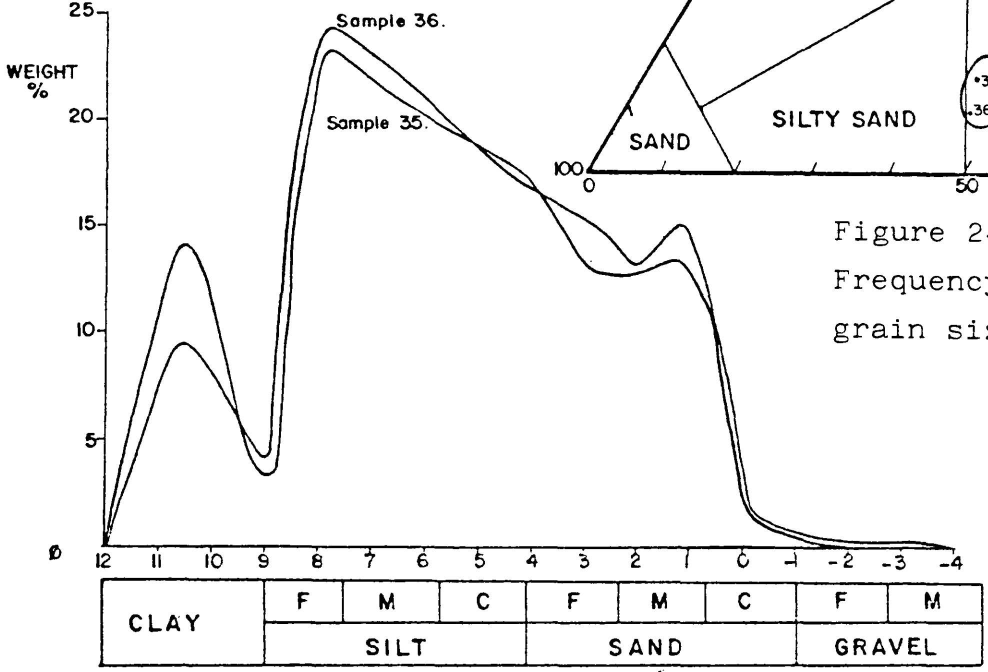

Figure 24b.
Frequency curve of the grain size distribution.

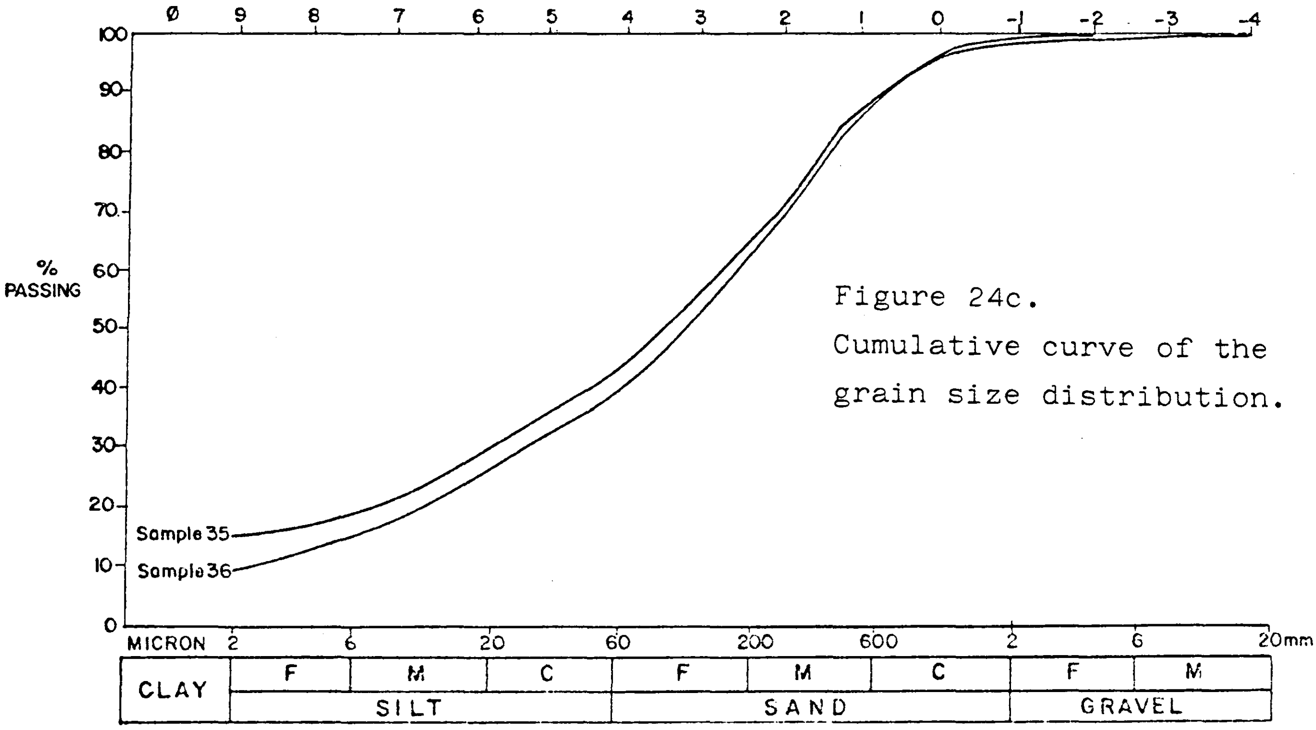

Figure 24c.
Cumulative curve of the grain size distribution.

Figure 24. Graphs of the sandy silt grain size distribution.

poorly sorted (Folk, 1968, p. 46). The sediment has a positive skewness of 0,35, indicating an excess of fine material. The kurtosis is 0,97 and the grain size distribution is thus normal or mesokurtic (Folk, 1968, p. 48).

The sandy silt horizon is coarser grained than the underlying clayey silt and contains more sand and less clay (Figures 21 and 24). The pebbly unconformity at the base of the sandy silt indicates that a period of erosion separated the deposition of the two soil types. Surface vegetation, particularly grass roots, and iron oxide precipitation have resulted in the sandy silt being more consolidated than the underlying clayey silt.

2. SEDIMENTARY HISTORY

Uplift of the Halfway House Granite in post-Transvaal times tilted the adjacent Transvaal Sequence up to 25° away from the dome (Jansen, 1977). Subsequent erosion stripped away the Pretoria Group to expose the underlying Chuniespoort Group. Groundwater apparently exploited structural and lithological weaknesses in the dolomites, and the karst topography in the study area is best developed along faults and dykes and in chert-poor dolomites. This episode of karst formation occurred in pre-Karoo times as Karoo outliers within the study area were deposited in existing karst forms. This period of dolomite weathering thus corresponds to the pre-Karoo karstification period suggested by Martini and Kavalieris (1976).

In contrast, Marker (1974 a) concludes that Karoo sediments in the Lyttelton quarry just south of the study area collapsed into the dolomites as the Karoo cover was eroded and that karst formation was post-Karoo. Jansen (1977) suggests that the palaeotopography prior to Karoo deposition resulted from glacial erosion in early Karoo times. The steep slopes around the two major karst depressions in the study area do not however support a glacial origin for these features.

The low intensity of deformation, size of the outliers and the orientation of mudclast conglomerate lobes into outlier J indicates that Karoo sedimentation within the study area took place into pre-existing surface irregularities. These deposits consist of a fining-upward sequence comprising basal diamictite grading up into sandstone, mudstone and shales, in response to a changing depositional environment. The Glossopteris leaves in the fossil-bearing shale confirm that the associated sequence of consolidated material is Karoo in age (Kovács-Endrödy, 1983, pers. comm.).

Initial Karoo sedimentation appears to have been debris flows of saturated local and transported material, which moved into the large surface depressions under the influence of gravity. Such flows can occur in almost any environment but the lithology and sedimentological features of the basal diamictites in the study area are analogous to fluvioglacial debris flow deposits of the Dwyka Formation found in the Northern Cape (Visser, 1983). The large chert breccia slabs in the diamictite and mudstone of the study area may originally have been ice-rafted material. The proposed debris flows were possibly related to melting of retreating Dwyka glaciers. As karstic surface depressions filled, fluvial activity may have laid down the sandy material associated with the diamictites.

The limited thickness, distribution and the fine-grained, organic-rich nature of the overlying carbonaceous shale suggests accumulation of sediment in a body of water with restricted circulation (Blatt et. al., 1972, p. 392). This implies that a small lake or swamp existed in the northern half of outlier F (Figure 4) after deposition of the diamictite.

The overlying mudstone was most likely deposited in similar lacustrine depressions. A large and constant influx of clay was necessary to produce the thick, massive mudstone deposits (Blatt et. al., 1972, p. 384; Collinson and Thompson, 1982, p. 57). This implies a clay-rich source close to the study area. Kaolinite is a common detrital clay mineral derived from granitic or gneissic terranes. The Halfway House Granite, 12km southwest of the study area, provides a likely source for such material.

Rivers draining this granitic area could have removed the clay and deposited it on entering the lakes. Localised debris flows deposited thin lenses of diamictite in these lacustrine mudstones.

Bennetts (1965), in discussing the origin of the clay deposits of the Transvaal, suggests that kaolinite derived from the Halfway House Granite was introduced into small, swampy basins by sluggish streams. The clay then flocculated in the fresh, acidic waters of the lakes to form massive mudstones.

The overlying mudclast conglomerate indicates penecontemporaneous erosion of the mudstone during and just after deposition of the clay (Selley, 1977, p. 105). Rivers flowing into the lakes probably generated currents which eroded and redeposited the clay as a mudclast conglomerate in fan-shaped lobes and channels. This conglomerate therefore formed in a fluviolacustrine palaeoenvironment and its distribution reveals the entry points of rivers suppling sediment to the lakes (Figures 13 and 14).

The well-laminated, fossil-bearing shale was deposited in a subaqueous palaeoenvironment with fluctuating physical or chemical conditions (Blatt et. al., 1972, p. 116). The flute structures and alternating laminae of clay and silt indicate flowing water with variable current velocities. The thin but laterally extensive nature of the horizon, and the preservation of fossil leaves, suggests a shallow water depositional palaeoenvironment, such as a floodplain or swamp with a generally flat palaeotopography. Surface depressions in the karst topography therefore seem to have been largely filled up by the Middle to Late Ecca period.

However, the more widespread sandstones which succeeded the fossil-bearing shales are thickest over pre-existing Karoo outliers. Widespread slickenside structures, bedding plane jointing and small scale folding within the older Karoo sediments indicates post-depositional movement of this material. This movement probably occurred after deposition of the fossil-bearing shales to produce surface depressions into which the sandstone accumulated.

This movement probably resulted either from continuing karst processes beneath the outliers, or by dewatering and compaction of the Karoo sediments. At the time of their deposition, clays may have water contents as high as 70% to 90% (Blatt et. al., 1972, p. 396). This is due to water present in the clay structure, absorbed onto clay surfaces and between clay flakes. Diagenetic pressure and temperature dehydrates such clay deposits, resulting in compaction. The high clay content and subaqueous origin of much of the Karoo sediments in the study area suggests this material had a high initial water content. Dewatering and compaction of this material could therefore have been sufficient to produce depositional sites for the Karoo sandstone.

The graded sandstone beds probably formed by deceleration of sediment-laden currents as they entered these depressions. Deposition most likely initially occurred in a fluviolacustrine palaeoenvironment and successive sedimentation became more fluvial as the depressions filled. The petrographic properties of the sandstone suggest a fairly nearby source of abundant sand-size quartz grains. Although no fluvial channel directions could be measured in the sandstones, similarities in grain textures of the sandstone and granitic soil samples (Appendix 3), suggest the most likely provenance areas are the Halfway House Granite. Quartzites of the Black Reef Formation and the Pretoria Group could have supplied additional material. All these lithologies are located within 12km of the study area (Figure 3). Absence of chert and dolomite grains in the sandstone implies the surrounding Chuniespoort Group was overlain by a more widespread Karoo cover during deposition of the sandstone.

The kaolinite fraction within the sandstone may have been derived from the Halfway House Granite and transported with the quartz grains. Erosion of the underlying Karoo sediments would also have contributed kaolinite to the fluvial deposits. Alternatively, the clay could be post-depositional, having been either washed in or produced in situ by breakdown of unstable detrital grains (Selley, 1977, p. 86).

A major period of karst formation appears to have occurred since the Karoo deposition and may be related to episodic uplift of the land surface (King, 1963). Sixteen sinkholes and dolines formed in the study area and were subsequently filled and covered by a second extensive period of sedimentation. Silt and lesser fine sand were laid down ; the size grading, mineralogical and textural maturity and quartz grain surface textures of this material suggest loessic depositional processes.

Silt found in major loess deposits of the world is usually glacial in origin, formed by glacial grinding of transported material. Silt can also be produced mechanically in hot, sandy deserts, although not enough to form large loess deposits (Smalley and Vita-Finzi, 1968). Loessic silt in Argentina has a volcanic-pyroclastic origin (Teruggi, 1957). Silt from all three possible sources is transported and deposited by wind.

Absence of post-Karoo glaciation and major volcanic-pyroclastic events in Southern Africa, and the presence of extensive post-Cretaceous desert sands of the Kalahari Group (Bond, 1948; Bond and Fernandes, 1974; Knight, 1961, 1963; Harmse, 1963; Baillieul, 1975) suggest a desert origin for silt found within the study area. Mixtures of different sized grains are unstable in deserts, as movement of sand grains exposes finer material which is removed by the wind (Smalley and Vita-Finzi, 1968). Silt is conveyed to desert fringes to form localised loessic deposits, such as the Be´er Sheva deposit in Israel (Smalley and Vita-Finzi, 1968). Clay and fine silt is transported much greater distances by major wind systems, and is often deposited in the oceans of the world (Chester <u>et</u>. <u>al</u>., 1972; Windom, 1975; Windom and Chamberlain, 1978).

The good sorting of the extensive Kalahari Group sands (Brain, 1958, p. 42; Harmse, 1963, p. 45; Baillieul, 1975) indicates that large quantities of fine-grained material may well have been removed. Deposition of silt-size sediment can be expected around the peripheries of the Kalahari desert. The lack of known loess deposits within South Africa suggests loessic deposition was localised and probably not recognised due to mixing, reworking and post-depositional alteration of this fine material.

Detailed examination of the clayey silt soil within the study area reveals its complex sedimentological history. Quartz-rich silt was mixed with local gravel - and sand-sized weathering products, such as chert and syenite, during deposition and filling of the karst topography. Minerals with a medium to high weatheribility would have broken down to form kaolinite with additional clay being washed into the soil from weathered rocks nearby. Iron oxide nodules and the red colour have developed in situ by precipitation of iron oxides.

Secondary alteration of the clayey silt took place due to climatic fluctuations and subsurface processes. The climate changed from possible arid conditions to a more temperate climate, with a resulting increase in surface water and vegetation (Knight, 1961, 1963). The higher permeability of the soil compared with the surrounding rocks would have concentrated groundwater flow into the soils. This water carried carbon dioxide and humic acids and aided in the continuous removal of weathering products. These conditions were ideal for the in situ decomposition of the soil.

Weinert (1974) demonstrates that present climatic conditions can be summarised in terms of an N value, derived by comparing evaporation during January with the annual precipitation. This value can indicate the type of weathering processes and weathering products that can be expected within a certain region. Pretoria has an N value of 2,4 and chemical decomposition is likely to be more pronounced than physical disintegration (Weinert, 1974).

Quartz, chert and kaolinite would remain after prolonged weathering with iron oxides precipitating to form ferricrete nodules. Similar weathering conditions during the Tertiary and Quaternary could have produced the clayey silt soil within the study area.

Fossil-bearing cave deposits of the Transvaal and Northern Cape exhibit similarities with the soil found in the study area. The cave deposits also consist of a mixture of local dolomitic weathering products and transported material, which accumulated in karst forms during the Late Tertiary to Middle Quaternary (Brain, 1958, p. 18; Marker, 1974b; Vrba, 1975; Beaumont et. al., 1978; Stiles and Partridge, 1979; South African Committee for Stratigraphy, 1980, p. 628-629). Although Brain (1958, p. 42) observes no primary aeolian sand or loess deposits in the Transvaal caves, Marker (1974b) reports that Kalahari Group sands are present in the Ulco deposits of the Northern Cape.

Transported material within the caves is recognised as having formed outside the caves and been washed in by sheetfloods during wetter periods (Brain, 1958, p. 42; Stiles and Partridge, 1979). Aeolian material appears to have mixed with local weathering products prior to filling the karst forms and therefore no true aeolian deposits accumulated in the Transvaal caves.

Following deposition of the clayey silt, a sandy silt layer developed within the study area. The massive, sandy nature of this horizon suggests it may represent aeolian Kalahari Group sand deposits. The basal coarser grained material indicates an erosional period existed prior to deposition. Surface weathering processes may also have modified the sandy silt since deposition, giving it a massive appearance. This relatively clay-poor sandy surface layer, with its lack of iron oxide nodules, may have experienced eluviation since deposition. Some of the clay and iron oxide nodules in the underlying clayey silt may have been derived from the sandy silt during surface weathering processes.

Karst processes are still operative in the study area and 36 surface sinkholes and dolines have developed since deposition of the red soils (Figure 5). Chert residuum and wad is therefore still accumulating. The syenite has been deeply weathered and is overlain by a kaolinitic soil.

IV. ENGINEERING PROPERTIES OF THE RED SOILS

In dolomitic areas of the Transvaal, post-Chuniespoort deposits have traditionally been assumed to offer more stable and safer ground conditions than the dolomitic bedrock. However, buildings in the study area have recently suffered cracking in zones underlai by unconsolidated surface soils. The engineering properties of these soils are therefore examined to assess the problems associated with construction on this material. Precautionary measures necessary for building are recommended.

The materials are described using the guide suggested by Jennings et. al. (1973). The engineering properties were determined from 75 disturbed and 23 undisturbed samples collected from the various soil-filled depressions (Figure 4). Properties of the two soil types were established from the Atterberg Limits, shear box test results, collapse potential tests and constant head field permeability tests.

1. CLAYEY SILT

Jennings et. al. (1973) suggest a method of describing a soil in the field which can facilitate an approximate quantitative assessment of the engineering properties of the material. To be reliable and consistent, each description should include the moisture condition, colour, consistency, structure, soil type and origin of the stratum. For the clayey silt, the moisture condition varies from slightly moist at the surface to moist with increasing depth. The soil is red to red-brown with a soft consistency and an intact structure. The material is a transported clayey silt.

The laboratory tests indicate the soil has relatively uniform engineering properties considering the range in sedimentological features. The Atterberg Limits of a soil reflect the change in strength or consistency of the material with a change in its water content (Capper and Cassie, 1976, p. 22; McCarthy, 1982, p. 77). The Liquid Limit is the moisture content at which a soil stops acting as a liquid and starts behaving as a plastic solid (Smith, 1978, p. 5). For the clayey silt, this occurs at a moisture content between 23,7 and 79,4%, with an average of 39,4% (Appendix 1).

The Plastic Limit is the moisture content at which a soil stops acting as a plastic solid and starts behaving as a brittle solid (Smith, 1978, p. 5). For the clayey silt, this occurs at a moisture content between 14,9 and 47,9%, with an average of 24,8% (Appendix 1). The Plasticity Index is the range of moisture content in which a soil remains plastic, and can be calculated by subtracting the Plastic Limit from the Liquid Limit. The clayey silt has a Plasticity Index between 9,1 and 31,5%, with an average of 14,6%. The Shrinkage Limit is the moisture content at which a further loss of moisture does not cause a decrease in the volume of a soil and will lead to cracking. For the clayey silt, this occurs between a moisture content of 5,1 and 16,4%, with an average of 8,4% (Appendix 1).

The Atterberg Limits can be used to classify different materials in terms of their mechanical and engineering properties. According to the Unified Soil Classification System, fine-grained sediments can be classified by comparing the Liquid Limit and Plasticity Index (Capper and Cassie, 1976, p. 15 and 24). The clayey silt classifies as an inorganic clay with a low to medium plasticity (CL type, Figure 25) or an inorganic silt with slight plasticity (ML type, Figure 25).

The Liquidity Index is the difference between the natural water content of a soil and the Plastic Limit, divided by the Plasticity Index (McCarthy, 1982, p. 80). For the clayey silt, the natural moisture content is between 5,2 and 12,9%, with an average of 8,7% and is always less than the Plastic Limit (Appendices 1 and 4). The Liquidity Index is -1,1, indicating the soil is

Figure 25. Unified Soil Classification of the clayey silt and sandy silt (Modified after Capper and Cassie, 1976, p. 15 and 24).

1-13 Average for each of the 13 clayey silt-filled depressions.

⊗ Average for the sandy silt.

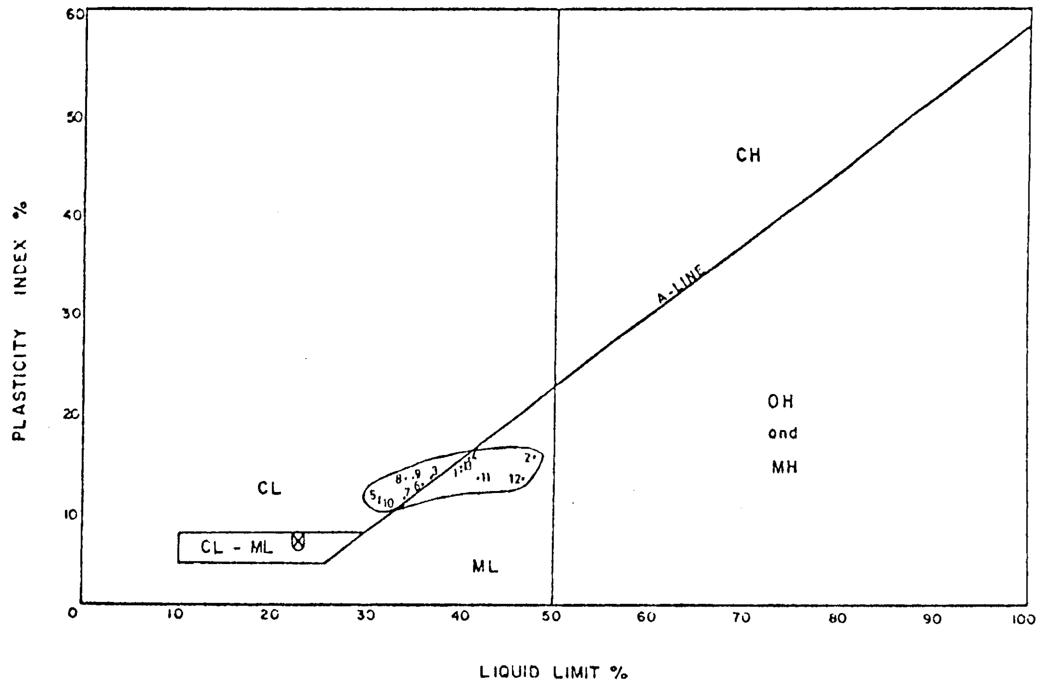

MAJOR DIVISIONS, GROUPS AND TYPICAL NAMES	GROUP SYMBOLS	VISUAL AND PHYSICAL CHARACTERISTICS
1. COARSE-GRAINED SOILS		
Gravel and gravelly soils		
Well-graded gravels or gravel-sand mixtures, little or no fines	GW	Large particles, easily seen; majority of particles larger than 1·5 mm
Poorly-graded gravels or gravel-sand mixtures, little or no fines	GP	
Silty gravels, gravel-sand-silt mixtures	GM	
Clayey gravels; gravel-sand-clay mixtures	GC	
Sand and sandy soils		
Well-graded sands or gravelly-sands, little or no fines	SW	Most of the particles can be seen without the aid of a magnifier, soils feel gritty to the fingers
Poorly graded sands or gravelly sands, little or no fines	SP	
Silty sands, sand-silt mixtures	SM	
Clayey sands, sand-clay mixtures	SC	
2. FINE-GRAINED SOILS		
Silts and clays (LL less than 50)		
Inorganic silts, very fine sands, rock flour, silty or clayey fine sands, or clayey silts with slight plasticity	ML	Not gritty to the fingers, but can be rolled into threads when moist. Shrinkage cracks appear on drying
Inorganic clays of low to medium plasticity, gravelly clays, sandy clays, silty clays, and lean clays	CL	
Organic silts and organic silt clays of low plasticity	OL	
Silts and clays (LL greater than 50)		
Inorganic silts, micaceous or diatomaceous fine sandy or silty soils, elastic silts	MH	Greasy to the touch. Can be rolled easily into threads when moist. Shrinks on drying. More than 40% clay particles
Inorganic clays of high plasticity, fat clays	CH	
Organic clays of medium to high plasticity, organic silts	OH	
3. HIGHLY ORGANIC SOILS		
Peat and other highly organic soils	Pt	Dark and fibrous

most likely a compressed sediment (Smith, 1978, p. 107). Soil in this state can be expected to have an undrained shear strength varying from 50 to 250 kN/m^2 (Smith, 1978, p. 108).

The low natural moisture content is probably due to the shallow depth of sampling (2m). The degree of saturation of the soil ranges between 15,4 and 35,7%,with an average of 21,5% (Appendix 4). This is the amount of water present in the voids of the soil (Smith, 1978, p. 11). The clayey silt is therefore partially saturated and the voids are filled mainly with air.

The amount of ground movement expected from a potentially expansive layer, due to changes in its natural moisture content, can be predicted using the method described by Van der Merwe (1964). By plotting the average clay content and Plasticity Index of the clayey silt within each of 13 soil-filled depressions, it appears the material has a low to medium potential expansiveness or activity (Figure 26). The activity averages 0,58 and the clay fraction can be classified as inactive (McCarthy, 1982, p. 81). No ground movement, such as heaving or swelling, is expected from the soil because the large clay content is composed entirely of kaolinite. Kaolinite is a stable clay mineral and undergoes no large volume changes with an increase in moisture content (McCarthy, 1982, p. 81).

The clayey silt contains an average of 25% clay, 48% silt, 17% sand and 10% gravel (Appendix 1) and is geologically poorly sorted but, from an engineering point of view, is well graded (Capper and Cassie, 1976, p. 19). Effective size and uniformity coefficient describe the grading of a material and are calculated from the grading curve (Capper and Cassie, 1976, p. 20). The effective size is the maximum particle size of the smallest 10% of a sample and the uniformity coefficient is the ratio of the maximum size of the smallest 60% to the effective size. The effective size of the clayey silt is 9,0 ϕ (0,002mm) because of the large clay content (Figure 21 b) and the uniformity coefficient is 29. The soil is therefore very well graded with

Figure 26. Potential expansiveness of the clayey silt and sandy silt (Modified after Van der Merwe, 1964).

1-13 Average for each of the 13 clayey silt-filled depressions.

⊗ Average for the sandy silt.

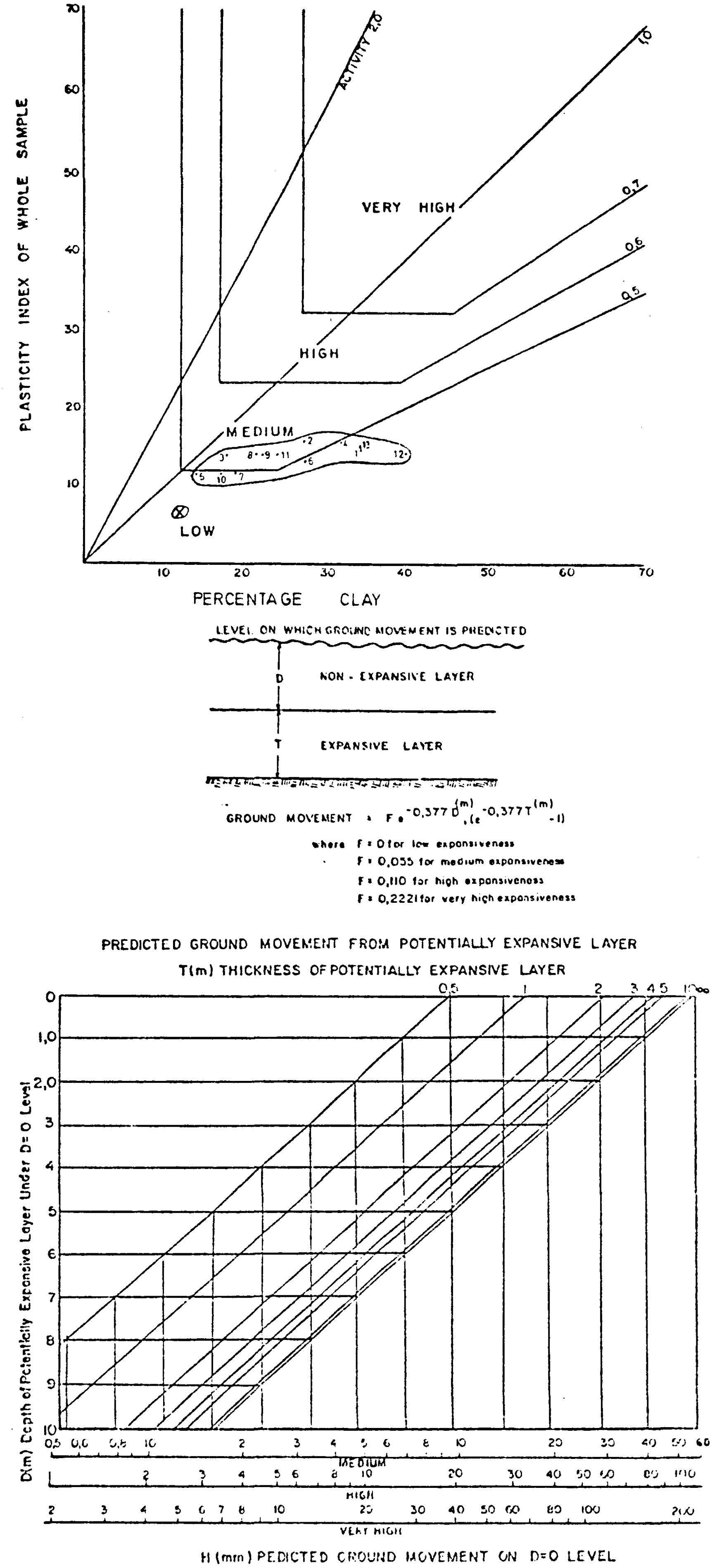

a very low degree of uniformity (McCarthy, 1982, p. 69).

Bulk density is the density of a soil in its natural state (Capper and Cassie, 1976, p. 27). For the clayey silt, the bulk density varies between 1175 and 1607 kgm^{-3}, with an average of 1411 kgm^{-3} (Appendix 4). Dry density is the density of a soil after water has been driven off (Capper and Cassie, 1976, p. 27). The dry density of the clayey silt ranges from 1044 to 1507 kgm^{-3}, with an average of 1301 kgm^{-3} (Appendix 4). Specific gravity of a soil is the ratio of the mass of a volume of grains to the mass of an equal volume of water (Smith, 1978, p. 12). For the clayey silt, the specific gravity varies between 2,37 and 2,67, with an average of 2,63 (Appendix 4), indicating a quartz-rich sediment.

Void ratio is a ratio of the volume of voids to the volume of solids in a soil (Smith, 1978, p.11). The void ratio of the clayey silt ranges from 0,77 to 1,56, with an average of 1,05 (Appendix 4). The volume of voids can also be related to the total volume, and is known as the porosity (Capper and Cassie, 1976, p. 27). For the clayey silt, the porosity ranges between 43,5 and 60,9%, with an average of 50,5% (Appendix 4). The average porosity and void ratio indicates the soil has a greater volume of voids than solids (Smith, 1978, p. 11).

Four constant head field permeability tests were carried out in three of the soil-filled depressions (Figure 4), using the method of Cedergren (1967). Permeability is a measure of the ability of water to flow through a material. The clayey silt has a permeability between $4,1 \times 10^{-5}$ and $10,1 \times 10^{-5}$ ms^{-1}, with an average of $8,5 \times 10^{-5}$ ms^{-1} (Appendix 4). A silt-clay mixture should have a very low permeability, between 10^{-6} and 10^{-9} ms^{-1}, and poor drainage properties (McCarthy, 1982, p. 94). The clayey silt therefore has a better permeability than expected and good drainage properties, which is most likely due to the high porosity and void ratio of this material.

Resistance of a soil against shear failure is a measure of its strength and comprises internal friction and cohesion. Internal friction is the resistance due to interlocking of soil particles and cohesion is resistance due to forces holding these particles together (Smith, 1978, p. 91). Drained shear box tests were used to determine the strength of the clayey silt, under natural moisture conditions. For normal stresses up to 150 kN/m^2, the soil has a cohesion between 40 and 63 kN/m^2, with an average of 55 kN/m^2 (Appendices 4 and 7). The angle of internal friction varies from 15° to 26°, with an average of 21°.

Collapse settlement is the rapid settlement of a partially saturated soil under increased load, following an increase in moisture conten (Jennings and Knight, 1975). Collapse potential is an index figure which can be used as a rough guide in predicting the severity of collapse of a material. The collapse potential of the clayey silt was determined from single consolidometer tests (Method modified after Jennings and Knight, 1975). After saturation at an applied load of 80 kN/m^2, the soil has a collapse potential between 4,8 and 11,9%, with an average of 8,2% (Appendices 4 and 5). The collapse potential could only be determined for soil in 7 of the soil-filled depressions as coarser grained samples crumbled before testing.

The low density, high porosity, permeability and void ratio and good drainage properties of the clayey silt, indicate that this soil has a very open grain structure with a high proportion of intergranular voids. The degree of saturation, natural moisture content and the deep groundwater level in excess of 100m, suggest these voids are filled mainly with air and the clayey silt is partially saturated. The cohesion and angle of internal friction,however, indicate that this soil has a relatively high strength under natural moisture conditions.

The anomalous properties of the clayey silt, with its open grain structure but relatively high strength, is further indicated by the high collapse potential. A rapid decrease in the natural volume and strength of this soil occurs with an increase in the moisture content under increased load conditions. The material collapses into a denser structure with a resultant increase in strength (Knight, 1961).

Engineering properties of the clayey silt are due to in situ weathering of this soil since deposition. Minerals with a high weatheribility broke down and were leached out, forming an open structure of stable quartz and chert grains (Knight, 1961). The deep groundwater level suggests rapid movement of infiltrating surface water through the soil, resulting in leaching and internal erosion of the material. Clay minerals were concentrated along quartz and chert grain contacts, possibly due to migration during seasonal fluctuations in moisture conditions (Knight, 1961). Concentration of this clay produced clay bridges which may have been cemented by secondary iron oxide precipitation.

Under natural moisture conditions, the clay bridges give the clayey silt a relatively high strength even with the open grain structure. This soil would have a fairly low erodibility because of the cohesive forces between grains and could support additional loading from surface structures. However, a subsequent rapid increase in moisture content and breaking of the bridges while the soil is under load, increase the erodibility of the largely silty material and the soil structure collapses.

2. <u>SANDY SILT</u>

The sandy silt has a dry moisture condition and is red to red-brown with a firm to stiff consistency. This soil has an intact structure and is a transported sandy silt.

The Liquid Limit of this horizon varies between 21,5 and 21,9%, with an average of 21,7% (Appendix 1). The Plastic Limit ranges from 14,8 to 15,1%, with an average of 15,0% and the

Plasticity Index varies between 6,4 and 7,1%, with an average of 6,7%. The Shrinkage Limit ranges from 3,3 to 4,0%, with an average of 3,7%. According to the Unified Soil Classification System, this soil classifies as an inorganic clay with a low to medium plasticity (CL type, Figure 25) or an inorganic silt with slight plasticity (ML type, Figure 25).

The natural moisture content of the sandy silt varies between 2,2 and 6,7%, with an average of 5,1% and is always less than the Plastic Limit (Appendices 1 and 4). The Liquidity Index is -1,5, indicating the soil is most likely a compressed sediment with an undrained shear strength between 50 and 250 kN/m^2 (Smith, 1978, p. 107 and 108).

The very low natural moisture content is probably due to the shallow depth of sampling (0,2m). The degree of saturation varies from 12,2 to 26,3%, with an average of 21,3% (Appendix 4). This soil is therefore partially saturated with the voids filled mainly with air (Smith, 1978, p. 11).

By plotting the average clay content and Placticity Index of the sandy silt, it appears this soil has a low potential expansiveness (Figure 26). The average activity is 0,57 and the clay fraction can be classified as inactive (McCarthy, 1982, p. 81). No ground movement is therefore expected from this horizon.

The sandy silt contains an average of 12% clay, 45% silt, 42% sand and 1% gravel (Appendix 1) and in an engineering sense, it is well graded (Capper and Cassie, 1976, p. 19). The effective size is 9,0 ø (0,002mm) and the uniformity coefficient is 80. The sandy silt is therefore very well graded with a very low degree of uniformity (McCarthy, 1982, p. 69).

The bulk density of the soil varies between 1635 and 1773 kgm^{-3}, with an average of 1712 kgm^{-3} (Appendix 4). The dry density ranges from 1532 to 1735 kgm^{-3}, with an average of 1630 kgm^{-3}. The specific gravity is between 2,53 and 2,67, with an average of 2,61, indicating a quartz-rich sediment. The soil has a void ratio between 0,46 and 0,74, with an average of 0,61 and a porosity from 31,5 to 42,5%, with an average of 37,6%. The sandy silt therefore has a greater volume of solids than voids (Smith, 1978, p. 11).

Results from single consolidometer tests indicate that little or no collapse occurs when the moisture content of the sandy silt is rapidly increased. After saturation at an applied load of 80 kN/m^2, this soil has a collapse potential between 0,4 and 3,3%, with an average of 1,6% (Appendices 4 and 6).

The higher density and lower void ratio and porosity of the sandy silt indicate this material has a less open grain structure than the clayey silt. The sandy silt mainly contains equal proportions of sand and silt which results in interlocking of grains and denser packing. The more consolidated nature and lower erodibility of the sandy silt is reflected in its low collapse potential and resistance to erosion.

3. ENGINEERING EVALUATION OF THE RED SOILS

A thorough evaluation of the engineering properties of the red soils is necessary for the safe design and construction of a building and its foundations on this material. Proposed development within the study area includes light structures, such as houses, and larger warehouses. Establishing the limitations of the soils is especially important to avoid the additional load of these new buildings exceeding the allowable bearing capacity of the substrata.

Engineering properties of the sandy silt indicate that no ground movement, such as heaving or swelling, or collapse can be expected from the horizon with an increase in moisture content. The soil also has a firm to stiff consistency and an intact structure.

The layer is however thin, erratically distributed and always underlain by clayey silt. Proposed structures must therefore be designed according to engineering properties of the clayey silt and the sandy silt layer is of minor importance.

The safe bearing capacity of a soil is the contact pressure which the material can be subjected to without the risk of shear failure and is therefore an important consideration in building and foundation design (Smith, 1978, p. 237; Smith and Pole, 1980, p. 1). Values of safe loading are based on soil strength and are determined by experience or testing against a factor of safety. Under natural moisture content and loading, the clayey silt can be expected to have a safe bearing capacity between 200 and 400 kN/m^2 (Smith, 1978, p. 251).

However, values of safe bearing capacity are for horizontal foundations at 0,6m depth and it is assumed the site and ground strata are reasonably level, there is no underlying softer layer and the site is protected from deterioration (Smith, 1978, p. 250). The underlying karst topography with thick accumulations of wad and chert residuum, and the fact that karst processe are still operative, makes an accurate estimation of the safe bearing capacity difficult. The large collapse potential of the clayey silt and the change in engineering properties with an increase in moisture content, will also result in an overestimation of the safe bearing capacity. Only by decreasing the threat of the karst materials and possible collapse of the clayey silt grain structure by controlling the inflow of surface water, can the standard tables of safe bearing capacity be used.

Jennings and Knight (1975) discuss the use of consolidometer test results as a guide to construction on materials exhibiting a collapsible grain structure. The collapse potential calculated from the test results can indicate the expected severity of collapse of a material.

The average collapse potential of the clayey silt is 8,2%, which suggests trouble can be expected in areas underlain by this soil.

Collapse settlement occurs when the moisture content of a material with a collapsible grain structure and under load, increases and does not necessarily require an additional increase in loading (Jennings and Knight, 1975). An increase in subsurface moisture content generally results from accumulation of surface water or leakage of water services.

Large structures within the study area were erected in zones underlain by more than 30m of clayey silt. Artificial entrapment of surface runoff occurs between these buildings. Numerous small scale depressions were created during construction and the natural slope was altered by leveling the ground around buildings. Water accumulates along the walls and corners of structures because gutter downpipes discharge rainwater directly into the soil. Loose backfill overlying recently installed stormwater pipes acts as french drains. Trenches and embankments were created during excavations. Water is also released from corrode or damaged water-bearing pipes. This alteration of the natural hydrology results in an increase in the subsurface moisture content and collapse of the soil grain structure.

The presence of a collapsible grain structure in the clayey silt and the predicted effect of an increase in the water content is supported by recent case histories. During 1980, extensive cracks up to 3mm wide developed in structures erected on soil-filled depression 6 (Figure 4), especially in the ablution facilities (Bénet, 1981). Larger displacements occurred in the walls and floors with minor cracks running diagonally down from the windows. This damage was related to the saturation and resultant collapse settlement of the soil following leakage of water-bearing pipes and surface accumulation of rainwater (Bénet, 1981).

In August 1981, noticeable sagging of a large tarred area overlying soil-filled depression 6 occurred (Jacobs, 1981). In December 1981, existing expansion-contraction joints in a nearby concrete floor opened up to 100mm. Large doors in the building could not close properly and the doors threatened to collapse. Removal of the concrete floor revealed a leaking 50mm diameter waterpipe that had saturated a 20m^3 zone of soil (Newham, 1981). A pneumatic percussion borehole was started but the force of the compressed air and the saturated, unconsolidated nature of the soil caused the borehole to cave in.

The underlying lithology is another factor to consider in evaluating the clayey silt. This soil is preserved in palaeosinkholes and dolines which can be reactivated through saturation by flowing water released from leaking pipes and poor surface drainage. In addition, lowering of the watertable allows overlying unconsolidated materials to move downwards into caverns previously filled with water (Brink and Partridge, 1965; Brink, 1979, p. 206; Foose, 1968; Martini and Kavalieris, 1976). Wad has a low density and a high void ratio and compacts easily, resulting in large settlements with loading or when the material is drained (Partridge, 1981). Thick accumulations of wad beneath the clayey silt can therefore also affect the stability of this soil.

Karoo sediments are generally considered to offer safe founding conditions (Enslin and Smit, 1955). The outliers are, however, preserved in orginally unstable zones, such as along faults and in karst depressions, and surface damage has been recorded in areas underlain by thick Karoo outliers (Chapman, in Kleywegt, 1981; Rauch, in Kleywegt, 1981; Wiid, 1981; van Rooy, 1983; Jones, 1984). This damage resulted from lowering of the watertable (Kleywegt and Enslin, 1973), dewatering of the Karoo sediments, seasonal fluctuations of perched watertables (Jones, 1984), possible microtectonic adjustments along zones of weakness in the bedrock (Wiid, 1981) or karstic processes in the underlying dolomites.

Four of the soil-filled zones within the study area are underlain by the major Karoo outlier and another two are partly underlain by this outlier (Figure 5). The soil is preserved in deep depressions which indicates post-Karoo movement of the outlier. Further movement of the Karoo material would pose a threat to surface stability and this possibility must be considered when evaluating clayey silt overlying a Karoo outlier.

4. RECOMMENDATIONS FOR CONSTRUCTION ON THE RED SOILS

The threat to the stability of structures sited on the clayey silt comes from the material itself and from the underlying lithology. Large variations in subsurface water conditions are, however, required to activate either threat. It is therefore necessary to avoid accidental leakage of water or the accumulation of rainwater and surface runoff.

To limit the subsurface percolation of water, the strict water precautionary measures pertaining to dolomitic areas (Bénet, 1981) must also be observed in zones underlain by red soils. All water-bearing pipes, drains and furrows should be watertight and fitted with flexible impermeable joints. Major water-bearing pipes should be placed above surface where any leaks can be easily detected. Taps, joints, drains and pipes must be inspected at regular intervals for possible damage or decay.

To avoid accumulation of surface water, the entire area to be developed must be properly drained. All artificial entrapment zones, especially between builings, and all roads and pathways must be rendered impervious by tarring or concreting. Furrows and drains must be installed to remove all surface runoff. Trenches and excavations must be properly backfilled with damp soil in layers of not more than 150mm. The backfilled areas must be compacted to prevent them functioning as french drains. The same order of permeability as the surrounding undisturbed soil should be attained. Gutter downpipes must discharge rainwater into drains or furrows. Water-borne sewerage reticulation must be installed instead of french drains.

To lessen the influence of the red soil and any underlying wad, a proposed structure can be founded below this material by piling or caissons (Wagener, 1981). Chert breccia and Karoo sediments have a greater safe bearing capacity and therefore offer more stable founding conditions. Piles may consist either of end-bearing piles, which transmit a load through weak or soft deposits onto an underlying firmer stratum, or of friction piles, which derive their support from the frictional resistance of the surrounding material (Smith and Pole, 1980, p. 55). The open grain structure of the clayey silt, however, makes friction piles unsuitable and cost is a limiting factor in the use of end-bearing piles.

It is possible to found a building within the red soil but only under strict controls. To minimise the possible collapse of the soil grain structure after development, the soil should be wetted and then compacted using an impact vibratory roller. Van der Merwe (in Mackechnie, 1968) suggests compacting trench inverts before continuing with conventional construction. Compaction induces collapse producing a denser, safer horizon. The resultant collapse potential should be less than 1% down to an acceptable depth of influence.

The red soils can also be removed and replaced with a more stable material, such as chert residuum or dumprock, to form a mattress (Jennings and Knight, 1975; Wagener, 1981). This mattress is normally compacted to a density of 95% Mod. AASHTO maximum dry density, producing a safe bearing capacity between 200 and 400 kN/m^2. A building is then founded as shallowly as possible on this mattress, usually by means of a raft-type foundation (Wagener, 1981).

The use of a mattress and a thick concrete raft foundation ensures an equal distribution of the load of a structure. Mackechnie (1968) recommends the use of ground floor slabs that are independent of the walls of a building. A bitumen skirt around a structure and a complete reticulation system at a shallow depth would control waterflow and prevent an increase in the subsurface moisture content.

V. CONCLUSIONS

The geology of the study area comprises Chuniespoort Group dolomites, overlain by younger sediments which are preserved in a karst topography. Chert-poor dolomite and wad of the Lyttelton Formation is overlain by chert-rich dolomite, chert breccia and chert residuum of the Eccles Formation and the succession dips at approximately 20° towards the east. A vertical syenite dyke in the east of the study area intruded parallel to the strike of the bedrock. Groundwater solution exploited lithological and structural weaknesses in the dolomites, producing a karst topography of sinkholes, bogazis and dolines.

Two major post-Chuniespoort periods of karst-fill deposition are identified. During Late Dwyka times, subaqueous debris flows of local and transported material slumped into 10 surface depressions. Sedimentation probably took place in a fluvioglacial palaeoenvironment. This period was followed by finer grained lacustrine deposition and fluvial channel sedimentation during Ecca times.

A second major episode of deposition occurred in Late Tertiary to Middle Quaternary times. Quartz silt was introduced to the study area under loessic conditions. Later sedimentary reworking mixed this silt with local weathering products and the resultant material filled 16 deep karst depressions. A younger, thin and erratically distributed sandy silt layer was then deposited in the study area.

Weathering processes have modified the reworked loessic deposits since deposition, producing a red clayey silt with a collapsible grain structure. Damage to structures has been experienced in areas underlain by thick accumulations of this soil. The case histories were found to be related to leakage of water-bearing pipes and poor drainage of surface water.

By decreasing the subsurface percolation of water and strict monitoring of all water-bearing facilities, the threat of collapse of the clayey silt grain structure can be lessened. Buildings can be founded within this scil by constructing a mattress or below it by piling. Once all the constructional constraints are observed, then the red soils will offer more favourable founding conditions than the surrounding dolomitic material.

VI. ACKNOWLEDGEMENTS

The author would like to thank the Chief Director of the Geological Survey, Dr. P.J. Smit for the use of information accumulated during my stay in the Engineering Geology Division. Sincere thanks also go to Dr. P. Roux for making this investigation possible and to Mr. J.L. van Rooy and my fellow workers at the Old Land Bank for their assistance.

The writer is indebted to Mr. E. Filmater and the staff of the Engineering Geology Laboratory for the grading analysis and engineering testing of the field samples. The work done by Mr. P.S. Chauke and the field staff at Visagie Street in the collection and storage of samples is acknowledged. Use of the numerous facilities at Visagie Street and the efforts of the related staff are greatly appreciated.

Sincere gratitude goes to my supervisors Dr. P. Eriksson and Prof. A. van Schalkwyk of the University of Pretoria for their continual support and guidance during this investigation.
The help received in the XRD analysis of samples by Mr. G. Botha and in the operation of the scanning electron microscope by Mr. A. Botha, both of the University of Pretoria, is acknowledged. Thanks also go to Mrs. J. Trebble for typing this thesis.

VII. REFERENCES

Access to reports and letter reports written by the Engineering Geology Division of the Geological Survey is restricted. Where these reports are listed, only the author's name, date and report number are given.

AL-SALEH,S. and KHALAF,F.I. (1982). Surface textures of quartz grains from various recent sedimentary environments in Kuwait. J. Sed. Pet., 52, 215-225.

BAKER,H.W. (1976). Environmental sensitivity of submicroscopic surface textures on quartz sand grains - a statistical evaluation. J. Sed. Pet., 46, 871-880.

BAILLIEUL, T.A. (1975). A reconnaissance survey of the cover sands in the Republic of Botswana. J. Sed. Pet., 45, 494-503.

BEAUMONT,P.B., DE VILLIERS,H. and VOGEL,J.C. (1978). Modern man in sub-Saharan Africa prior to 49 000 years B.P. : A review and evaluation with particular reference to Border Cave. S. Afr. J. Sci., 74, 409-417.

BÉNET,M.J.F. (1981). Restricted report. Geol. Surv. S.Afr., 1981-0083.

BENNETTS,K.P. and PIETERSE,J.J. (1963). Bulk density-apparent porosity relationship in Transvaal flint-clays. Ann. Geol. Surv. S.Afr., 2, 152-159.

BENNETTS,K.P. (1965). The flint-clay deposits of the area between Pretoria and Belfast, Transvaal. Bull. Geol. Surv. S.Afr., 45, 79 p.

BLATT,H., MIDDLETON,G. and MURRAY,R. (1972). Origin of sedimentary rocks. Prentice-Hall, New Jersey, 634 p.

BOND,G. (1948). The direction of origin of the Kalahari sand of Southern Rhodesia. Geol. Mag., 85, 305-315.

BOND,G. and FERNANDES,T.R.C. (1974). Scanning electron microscopy applied to quartz grains from Kalahari type sands. Trans. Geol. Soc. S.Afr., 77, 191-199.

BRAIN,C.K. (1958). The Transvaal ape-man-bearing cave deposits. Mem. Transvaal Museum, 11, 131 p.

BREDELL,J.H. (1974). pH as a guide to the genesis and quality of Transvaal refractory clays. Ann. Geol. Surv. S.Afr., 10, 23-29.

BREDELL,J.H. (1978). Prospecting for refractory clay on the East Rand. Bull. Geol. Surv. S.Afr., 62, 20 p.

BRINK,A.B.A. and PARTRIDGE,T.C. (1965). Transvaal karst : some consideration of development and morphology, with special reference to sinkholes and subsidences on the Far West Rand. S.Afr. Geogr. J., 47, 11-34.

BRINK,A.B.A. (1979). Engineering geology of Southern Africa. 1, Building Publications, Pretoria, 319 p.

BRINK,A.B.A. (1981). Geology and geomorphology of dolomite : Seminar on the engineering geology of dolomite areas. Univ. Pretoria, 62-65.

BULL,P.A. (1981). Environmental reconstruction by electron microscopy. Progress Phy. Geog., 5, 368-387.

CAPPER,P.L. and CASSIE,W.F. (1976). The mechanics of engineering soils. 6th ed., John Wiley and Sons, New York, 376 p.

CARVER,R.E. (1971). Procedures in sedimentary petrology. John Wiley and Sons, New York, 653 p.

CEDERGREN,H.R. (1967). Seepage, drainage and flow nets. John Wiley and Sons, New York, 489 p.

CHESTER,R., ELDERFIELD,H., GRIFFIN,J.J., JOHNSON,L.R. and PADGHAM,R.C. (1972). Eolian dust along the eastern margins of the Atlantic Ocean. Marine Geol., 13, 91-105.

COETZEE,C.B. (1968). Kaolin deposits of the Republic of South Africa. 23rd Int. Geol. Cong., 16, 61-65.

COLLINSON,J.D. and THOMPSON,D.B. (1982). Sedimentary structures. Allen and Unwin, London, 194 p.

ENSLIN,J.F. (1950). Restricted letter report. Geol. Surv. S.Afr., 16/25/2528 CC/10/01.

ENSLIN,J.F. and SMIT,P.J. (1955). Geophysical surveys for foundations in South Africa with special reference to the sinkholes in the dolomites south of Pretoria. Trans. S.Afr. Inst. Civ. Eng., 5, 318-322.

FOLK,R.L. and WARD,W.C. (1957). Brazos River bar : a study in the significance of grain size parameters. J. Sed. Pet., 27, 3-27.

FOLK,R.L. (1968). Petrology of sedimentary rocks. Hemphill's, Austin, 170 p.

FOLK,R.L. (1976). Reddening of desert sands : Simpson Desert, N.T., Australia. J. Sed. Pet., 46, 604-615.

FOOSE,R.M. (1968). Surface subsidence and collapse caused by ground water withdrawal in carbonate rock areas. 23rd Int. Geol. Congr., 12, 155-166.

GEOLOGICAL SURVEY. (1971). Residual gravity map Ghp 3426, 1:10 000. Geol. Surv. S.Afr.

GEOLOGICAL SURVEY. (1973). Geological sheet 2528 CC (Lyttelton), 1:50 000. Geol. Surv. S.Afr.

GRIFFITHS,J.C. (1967). Scientific method in analysis of sediments. McGraw-Hill, New York, 508 p.

HAMMERBECK,E.C.I. (1972). Investigation of refractory clay at Westwood Small Holdings, Boksburg North. Bull. Geol. Surv. S.Afr., 56, 19 p.

HARMSE,H.J. von M. (1963). The sedimentary petrology of the aeolian sands in the north-western Orange Free State. Unpubl. M. Sc. thesis, Univ. Potch, 101 p.

HIGGS,R. (1979). Quartz-grain surface features of Mesozoic-Cenozoic sands from the Labrador and western Greenland continental margins. J. Sed. Pet., 49, 599-610.

HUBERT,J.F. and REED,A.A. (1978). Red-bed diagenisis in the East Berlin Formation, Newark Group, Connecticut Valley. J. Sed. Pet., 48, 175-184.

JACOBS,C.J. (1981). Restricted letter report. Geol. Surv. S.Afr., 16/25/2528 CC /10/02.

JAKUCS,L. (1977). Morphogenetics of karst regions. Adam Hilger, Bristol, 284 p.

JANSEN,H. (1977). The geology of the country around Pretoria : Expl. Sheets 2527 DA, DB, DC, DD and 2528 CA, CB, CC, CD, 1:50 000. Geol. Surv. S.Afr, 141 p.

JENNINGS,J.E., BRINK,A.B.A. and WILLIAMS,A.A.B. (1973). Revised guide to soil profiling for civil engineering purposes in Southern Africa. Trans. S.Afr. Inst. Civ. Eng., 15, 3-12.

JENNINGS,J.E. and KNIGHT,K. (1975). A guide to construction on or with materials exhibiting additional settlement due to "collapse" of grain structure. Proc. 6th Reg. Conf. Soil Mech. Found. Eng., 99-105.

JONES,D.H. (1984). Unstable ground conditions associated with Karoo outliers in the dolomitic environment of the Far West Rand. Unpubl. Ph.D. thesis, Univ. Pretoria, 235 p.

KAEY,G.M. (1949). Restricted letter report. Geol. Surv. S.Afr., 16/25/2528 CC/10/01.

KING,L.C. (1963). South African scenery. 3rd ed., Oliver and Boyd, Edinburgh, 308 p.

KLEYWEGT,R.J. and ENSLIN,J.F. (1973). The application of the gravity method to the problem of ground settlement and sinkhole formation in dolomite on the Far West Rand, South Africa. Proc. Int. Assoc. Eng. Geol. Symp. : Sinkholes and Subsidence, T3-01 - T3-015.

KLEYWEGT,R.J. (1981). Discussion on engineering evaluation of dolomite areas : Seminar on the engineering geology of dolomite areas. Univ. Pretoria, 285-295.

KNIGHT,K. (1958). Problems of foundations on collapsing soils. Trans. S.Afr. Inst. Civ. Eng., 8, 304-307.

KNIGHT,K. (1961). The collapse of structure of sandy subsoils on wetting. Unpubl. Ph.D. thesis, Univ. Wits, 95 p.

KNIGHT,K. and DEHLEN,G.L. (1963). The failure of a road constructed on a collapsing soil. Proc. 3rd Reg. Conf. Soil Mech. Found. Eng., 31-34.

KNIGHT,K. (1963). The origin and occurrence of collapsing soils. Proc. 3rd Reg. Conf. Soil Mech. Found. Eng., 127-130.

KOVÁCS-ENDRÖDY,E. (1977). The systematic position of the genus _Gangamopteris McCoy_. _Bull. Geol. Surv. S.Afr._, 60, 19-71.

KOVÁCS-ENDRÖDY,E. (1979). A re-evaluation of the venation structure of _Glossopteris_. _Ann. Geol. Surv. S.Afr._, 12, 107-141.

KOVÁCS-ENDRÖDY,E. (1981). "Broad sense interpretation" of _Glossopteris_ leaves : a critique. _Palaeont. Afr._, 24,35-38.

KRINSLEY,D.H. and DOORNKAMP,J.C. (1973). _Atlas of quartz sand surface textures_. Cambridge Univ. Press, London, 91 p.

LOMBARD,P.J.A. and LOURENS,P.G. (1983). Restricted report. _Geol. Surv. S.Afr._, 1983-0171.

LOWE,D.R. (1982). Sediment gravity flows : II. Depositional models with special reference to the deposits of high-density turbidity currents. _J. Sed. Pet._, 52, 279-297.

LY,C.K. (1978). Grain surface features in environmental determination of late Quaternary deposits in New South Wales. _J. Sed. Pet._, 48, 1219-1226.

MACKECHNIE,W.R. (1968). Collapse soils. _Proc. 4th Reg. Conf. Soil Mech. Found. Eng._, 394-396.

MANKER,J.P. and PONDER,R.D. (1978). Quartz grain surface features from fluvial environments of northeastern Georgia. _J. Sed. Pet._, 48, 1227-1232.

MARGOLIS,S. and KRINSLEY,D. (1974). Processes of formation and environmental occurrence of micro-features on detrital grains. _Amer. J. Sci._, 274, 449-464.

MARKER,M.E. (1971). _Karst landforms of the northeastern Transvaal_. Unpubl. Ph.D. thesis, Univ. Wits, 261 p.

MARKER,M.E. (1974 a). A note on the occurrence of Karoo sediments near Pretoria and its relevance to the dating of karst weathering. Trans. Geol. Soc. S.Afr., 77, 69-70.

MARKER,M.E. (1974 b). Dating Quaternary climatic oscillations using cave and tufa deposits. S.Afr. Archaeol. Soc., Goodwin Ser., 2, 13-19.

MARKER,M.E. (1980). A systems model for karst development with relevance for southern Africa. S.Afr. Geogr. J., 62, 151-163.

MARTINI,J. and KAVALIERIS,I. (1976). The karst of the Transvaal (South Africa). Int. J. Speleol., 8, 229-251.

MARZOLF,J.E. (1976). Sand-grain frosting and quartz overgrowth examined by scanning electron microscopy : the Navajo Sandstone (Jurassic (?)), Utah. J. Sed. Pet., 46, 906-912.

MCCARTHY,D.F. (1982). Essentials of soil mechanics and foundations. 2nd ed., Reston, Virginia, 632 p.

MINNETT,R.C.A. and WITHERS,A.W. (1980). The geology and ground conditions over the Malmani Dolomite in the Pretoria area as interpreted from Thermal Infrared Imagery. Spectral Africa, 31A (SES 30), 40 p.

NEWHAM,M.R. (1981). Restricted letter report. Geol. Surv. S.Afr., 16/25/2528 CC/10/02.

PARTRIDGE,T.C. (1981). Geology and geomorphology of dolomite : Seminar on the engineering geology of dolomite areas. Univ. Pretoria, 66-70.

PETTIJOHN,F.J., POTTER,P.E. and SIEVER,R. (1972). Sand and sandstone. Springer-Verlag, New York, 618 p.

RHODES,R.C. (1968). Some aspects of the post-depositional history of the red sands in coastal Natal. S.Afr. J. Sci., 64, 145-149.

ROUX,P. (1981). Evaluasie van nie-ontwaterde dolomitiese gebiede : Seminar on the engineering geology of dolomite areas. Univ. Pretoria, 230-241.

SCHLUGER,P.R. (1976). Petrology and origin of the red beds of the Perry Formation, New Brunswick, Canada, and Maine, USA. J. Sed. Pet., 46, 22-37.

SCHMIDT,E.R. (1976). Clay. In : C.B. Coetzee (Ed.), Mineral Resources of the Republic of South Africa. 5th ed., Handb. Geol. Surv. S.Afr., 7, 275-287.

SELLEY,R.C. (1977). An introduction to sedimentology. Academic Press, London, 408 p.

SHEPARD,F.P. (1954). Nomenclature based on sand-silt-clay ratios. J. Sed. Pet., 24, 151-158.

SKAWRAN,D.W. (1971). Ceramic raw materials of southern Africa. Nat. Build. Res. Inst., C.S.I.R., X/BOU-KER series, 31 p.

SMALLEY,I.J. and VITA-FINZI,C. (1968). The formation of fine particles in sandy deserts and the nature of 'desert' loess. J. Sed. Pet., 38, 766-774.

SMITH,G.N. (1978). Elements of soil mechanics for civil and mining engineers. 4th ed., Granada, London, 424 p.

SMITH,G.N. and POLE,E.L. (1980). Elements of foundation design. Granada, London, 222 p.

SNEED,E.D. and FOLK,R.L. (1958). Pebbles in the Lower Colorado River, Texas, a study in particle morphogenesis. J. Geol., 66, 114-150.

SOUTH AFRICAN COMMITTEE FOR STRATIGRAPHY (1980). Stratigraphy of South Africa, Part 1. Lithostratigraphy of the Republic of South Africa, South West Africa/Namibia, and the Republics of Bophuthatswana, Transkei and Venda. Handb. Geol. Surv. S.Afr., 8, 690 p.

STILES,D.N. and PARTRIDGE,T.C. (1979). Results of recent archaeological and palaeoenvironmental studies at the Sterkfontein Extension site. S.Afr. J. Sci., 75, 346-352.

SUBRAMANIAN,V. (1975). Origin of surface pits on quartz as revealed by scanning electron microscopy. J. Sed. Pet., 45, 530-534.

TERUGGI,M.E. (1957). The nature and origin of Argentine loess. J. Sed. Pet., 27, 322-332.

VAN DER MERWE,D.H. (1964). The prediction of heave from the plasticity index and percentage clay fraction of soils. Civ. Eng. S.Afr., 6, 103-107.

VAN ROOY,J.L. (1983). Restricted letter report. Geol. Surv. S.Afr., 16/25/2528 CC/10/21.

VISSER,J.N.J. (1983). The problems of recognizing ancient subaqueous debris flow deposits in glacial sequences. Trans. Geol. Soc. S.Afr., 86, 127-135.

VRBA,E. (1975). The life and times of the Transvaal ape-man. S.Afr. J. Sci., 71, 298-299.

WAGENER,F. VON M. (1981). Engineering uses of dolomite and chert gravel : Seminar on the engineering geology of dolomite areas. Univ. Pretoria, 201-212.

WAGENER,F. VON M. (1983). Engineering construction on dolomite. Unpubl. Ph.D. thesis, Univ. Natal, 328 p.

WALKER,T.R. (1967). Formation of red beds in modern and ancient deserts. Geol. Soc. Amer. Bull., 78, 353-368.

WEINERT,H.H. (1974). A climatic index of weathering and its application in road construction. Geotech., 24, 475-488.

WIID,B.L. (1981). Are Karoo outliers and similar geological bodies within the dolomites completely stable ? : Seminar on the engineering geology of dolomite areas. Univ. Pretoria, 261-271.

WINDOM,H.L. (1975). Eolian contributions to marine sediments. J. Sed. Pet., 45, 520-529.

WINDOM,H.L. and CHAMBERLAIN,C.F. (1978). Dust-storm transport of sediments to the North Atlantic Ocean. J. Sed. Pet., 48, 385-388.

Appendix 1. Results of the grain size analysis and the Atterberg Limits for the clayey silt, sandy silt and Karoo Sequence sandstone.

SAMPLE TYPE: CLAYEY SILT

POCKET NUMBER	1					2				
SAMPLE NUMBER	1				AVE	2				AVE
SAMPLE DEPTH (m) / (φ) (mm)	4,5	10	20	30		4,5	10	20	30	
-4,0 / 14,0	0,0	0,0	0,0	0,0	0,0	0,0	0,0	0,0	0,0	0,0
-2,66 / 6,3	0,0	0,1	0,0	0,4	0,1	4,1	8,4	4,1	2,9	4,9
-2,0 / 4,0	0,4	0,3	0,4	0,4	0.4	4,9	6,6	6,7	5,4	5,9
-1,0 / 2,0	1,4	1,6	2,0	2,2	1,8	8,8	9,4	10,9	10,6	9,9
-0,24 / 1,18	1,3	1,9	2,1	2,2	1,9	5,9	5,0	6,1	6,8	6,0
1,24 / 0,425 (%)	3,6	3,6	4,4	3,8	3,9	7,3	6,6	6,5	8,6	7,2
2,0 / 0,250	1,5	2,2	1,7	1,8	1,8	2,1	1,9	2,9	2,4	2,3
2,75 / 0,150	1,7	2,3	2,2	2,2	2,1	2,3	1,9	3,1	2,5	2,5
4,34 / 0,050	8,8	14,5	12,0	12,4	11,9	13,2	7,6	9,5	8,3	9,6
7,67 / 0,005	36,3	34,5	37,7	36,2	36,2	20,0	17,9	23,5	20,2	20,4
9,0 / 0,002	5,2	5,2	5,8	5,1	5,3	3,6	3,2	4,3	3,3	3,6
<9,0 / <0,002	39,8	33,8	31,7	33,3	34,6	27,8	31,5	22,4	29,0	27,7
GRAVEL	1,8	2,0	2,4	3,0	2,3	17,8	24,4	21,7	18,9	20,7
SAND	8,1	10,0	10,4	10,0	9,7	17,6	15,4	18,6	20,3	18,0
SILT (%)	50,3	54,2	55,5	53,7	53,4	36,8	28,7	37,3	31,8	33,6
CLAY	39,8	33,8	31,7	33,3	34,6	27,8	31,5	22,4	29,0	27,7
LIQUID LIMIT	42,4	41,8	37,1	38,7	40,0	46,2	50,4	49,1	58,1	51,0
PLASTIC LIMIT	26,4	26,1	24,5	22,9	25,0	29,8	33,2	33,2	36,9	33,3
PLASTICITY INDEX (%)	16,0	15,7	12,6	15,8	15,0	15,4	17,2	15,9	21,2	17,7
SHRINKAGE LIMIT	10,3	9,4	8,5	9,9	9,5	9,1	9,3	9,9	11,5	10,0
MOMENT MEAN	7,4	6,8	6,7	6,8	6,9	4,8	4,6	4,3	4,7	4,6
UNDERLYING STRATA	CHERT RESIDUUM					CHERT RESIDUUM				

POCKET NUMBER	3				4					5		
SAMPLE NUMBER	3			AVE	4		5		AVE	6		AVE
SAMPLE DEPTH (m) / (φ) (mm)	10	20	30		4,5	10	4,5	10		4,5	10	
-4,0 / 14,0	0,0	0,0	0,0	0,0	0,0	0,0	0,0	0,0	0,0	0,0	2,1	1,0
-2,66 / 6,3	3,4	12,6	16,4	10,8	2,1	0,5	0,1	0,3	0,7	3,0	15,0	9,0
-2,0 / 4,0	0,8	6,4	9,4	5,5	2,0	1,1	1,6	2,8	1,9	4,6	8,4	6,5
-1,0 / 2,0	1,1	7,0	8,8	5,6	5,4	3,5	7,3	7,8	6,0	10,2	13,3	11,8
-0,24 / 1,18	1,1	4,8	4,8	3,6	3,7	3,7	4,9	8,7	5,3	5,7	7,4	6,6
1,24 / 0,425 (%)	3,0	7,1	6,5	5,5	5,3	6,7	5,7	14,1	8,0	8,2	10,5	9,3
2,0 / 0,250	2,4	4,2	4,5	3,7	1,9	2,9	2,7	2,5	2,5	2,6	3,2	2,9
2,75 / 0,150	2,2	3,5	3,5	3,1	2,1	2,5	3,2	2,4	2,5	2,6	3,2	2,9
4,34 / 0,050	11,1	10,9	11,5	11,2	10,3	9,0	12,1	9,9	10,3	10,7	8,2	9,5
7,67 / 0,005	37,4	25,0	21,7	28,0	29,9	29,8	29,0	20,9	27,4	28,7	18,4	23,5
9,0 / 0,002	6,7	3,7	3,1	4,5	5,7	5,1	4,3	4,0	4,8	4,5	2,6	3,6
<9,0 / <0,002	30,8	14,8	9,8	18,5	31,6	35,2	29,1	26,6	30,6	19,2	7,7	13,4
GRAVEL	5,3	26,0	34,6	21,9	9,5	5,1	9,0	10,9	8,6	17,8	38,8	28,3
SAND	8,7	19,6	19,3	15,9	13,0	15,8	16,5	27,7	18,3	19,1	24,3	21,7
SILT (%)	55,2	39,6	36,3	43,7	45,9	43,9	45,4	34,8	42,5	43,9	29,2	36,6
CLAY	30,8	14,8	9,8	18,5	31,6	35,2	29,1	26,6	30,6	19,2	7,7	13,4
LIQUID LIMIT	42,8	35,1	34,4	37,4	43,9	46,2	36,1	39,8	41,5	35,8	23,7	29,8
PLASTIC LIMIT	26,1	22,1	22,1	23,4	23,9	25,1	24,3	27,6	25,2	20,3	14,9	17,6
PLASTICITY INDEX (%)	16,7	13,0	12,3	14,0	20,0	21,1	11,8	12,2	16,3	15,5	8,8	12,2
SHRINKAGE LIMIT	9,7	8,0	8,7	8,8	8,3	8,9	8,1	8,1	8,4	7,3	5,1	6,2
MOMENT MEAN	6,6	3,3	2,3	4,1	6,0	6,3	5,7	4,9	5,8	4,4	1,7	3,0
UNDERLYING STRATA	CHERT BRECCIA				CHERT RESIDUUM, KAROO SANDSTONE					CHERT RESIDUUM		

POCKET NUMBER	6														
SAMPLE NUMBER	10		11				13				14			AVE
SAMPLE DEPTH (m) / (φ) (mm)	4,5	10	4,5	10	20	30	4,5	10	20	30	4,5	10	20	
-4,0 / 14,0	0,0	0,0	0,0	0,0	0,0	0,0	0,0	0,0	0,0	0,0	0,0	0,0	0,0	0,0
-2,66 / 6,3	0,4	0,2	0,0	0,1	0,0	0,7	0,0	0,0	0,0	0,0	0,0	0,0	0,0	0,1
-2,0 / 4,0	1,0	0,1	0,3	0,1	0,1	0,3	0,3	0,1	0,2	0,0	0,2	0,1	0,1	0,2
-1,0 / 2,0	3,0	0,7	3,4	0,8	2,2	1,0	4,7	2,0	0,6	0,2	2,8	0,7	1,3	1,8
-0,24 / 1,18	3,5	1,6	4,1	2,8	3,3	1,8	4,7	3,9	1,5	1,5	3,3	1,9	3,2	2,9
1,24 / 0,425 (%)	6,1	6,8	8,2	7,1	8,4	6,8	4,4	10,5	7,4	5,9	4,9	10,7	14,4	7,8
2,0 / 0,250	5,1	3,6	5,8	6,8	6,0	4,7	3,2	5,3	3,6	2,9	3,0	4,3	5,8	4,6
2,75 / 0,150	3,8	4,8	5,0	6,2	4,7	5,6	4,3	4,9	3,0	4,2	3,8	3,1	3,1	4,3
4,34 / 0,050	10,3	14,1	14,5	18,6	13,0	22,9	15,1	12,6	15,1	20,2	25,0	12,5	10,6	15,7
7,67 / 0,005	26,7	32,8	41,4	43,3	39,4	38,9	31,4	27,5	27,6	31,8	28,6	26,8	13,0	31,5
9,0 / 0,002	4,8	5,4	3,7	1,9	5,7	3,2	3,9	4,3	4,3	5,0	6,2	3,5	3,6	4,3
<9,0 / <0,002	35,3	29,9	13,6	12,3	17,2	14,1	28,0	28,9	36,7	28,3	22,2	36,4	44,9	26,8
GRAVEL	4,4	1,0	3,7	1,0	2,3	2,0	5,0	2,1	0,8	0,2	3,0	0,8	1,4	2,1
SAND	18,5	16,8	23,1	22,9	22,4	18,9	16,6	24,6	15,5	14,5	15,0	20,0	26,5	19,6
SILT (%)	41,8	52,3	59,3	63,8	58,1	65,0	50,4	44,4	47,0	57,0	59,8	42,8	27,2	51,5
CLAY	35,3	29,9	13,6	12,3	17,2	14,1	28,0	28,9	36,7	28,3	22,2	36,4	44,9	26,8
LIQUID LIMIT	38,3	55,7	34,8	32,6	32,0	34,4	37,2	35,2	36,2	37,2	35,0	37,1	42,0	37,5
PLASTIC LIMIT	28,9	35,7	22,9	21,4	19,9	22,2	24,5	23,4	23,9	24,6	24,7	23,4	19,8	24,3
PLASTICITY INDEX (%)	9,4	20,0	11,9	11,2	12,0	12,2	12,7	11,8	12,2	12,6	10,3	13,7	22,2	13,2
SHRINKAGE LIMIT	7,3	12,0	6,9	7,6	8,0	8,3	7,1	7,5	7,5	8,1	7,3	7,6	10,2	8,1
MOMENT MEAN	6,4	6,4	5,0	5,1	5,4	5,2	5,9	5,9	6,8	6,4	5,7	6,6	6,7	6,0
UNDERLYING STRATA	SYENITE, CHERT RESIDUUM						KAROO DIAMICTITE, MUDSTONE							

POCKET NUMBER	7			8								
SAMPLE NUMBER	12		AVE	15		16		17		18		AVE
SAMPLE DEPTH (m) / (φ) (mm)	4,5	10		4,5	10	4,5	10	4,5	10	4,5	10	
-4,0 / 14,0	0,0	0,0	0,0	0,0	0,0	0,0	0,0	0,0	0,0	0,0	0,0	0,0
-2,66 / 6,3	3,4	1,4	2,4	0,5	3,0	0,0	0,0	0,0	0,2	0,0	0,0	0,5
-2,0 / 4,0	1,9	5,6	3,8	0,1	2,7	0,2	0,1	0,1	2,3	0,1	0,2	0,7
-1,0 / 2,0	5,8	13,6	9,7	1,6	7,0	1,1	1,1	1,6	10,4	2,2	0,9	3,1
-0,24 / 1,18	3,2	6,5	4,8	4,5	4,4	3,2	2,9	4,2	8,2	3,2	1,9	4,1
1,24 / 0,425 (%)	5,2	5,3	5,3	13,3	6,0	8,3	8,7	8,9	11,0	6,4	3,6	8,3
2,0 / 0,250	4,7	3,0	3,8	7,0	3,2	3,7	6,4	7,1	5,4	4,2	1,6	4,8
2,75 / 0,150	6,4	3,7	5,0	3,6	2,8	3,7	5,1	6,6	4,7	3,2	1,6	4,2
4,34 / 0,050	17,9	14,7	16,3	19,7	14,1	18,2	22,1	18,1	14,2	17,6	14,9	17,4
7,67 / 0,005	26,4	23,1	24,8	31,9	31,0	32,7	32,6	31,8	27,6	36,7	38,9	32,9
9,0 / 0,002	4,8	4,7	4,8	4,6	3,7	6,4	3,3	2,7	3,4	5,8	8,4	4,8
<9,0 / <0,002	20,3	18,4	19,3	11,2	22,1	22,5	17,5	18,9	12,6	20,6	28,0	19,2
GRAVEL	11,1	20,6	15,9	2,2	12,7	1,3	1,2	1,7	12,9	2,3	1,1	4,3
SAND	19,5	18,5	18,9	30,4	16,4	18,9	23,1	26,8	29,3	17,0	8,7	21,4
SILT (%)	49,1	42,5	45,9	56,2	48,8	57,3	58,2	52,6	45,2	60,1	62,2	55,1
CLAY	20,3	18,4	19,3	11,2	22,1	22,5	17,5	18,9	12,6	20,6	28,0	19,2
LIQUID LIMIT	34,1	33,6	33,8	27,6	35,0	37,8	37,7	30,7	32,8	36,4	34,8	34,1
PLASTIC LIMIT	20,3	24,3	22,3	15,2	17,7	23,1	19,9	19,2	20,3	21,4	20,0	19,6
PLASTICITY INDEX (%)	13,7	9,3	11,5	12,4	17,3	14,7	17,8	11,5	12,5	15,0	14,8	14,5
SHRINKAGE LIMIT	7,4	7,2	7,3	5,1	8,3	7,3	8,7	5,7	7,2	8,7	8,7	7,5
MOMENT MEAN	4,9	4,1	4,5	4,6	3,0	5,8	5,3	5,2	3,9	5,7	6,7	5,3
UNDERLYING STRATA	CHERT RESID., KAROO SED.			KAROO SANDSTONE, DIAMICTITE, MUDSTONE								

SAMPLE TYPE	CLAYEY SILT												
POCKET NUMBER	9												
SAMPLE NUMBER	19				20			21			22		AVE
SAMPLE DEPTH (m)	4,5	10	20	30	4,5	10	20	4,5	10	20	4,5	10	
(Ø) (mm) (%) -4,0 14,0	0,0	0,0	0,0	0,0	0,0	0,0	0,0	0,0	0,0	0,0	0,0	0,0	0,0
-2,66 6,3	0,0	0,0	1,9	0,0	0,0	0,0	2,7	0,9	0,0	0,0	0,0	0,0	0,5
-2,0 4,0	0,4	0,1	0,9	0,4	0,6	0,1	4,5	0,8	0,0	0,8	0,4	0,0	0,8
-1,0 2,0	2,5	0,1	2,3	1,9	2,2	1,8	3,9	1,4	1,8	5,3	1,9	1,6	2,2
-0,24 1,18	1,7	0,5	3,8	3,8	3,8	2,4	2,0	4,0	7,1	4,2	5,2	3,4	3,5
1,24 0,425	3,9	2,2	7,2	8,1	6,9	5,8	3,7	9,8	15,9	9,1	7,3	7,7	7,3
2,0 0,250	2,1	0,9	3,6	4,7	7,2	4,2	1,9	6,1	5,3	3,5	6,4	4,7	4,2
2,75 0,150	2,9	1,9	3,4	3,6	5,7	4,0	2,6	4,4	3,9	2,8	5,3	3,7	3,6
4,34 0,050	20,0	15,2	15,8	16,0	17,0	20,1	16,1	14,4	15,7	15,5	23,1	19,6	17,4
7,67 0,005	40,2	37,9	36,9	34,5	30,3	35,4	41,1	32,6	28,0	33,5	34,5	38,5	35,3
9,0 0,002	2,9	2,9	2,4	3,3	4,3	2,3	2,2	4,3	3,8	1,6	1,7	2,3	2,8
< 9,0 < 0,002	23,4	38,3	21,8	23,7	22,0	23,9	19,3	21,3	18,5	23,7	14,2	19,0	22,4
GRAVEL (%)	2,9	0,2	5,1	2,3	2,8	1,9	11,1	3,1	1,8	6,1	2,3	1,6	3,5
SAND	10,6	5,5	18,0	20,2	23,6	16,4	10,2	24,3	32,2	19,6	24,2	19,0	18,6
SILT	63,1	56,0	55,1	53,8	51,6	57,8	59,4	51,3	47,5	50,6	59,3	60,4	55,5
CLAY	23,4	38,3	21,8	23,7	22,0	23,9	19,3	21,3	18,5	23,7	14,2	19,0	22,4
LIQUID LIMIT (%)	42,0	39,8	38,4	41,2	33,7	35,3	36,3	32,3	30,1	33,2	31,3	32,3	35,5
PLASTIC LIMIT	26,5	24,5	22,0	22,9	22,6	23,3	22,7	18,6	15,9	16,8	21,5	18,3	21,3
PLASTICITY INDEX	15,5	15,3	16,4	18,3	11,1	12,0	13,6	13,7	14,2	16,4	9,8	14,0	14,2
SHRINKAGE LIMIT	8,7	8,3	8,3	9,5	6,6	7,2	7,7	6,7	6,5	7,1	6,3	7,7	7,6
MOMENT MEAN	6,0	7,4	5,3	5,7	5,5	5,9	5,2	5,4	4,9	5,4	4,8	5,3	5,6
UNDERLYING STRATA	KAROO DIAMICTITE, SANDSTONE												

SAMPLE TYPE	CLAYEY SILT													
POCKET NUMBER	10								—	11				
SAMPLE NUMBER	23	24			25	26		AVE	27	28		29		AVE
SAMPLE DEPTH (m)	4,5	4,5	10	20	10	4,5	10		4,5	10	20	4,5	10	
(Ø) (mm) (%) -4,0 14,0	0,0	0,0	0,0	0,0	0,0	0,0	0,0	0,0	0,0	0,0	0,0	0,0	0,0	0,0
-2,66 6,3	1,2	0,2	0,0	0,0	0,2	0,1	0,9	0,4	0,0	1,9	0,0	8,4	4,5	3,7
-2,0 4,0	2,4	0,4	0,4	0,3	0,1	0,4	1,0	0,7	0,2	3,8	0,9	4,6	4,0	3,3
-1,0 2,0	10,0	0,9	3,2	2,3	1,3	7,4	4,4	4,1	1,1	12,9	1,8	8,1	5,5	7,1
-0,24 1,18	5,4	2,4	2,1	3,9	3,2	4,5	5,6	3,9	0,8	3,8	0,6	4,9	2,7	3,0
1,24 0,425	10,0	6,7	6,6	9,7	7,8	7,2	9,4	8,2	1,8	3,2	1,3	6,0	3,4	3,5
2,0 0,250	6,0	5,6	7,8	5,7	3,9	5,7	6,4	5,9	3,7	1,5	1,2	3,1	1,9	1,9
2,75 0,150	4,2	8,4	5,9	5,7	3,6	5,2	5,9	5,5	5,6	2,1	2,0	3,4	3,3	2,7
4,34 0,050	14,4	21,4	17,8	15,9	15,7	15,8	18,6	17,1	16,3	16,0	17,8	13,1	17,3	16,1
7,67 0,005	25,1	32,4	35,6	35,1	33,6	32,3	31,2	32,2	31,7	24,7	33,0	31,4	35,7	31,2
9,0 0,002	3,1	2,3	2,5	4,3	3,8	4,8	2,1	3,3	4,8	3,0	5,7	2,5	3,0	3,5
< 9,0 < 0,002	18,2	19,3	18,1	17,1	26,8	16,6	14,5	18,7	34,0	27,1	35,7	14,5	18,7	24,0
GRAVEL (%)	13,6	1,5	3,6	2,6	1,6	7,9	6,3	5,2	1,3	18,6	2,7	21,1	14,0	14,1
SAND	25,6	23,1	22,4	25,0	18,5	22,6	27,3	23,5	11,9	10,6	5,1	17,4	11,3	11,1
SILT	42,6	56,1	55,9	55,3	53,1	52,9	51,9	52,6	52,8	43,7	56,5	47,0	56,0	50,8
CLAY	18,2	19,3	18,1	17,1	26,8	16,6	14,5	18,7	34,0	27,1	35,7	14,5	18,7	24,0
LIQUID LIMIT (%)	33,1	31,9	28,8	30,2	31,0	31,4	28,5	30,7	56,3	44,7	54,4	35,6	35,2	42,5
PLASTIC LIMIT	18,9	22,8	16,2	17,4	17,9	19,4	18,8	18,8	37,2	30,8	37,4	23,3	21,1	28,2
PLASTICITY INDEX	14,2	9,1	12,6	12,8	13,1	12,0	9,7	11,9	19,1	13,9	17,0	12,3	14,1	14,3
SHRINKAGE LIMIT	7,5	6,3	7,0	6,7	8,1	6,9	5,7	6,9	9,6	9,3	9,3	7,7	7,8	8,5
MOMENT MEAN	4,3	5,3	5,2	5,2	6,0	4,9	4,5	5,1	6,8	5,0	7,1	3,8	4,9	5,2
UNDERLYING STRATA	CHERT RESIDUUM								SYEN	CHERT RESIDUUM, SYENITE				

SAMPLE TYPE	CLAYEY SILT											
POCKET NUMBER	12						13					AVE
SAMPLE NUMBER	30	31		32	33	AVE	34				AVE	
SAMPLE DEPTH (m)	4,5	4,5	10	4,5	4,5		4,5	10	20	30		
(Ø) (mm) (%) -4,0 14,0	0,0	0,0	0,0	0,0	0,0	0,0	0,0	0,0	0,0	0,0	0,0	0,0
-2,66 6,3	1,5	0,2	0,0	1,4	0,7	0,8	0,1	0,0	0,0	0,0	0,0	2,6
-2,0 4,0	0,5	0,2	0,0	1,0	0,3	0,4	0,7	0,1	0,1	0,1	0,3	2,3
-1,0 2,0	1,0	1,0	0,1	2,9	1,9	1,4	1,5	0,6	0,5	0,5	0,8	5,1
-0,24 1,18	0,7	0,9	0,3	1,4	2,7	1,2	1,4	1,2	0,9	1,5	1,2	3,7
1,24 0,425	2,3	1,8	1,8	3,2	4,8	2,8	5,8	5,4	4,2	7,8	5,8	6,4
2,0 0,250	2,5	1,6	1,1	1,6	4,1	2,2	3,1	2,6	2,3	3,0	2,8	3,3
2,75 0,150	3,6	2,6	1,7	2,6	8,2	3,7	2,9	2,0	1,8	2,2	2,2	3,4
4,34 0,050	10,4	8,6	12,1	12,4	23,7	13,4	11,8	12,7	12,7	11,9	12,3	13,7
7,67 0,005	33,6	24,8	28,5	40,1	32,6	31,9	36,9	33,9	33,7	39,7	36,0	30,1
9,0 0,002	4,3	5,9	3,5	2,4	3,4	3,9	5,2	7,8	5,3	1,6	5,0	4,2
< 9,0 < 0,002	39,6	52,4	50,9	31,0	17,6	38,3	30,6	33,7	38,5	31,7	33,6	25,2
GRAVEL (%)	3,0	1,4	0,1	5,3	2,9	2,6	2,3	0,7	0,6	0,6	1,1	10,0
SAND	9,1	6,9	4,9	8,8	19,8	9,9	13,2	11,2	9,2	14,5	12,0	16,8
SILT	48,3	39,3	44,1	54,9	59,7	49,2	53,9	54,4	51,7	53,2	53,3	48,0
CLAY	39,6	52,4	50,9	31,0	17,6	38,3	30,6	33,7	38,5	31,7	33,6	25,2
LIQUID LIMIT (%)	53,0	69,9	79,4	49,8	36,7	57,8	43,1	40,0	39,6	38,5	40,3	39,4
PLASTIC LIMIT	35,0	43,2	47,9	36,4	26,4	37,8	24,1	26,5	25,9	26,1	25,7	24,8
PLASTICITY INDEX	18,0	26,7	31,5	13,4	10,3	20,0	19,0	13,5	13,7	12,4	14,6	14,6
SHRINKAGE LIMIT	11,0	12,7	16,4	9,7	5,5	11,1	8,7	8,8	9,2	8,2	8,7	8,4
MOMENT MEAN	7,2	8,1	8,1	6,5	5,3	7,0	6,6	7,0	7,3	6,6	6,9	5,4
UNDERLYING STRATA	SYENITE						CHERT RESIDUUM					

SAMPLE TYPE	SANDY SILT			KAROO SANDSTONE						
POCKET NUMBER	—	—	AVE	4	6		8			AVE
SAMPLE NUMBER	35	36		5	7		15	17		
SAMPLE DEPTH (m)	0,2	0,2		16	7	10	14	12	14	
(Ø) (mm) (%) -4,0 14,0	0,0	0,0	0,0	0,0	0,0	0,0	0,0	0,0	0,0	0,0
-2,66 6,3	0,2	0,0	0,1	0,0	0,0	0,0	0,1	0,2	0,6	0,2
-2,0 4,0	0,2	0,0	0,1	0,3	0,2	0,3	0,5	0,3	1,4	0,5
-1,0 2,0	0,6	0,5	0,6	2,8	2,2	5,2	2,7	1,5	10,0	4,1
-0,24 1,18	1,7	1,6	1,6	12,5	14,6	15,8	5,9	5,3	16,5	11,8
1,24 0,425	13,4	15,0	14,2	41,1	44,4	34,4	20,0	27,4	40,2	34,6
2,0 0,250	12,8	13,0	12,9	14,4	11,4	14,0	21,1	25,4	9,4	15,9
2,75 0,150	12,7	15,0	13,9	9,3	7,6	9,1	16,0	12,0	5,3	9,8
4,34 0,050	17,7	17,1	17,4	6,4	7,5	7,5	11,8	10,0	6,7	8,3
7,67 0,005	23,2	24,2	23,7	7,9	6,6	8,5	12,7	9,4	7,0	8,7
9,0 0,002	3,4	4,1	3,7	1,6	1,0	1,0	1,6	1,7	1,1	1,3
< 9,0 < 0,002	14,1	9,5	11,8	3,7	4,5	4,2	7,6	6,8	1,8	4,8
GRAVEL (%)	1,0	0,5	0,8	3,1	2,4	5,3	3,3	2,0	12,0	4,8
SAND	40,6	44,6	42,6	77,3	78,0	73,3	63,0	70,1	71,4	72,1
SILT	44,3	45,4	44,8	15,9	15,1	17,0	26,1	21,1	14,8	18,3
CLAY	14,1	9,5	11,8	3,7	4,5	4,2	7,6	6,8	1,8	4,8
LIQUID LIMIT (%)	21,9	21,5	21,7	TOO SANDY						
PLASTIC LIMIT	14,9	15,1	15,0							
PLASTICITY INDEX	7,1	6,4	6,7							
SHRINKAGE LIMIT	4,0	3,3	3,7							
MOMENT MEAN	4,5	4,1	4,3	3,0	2,7	1,3	1,9	1,9	2,0	2,1
UNDERLYING STRATA	CLAYEY SILT			KAROO DIAMICTITE, MUDSTONE						

Appendix 2. Composition of the clayey silt and Karoo Sequence sandstone (% per size fraction).

SAMPLE TYPE		CLAYEY SILT																					
POCKET NUMBER		1					2					3				4					5		
SIZE FRACTION	SAMPLE NUMBER	1				AVE	2				AVE	3			AVE	4		5		AVE	6		AVE
	SAMPLE DEPTH	4,5	10	20	30		4,5	10	20	30		10	20	30		4,5	10	4,5	10		4,5	10	
-1,0 ϕ > 2,0 mm	QUARTZ	13	14	16	10	13	28	40	35	27	33	10	14	12	12	18	20	19	15	18	17	10	14
	CHERT	51	55	52	55	53	68	58	62	69	64	83	81	82	82	29	40	29	43	35	42	78	60
	IRON OXIDES	36	31	32	35	34	4	2	3	4	3	7	5	6	6	53	40	52	42	47	41	12	26
	SYENITE	-	-	-	-	-	-	-	-	-	-	-	-	-	-	-	-	-	-	-	-	-	-
-0,24 ϕ 1,18 mm	QUARTZ	22	28	22	15	22	32	35	39	27	33	32	21	14	22	20	22	28	28	25	9	5	7
	CHERT	61	60	61	66	62	64	62	58	68	63	45	74	78	66	22	57	20	47	36	59	80	69
	IRON OXIDES	17	12	17	19	16	4	3	3	5	4	23	5	8	12	58	21	52	25	39	32	15	24
	SYENITE	-	-	-	-	-	-	-	-	-	-	-	-	-	-	-	-	-	-	-	-	-	-
1,24 ϕ 0,425mm	QUARTZ	70	80	80	79	77	25	29	33	25	28	40	46	47	44	35	40	34	60	42	15	10	13
	CHERT	22	16	15	17	18	70	67	64	69	67	50	50	50	50	30	50	16	20	29	60	75	67
	IRON OXIDES	8	4	5	4	5	5	4	3	6	5	10	4	3	6	35	10	50	20	29	25	15	20
	SYENITE	-	-	-	-	-	-	-	-	-	-	-	-	-	-	-	-	-	-	-	-	-	-
2,0 ϕ 0,250mm	QUARTZ	88	93	95	93	92	41	42	41	40	41	60	58	59	59	79	73	89	82	81	60	26	43
	CHERT	8	4	2	5	5	54	54	56	57	55	34	38	37	36	15	21	5	12	13	30	64	47
	IRON OXIDES	4	3	3	2	3	5	4	3	3	4	6	4	4	5	6	6	6	6	6	10	10	10
	SYENITE	-	-	-	-	-	-	-	-	-	-	-	-	-	-	-	-	-	-	-	-	-	-
2,75 ϕ 0,150mm	QUARTZ	93	96	95	94	94	30	30	28	30	30	80	78	74	77	80	80	90	82	83	60	25	43
	CHERT	5	3	3	4	4	67	68	70	68	68	15	19	23	19	14	17	5	13	12	35	65	50
	IRON OXIDES	2	1	2	2	2	3	2	2	2	2	5	3	3	4	6	3	5	5	5	5	10	7
	SYENITE	-	-	-	-	-	-	-	-	-	-	-	-	-	-	-	-	-	-	-	-	-	-
2,75 - 9,0 ϕ 0,150 - 0,002mm	QUARTZ	93	95	93	93	94	66	69	67	65	67	79	77	78	78	89	87	89	88	88	51	36	44
	CHERT	4	3	4	5	4	30	28	31	33	30	18	21	20	20	7	9	8	10	9	45	61	53
	IRON OXIDES	3	2	3	2	2	4	3	2	2	3	3	2	2	2	4	4	3	2	3	4	3	3
	SYENITE	-	-	-	-	-	-	-	-	-	-	-	-	-	-	-	-	-	-	-	-	-	-
< 9,0 ϕ 0,002mm	KAOLINITE	100	100	100	100	100	100	100	100	100	100	100	100	100	100	100	100	100	100	100	100	100	100

SAMPLE TYPE		CLAYEY SILT																									
POCKET NUMBER		6														7			8								
SIZE FRACTION	SAMPLE NUMBER	10		11				13				14			AVE	12		AVE	15		16		17		18		AVE
	SAMPLE DEPTH	4,5	10	4,5	10	20	30	4,5	10	20	30	4,5	10	20		4,5	10		4,5	10	4,5	10	4,5	10	4,5	10	
-1,0 ϕ > 2,0 mm	QUARTZ	23	22	19	35	21	14	38	29	28	40	34	32	31	28	31	13	22	47	38	43	49	63	67	38	43	44
	CHERT	23	30	60	49	62	44	13	12	13	10	17	24	18	29	30	37	34	13	22	25	32	9	16	21	23	20
	IRON OXIDES	54	46	21	16	15	3	49	59	59	50	49	44	51	40	39	50	44	40	40	32	19	28	37	41	34	34
	SYENITE	■	2	■	■	2	39	-	-	-	-	-	-	-	3	-	-	-	-	-	-	-	-	-	-	-	-
-0,24 ϕ 1,18 mm	QUARTZ	61	41	33	43	33	26	57	58	62	67	60	51	53	50	38	18	28	64	51	75	73	87	63	68	62	68
	CHERT	11	20	54	42	54	39	7	6	8	8	9	9	8	21	26	47	37	5	16	12	14	4	16	9	15	11
	IRON OXIDES	28	39	13	15	13	5	36	36	30	25	31	40	39	27	36	35	35	31	33	13	13	9	21	25	23	21
	SYENITE	■	■	■	■	■	30	-	-	-	-	-	-	-	2	-	-	-	-	-	-	-	-	-	-	-	-
1,24 ϕ 0,425mm	QUARTZ	80	53	72	74	67	58	75	80	89	88	77	85	89	76	55	52	54	90	81	90	92	93	89	91	88	89
	CHERT	11	10	18	17	25	15	10	8	3	4	8	5	4	11	35	40	37	4	9	7	4	3	5	4	6	5
	IRON OXIDES	8	7	10	8	8	2	15	12	8	8	15	10	7	9	10	8	9	6	10	3	4	4	6	5	6	6
	SYENITE	1	30	■	1	■	25	■	■	■	■	■	■	■	4	-	-	-	■	■	■	■	■	■	■	■	■
2,0 ϕ 0,250mm	QUARTZ	89	49	90	86	86	79	87	86	87	88	87	86	85	83	82	70	76	96	87	96	95	95	89	95	88	93
	CHERT	6	5	6	8	9	3	5	6	5	4	5	4	6	6	12	22	17	1	7	1	2	1	5	2	8	3
	IRON OXIDES	5	6	4	6	5	6	8	8	8	8	8	10	9	7	6	8	7	3	6	3	3	4	6	3	4	4
	SYENITE	■	40	■	■	■	12	■	■	■	■	■	■	■	4	-	-	-	■	■	■	■	■	■	■	■	■
2,75 ϕ 0,150mm	QUARTZ	90	60	93	93	93	84	90	92	91	94	89	91	88	88	83	67	75	95	90	95	94	93	93	93	91	93
	CHERT	4	4	4	3	4	2	5	3	3	2	6	2	5	4	12	25	19	1	4	1	2	2	3	2	5	3
	IRON OXIDES	6	6	3	4	3	6	5	5	6	4	5	7	7	5	5	8	6	4	6	4	4	5	4	5	4	4
	SYENITE	■	30	■	■	■	8	■	■	■	■	■	■	■	3	-	-	-	■	■	■	■	■	■	■	■	■
2,75 - 9,0 ϕ 0,150 - 0,002mm	QUARTZ	89	69	91	93	94	87	89	90	93	94	89	92	92	90	84	84	84	91	91	94	94	92	93	92	91	92
	CHERT	5	4	5	4	4	3	4	5	3	4	5	4	3	4	10	12	11	4	5	3	4	3	5	4	6	4
	IRON OXIDES	6	7	4	3	2	2	7	5	4	2	6	4	5	4	6	4	5	5	4	3	2	5	2	4	3	4
	SYENITE	■	20	■	■	■	8	■	■	■	■	■	■	■	2	-	-	-	■	■	■	■	■	■	■	■	■
< 9,0 ϕ 0,002mm	KAOLINITE	100	100	100	100	100	100	100	100	100	100	100	100	100	100	100	100	100	100	100	100	100	100	100	100	100	100

SIZE FRACTION	SAMPLE TYPE	CLAYEY SILT												
	POCKET NUMBER	9												
	SAMPLE NUMBER	19				20			21			22		AVE
	SAMPLE DEPTH	4,5	10	20	30	4,5	10	20	4,5	10	20	4,5	10	
-1,0 ϕ > 2,0 mm	QUARTZ	39	50	44	46	49	64	51	40	70	46	64	60	52
	CHERT	19	19	20	20	19	9	14	44	11	13	11	9	17
	IRON OXIDES	42	31	36	34	32	27	35	16	19	41	25	31	31
	SYENITE	-	-	-	-	-	-	-	-	-	-	-	-	-
-0,24 ϕ 1,18 mm	QUARTZ	62	76	66	67	76	84	72	77	78	73	71	71	73
	CHERT	6	7	7	7	6	4	6	11	4	3	7	6	6
	IRON OXIDES	32	17	27	26	18	12	22	12	18	24	22	23	21
	SYENITE	-	-	-	-	-	-	-	-	-	-	-	-	-
1,24 ϕ 0,425 mm	QUARTZ	91	91	91	92	88	90	87	90	90	90	89	91	90
	CHERT	4	3	3	3	7	3	6	7	5	4	5	4	5
	IRON OXIDES	5	6	6	5	5	7	7	3	5	6	6	5	5
	SYENITE	■	■	■	■	■	■	■	■	■	■	■	■	■
2,0 ϕ 0,250 mm	QUARTZ	93	93	92	93	91	93	93	91	94	94	91	90	92
	CHERT	2	3	3	3	4	3	4	2	2	2	3	4	3
	IRON OXIDES	5	4	5	4	5	4	3	7	4	4	6	6	5
	SYENITE	■	■	■	■	■	■	■	■	■	■	■	■	■
2,75 ϕ 0,150 mm	QUARTZ	95	95	95	95	92	93	93	90	95	95	94	95	94
	CHERT	1	2	2	2	3	3	3	8	4	3	2	2	3
	IRON OXIDES	4	3	3	3	5	4	4	2	1	2	4	3	3
	SYENITE	■	■	■	■	■	■	■	■	■	■	■	■	■
2,75 - 9,0 ϕ 0,150 - 0,002 mm	QUARTZ	92	94	94	93	94	92	94	92	94	93	93	92	93
	CHERT	5	4	4	5	3	4	3	4	4	5	4	5	4
	IRON OXIDES	3	2	2	2	3	4	3	4	2	2	3	3	3
	SYENITE	■	■	■	■	■	■	■	■	■	■	■	■	■
< 9,0 ϕ 0,002 mm	KAOLINITE	100	100	100	100	100	100	100	100	100	100	100	100	100

SIZE FRACTION	SAMPLE TYPE	CLAYEY SILT													
	POCKET NUMBER	10								–	11				
	SAMPLE NUMBER	23	24			25	26		AVE	27	28		29		AVE
	SAMPLE DEPTH	4,5	4,5	10	20	10	4,5	10		4,5	10	20	4,5	10	
-1,0 ϕ > 2,0 mm	QUARTZ	29	22	19	15	31	20	15	22	25	21	19	22	17	20
	CHERT	38	41	43	46	47	43	40	43	31	65	70	62	73	67
	IRON OXIDES	33	37	38	39	22	37	45	35	23	13	7	15	10	11
	SYENITE	■	■	■	■	■	■	■	■	21	1	4	1	■	2
-0,24 ϕ 1,18 mm	QUARTZ	51	40	34	25	45	28	27	36	30	20	13	36	32	26
	CHERT	26	32	35	36	30	47	36	34	40	69	71	48	54	60
	IRON OXIDES	23	28	31	39	25	25	37	30	20	8	10	8	10	9
	SYENITE	■	■	■	■	■	■	■	■	10	3	6	8	4	5
1,24 ϕ 0,425 mm	QUARTZ	69	66	65	63	65	67	55	64	30	30	35	30	20	29
	CHERT	20	20	23	25	25	23	30	24	30	60	42	54	67	56
	IRON OXIDES	10	13	12	12	10	8	15	11	20	8	8	10	6	8
	SYENITE	1	1	■	■	■	2	■	1	20	2	15	6	7	7
2,0 ϕ 0,250 mm	QUARTZ	88	86	81	79	85	85	78	83	25	63	54	60	55	58
	CHERT	5	5	11	14	8	7	12	9	25	13	10	15	30	17
	IRON OXIDES	5	7	7	6	6	5	8	6	10	7	6	10	8	8
	SYENITE	2	2	1	1	1	3	2	2	40	15	30	15	7	17
2,75 ϕ 0,150 mm	QUARTZ	91	87	88	87	90	88	83	88	20	70	60	63	50	61
	CHERT	4	6	7	8	5	5	9	6	20	12	4	12	30	15
	IRON OXIDES	4	5	4	4	4	4	6	4	15	8	6	10	10	8
	SYENITE	1	2	1	1	1	3	2	2	45	10	30	15	10	16
2,75 - 9,0 ϕ 0,150 - 0,002 mm	QUARTZ	89	89	90	89	90	91	89	90	52	73	68	67	70	70
	CHERT	5	5	6	7	5	4	5	5	7	5	6	8	10	7
	IRON OXIDES	4	4	3	3	4	4	5	4	6	7	6	9	7	7
	SYENITE	2	2	1	1	1	1	1	1	35	15	20	16	13	16
< 9,0 ϕ 0,002 mm	KAOLINITE	100	100	100	100	100	100	100	100	100	100	100	100	100	100

SIZE FRACTION	SAMPLE TYPE	CLAYEY SILT											
	POCKET NUMBER	12						13					ω > <
	SAMPLE NUMBER	30	31		32	33	AVE	34				AVE	
	SAMPLE DEPTH	4,5	4,5	10	4,5	4,5		4,5	10	20	30		
-1,0 ϕ > 2,0 mm	QUARTZ	16	17	10	34	30	21	29	34	36	31	33	26
	CHERT	62	70	36	31	40	48	30	43	37	38	37	45
	IRON OXIDES	18	12	39	24	18	22	41	23	27	31	30	28
	SYENITE	4	1	15	11	12	9	-	-	-	-	-	1
-0,24 ϕ 1,18 mm	QUARTZ	29	25	17	29	25	25	45	52	56	56	52	36
	CHERT	46	41	28	45	63	41	21	22	25	29	25	41
	IRON OXIDES	20	30	25	21	22	23	34	26	19	15	23	22
	SYENITE	5	4	30	5	10	11	-	-	-	-	-	1
1,24 ϕ 0,425 mm	QUARTZ	65	65	52	55	52	58	88	89	89	87	88	58
	CHERT	15	10	10	10	12	11	5	5	6	7	6	30
	IRON OXIDES	5	7	8	13	12	9	7	6	5	8	6	10
	SYENITE	15	18	30	22	24	22	■	■	■	■	■	2
2,0 ϕ 0,250 mm	QUARTZ	58	53	45	45	38	48	90	92	93	88	91	72
	CHERT	5	6	3	5	9	5	6	5	4	7	6	17
	IRON OXIDES	7	6	8	8	10	8	4	3	3	5	3	6
	SYENITE	30	35	44	42	43	39	■	■	■	■	■	5
2,75 ϕ 0,150 mm	QUARTZ	49	45	40	42	43	44	89	94	93	89	91	74
	CHERT	4	3	2	4	6	4	5	2	3	5	4	16
	IRON OXIDES	7	7	8	8	6	7	6	4	4	6	5	5
	SYENITE	40	45	50	46	45	45	■	■	■	■	■	5
2,75 - 9,0 ϕ 0,150 - 0,002 mm	QUARTZ	49	45	44	49	49	47	89	91	93	90	91	79
	CHERT	5	6	4	5	6	5	6	5	4	6	5	12
	IRON OXIDES	6	6	4	6	7	6	5	4	3	4	4	4
	SYENITE	40	43	48	40	38	42	■	■	■	■	■	5
< 9,0 ϕ 0,002 mm	KAOLINITE	100	100	100	100	100	100	100	100	100	100	100	100

SIZE FRACTION	SAMPLE TYPE	KAROO SANDSTONE						
	POCKET NUMBER	4	6		8			ω > <
	SAMPLE NUMBER	5	7		15	17		
	SAMPLE DEPTH	16	7	10	14	12	14	
-1,0 ϕ > 2,0 mm	QUARTZ	99	98	99	100	100	100	99
	CHERT	■	■	■	■	■	■	■
	IRON OXIDES	1	2	1	■	■	■	1
	SYENITE	-	-	-	-	-	-	-
-0,24 ϕ 1,18 mm	QUARTZ	99	99	99	100	99	100	99
	CHERT	■	■	■	■	■	■	■
	IRON OXIDES	1	1	1	■	1	■	1
	SYENITE	-	-	-	-	-	-	-
1,24 ϕ 0,425 mm	QUARTZ	99	98	99	100	99	100	99
	CHERT	■	■	■	■	■	■	■
	IRON OXIDES	1	2	1	■	1	■	1
	SYENITE	-	-	-	-	-	-	-
2,0 ϕ 0,250 mm	QUARTZ	99	99	99	100	99	100	99
	CHERT	■	■	■	■	■	■	■
	IRON OXIDES	1	1	1	■	1	■	1
	SYENITE	-	-	-	-	-	-	-
2,75 ϕ 0,150 mm	QUARTZ	99	98	99	100	99	100	99
	CHERT	■	■	■	■	■	■	■
	IRON OXIDES	1	2	1	■	1	■	1
	SYENITE	-	-	-	-	-	-	-
2,75 - 9,0 ϕ 0,150 - 0,002 mm	QUARTZ	98	98	99	100	100	100	99
	CHERT	■	■	■	■	■	■	■
	IRON OXIDES	2	2	1	■	■	■	1
	SYENITE	-	-	-	-	-	-	-
< 9,0 ϕ 0,002 mm	KAOLINITE	100	100	100	100	100	100	100

Appendix 3. Grain textures of the clayey silt, Karoo Sequence sandstone and Halfway House Granite soil.

% GRAINS SHOWING TEXTURE	Sample Type	CLAYEY SILT							KAROO SST.	H.H.G. SOIL
	Grain Type	QUARTZ		CHERT		IRON OXIDES	SYENITE		QUARTZ	QUARTZ
	Grain Size	GRAVEL SAND	SILT	GRAVEL SAND	SILT	GRAVEL SAND	GRAVEL SAND	SILT	SAND	SAND SILT
RELIEF	Low	10	90	100		80				20
	Medium	60 - 80			100				100	80
	High	10 - 40	10			20	100	100		
SPHERICITY	Low	10 - 40	5							80
	Medium	60 - 80	5	100	100	20	100	100	100	
	High	10	90			80				20
ROUNDNESS	1	10 - 40	5	95			100	100		
	2				100	20			100	80
	3	60 - 80	5	5						
	4	10				80				20
	5		90							
FORM	C	60 - 90	95	70	100	80				20
	CP									
	CB									
	CE					20	100	100	100	80
	P		5	30						
	B									
	E	10-40								
	VP									
	VB									
	VE									
COLOUR		GREEN 10-40 C.LESS 60-90		GREEN 30 YELLOW 70		BLACK 80 BROWN 20	WHITE	WHITE	C.LESS	RED 10 C.LESS 90
FRESHNESS	Fresh	10 - 40		30		80			100	80
	Interm.	60-90	100	70	100	20				20
	Weath.						100	100		

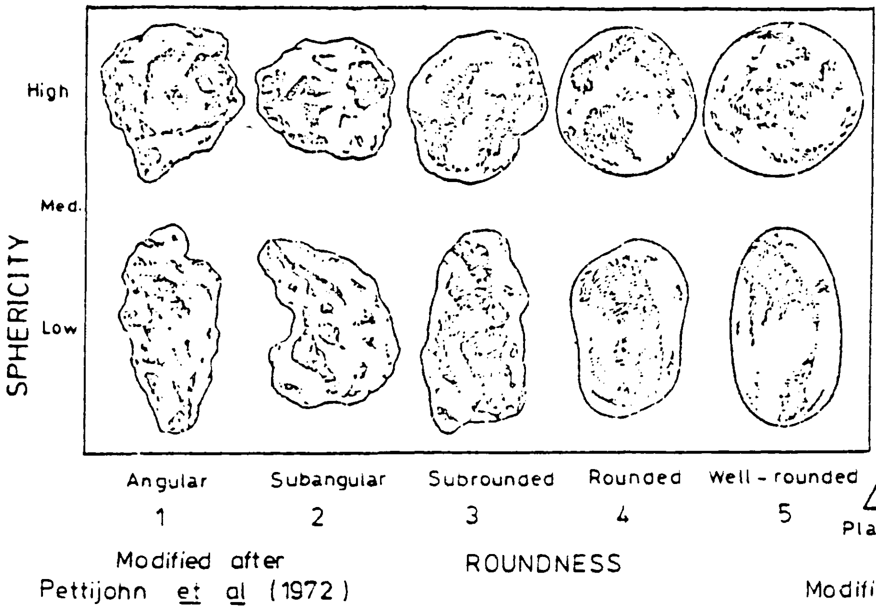

Modified after
Pettijohn *et al* (1972)

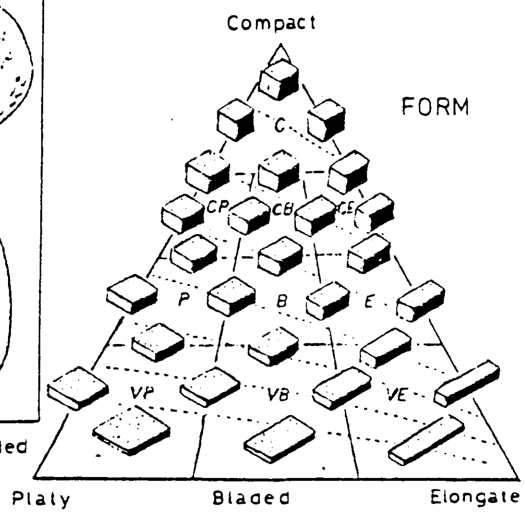

Modified after Sneed and Folk (1958)

Appendix 4. Engineering test results for the clayey silt and sandy silt.

SAMPLE TYPE	CLAYEY SILT																					SANDY SILT					
POCKET NUMBER	1	2	5	6						8			9	10				-	11	12		AVE	4	9	13	-	-	AVE
SAMPLE NUMBER	1	2	6	7	8	9	10	11	AVE	16	18	AVE	20	23	25	26	AVE	27	29	32	33		4	19	34	35	36	
SAMPLE DEPTH (m)	2	2	2	2	2	2	2	2		2	2		2	2	2	2		2	2	2	2		0,2	0,2	0,2	0,2	0,2	
MOISTURE CONTENT (%)	5,2	5,7		10,1	11,7	12,4	11,2	11,4	11,4	8,9	6,6	7,8	10,4	5,6	12,9	8,4	9,0	7,2	12,6			8,7	5,5	2,2	4,3	6,7	6,7	5,1
DEGREE OF SATURATION (%)	16,1	17,2		22,3	25,8	31,1	27,8	35,7	28,5	22,2	22,8	22,5	24,9	18,3	35,2	24,9	26,1	15,4	21,6			21,5	23,5	12,2	20,3	26,3	24,0	21,3
BULK DENSITY (kgm^{-3})	1470	1467		1460	1491	1483	1428	1540	1480	1405	1607	1506	1395	1590	1507	1443	1513	1283	1175			1411	1711	1773	1748	1694	1635	1712
DRY DENSITY (kgm^{-3})	1397	1388		1382	1375	1361	1283	1312	1343	1290	1507	1399	1263	1506	1335	1331	1391	1186	1044			1301	1621	1735	1676	1588	1532	1630
SPECIFIC GRAVITY	2,56	2,56		2,45	2,37	2,61	2,66	2,58	2,53	2,67	2,67	2,67	2,67	2,67	2,67	2,67	2,67	2,67	2,67			2,63	2,62	2,54	2,53	2,67	2,67	2,61
eo	0,83	0,84	SAMPLE CRUMBLED	0,86	0,87	0,93	1,07	0,97	0,94	1,07	0,77	0,92	1,11	0,77	0,97	1,01	0,92	1,25	1,56	SAMPLE CRUMBLED	SAMPLE CRUMBLED	1,05	0,62	0,46	0,54	0,68	0,74	0,61
COLLAPSE POTENTIAL (%)	9,2	11,9		8,1	7,7	7,2	7,5	4,8	7,1	9,1	6,6	7,9	10,4	7,2	-	9,3	8,3	5,9	5,1			8,2	3,3	0,6	0,4	2,4	1,2	1,6
COHESION (kN/m^2)	-	-		-	63	55	-	-	59	60	40	50	-	-	-	-	-	-	-			55	-	-	-	-	-	-
INTERNAL FRICTION (°)	-	-		-	19	21	-	-	20	15	26	21	-	-	-	-	-	-	-			21	-	-	-	-	-	-
POROSITY (%)	45,4	45,7		46,2	46,5	48,2	51,7	49,2	48,4	51,7	43,5	47,6	52,6	43,5	49,2	50,2	47,6	55,5	60,9			50,5	38,3	31,5	35,1	40,5	42,5	37,6
PERMEABILITY ($\times 10^{-5} ms^{-1}$)	-	-		-	-	-	8,2	4,1	6,2	10,1	-	10,1	9,3	-	-	-	-	-	-			8,5	-	-	-	-	-	-

- NOT TESTED

Appendix 5. Single consolidometer test results for the clayey silt (Saturated at an applied load of 80 kN/m^2).

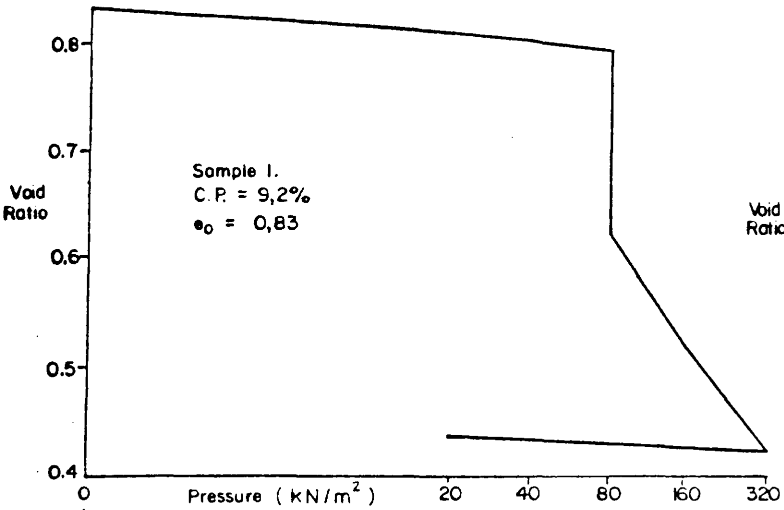

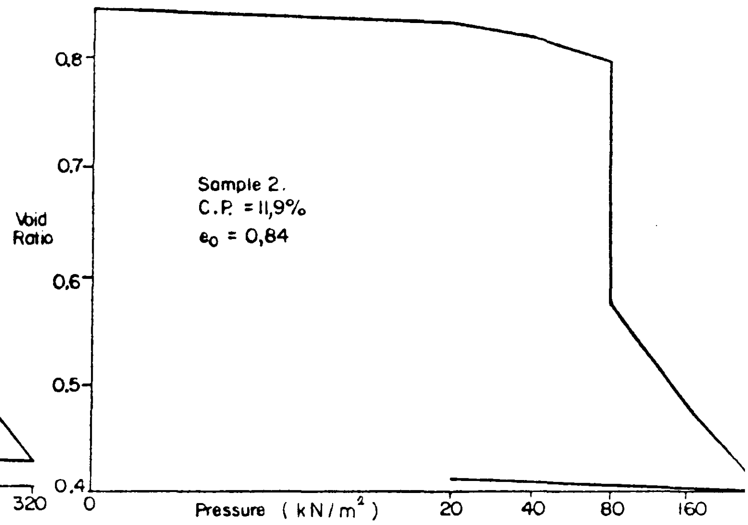

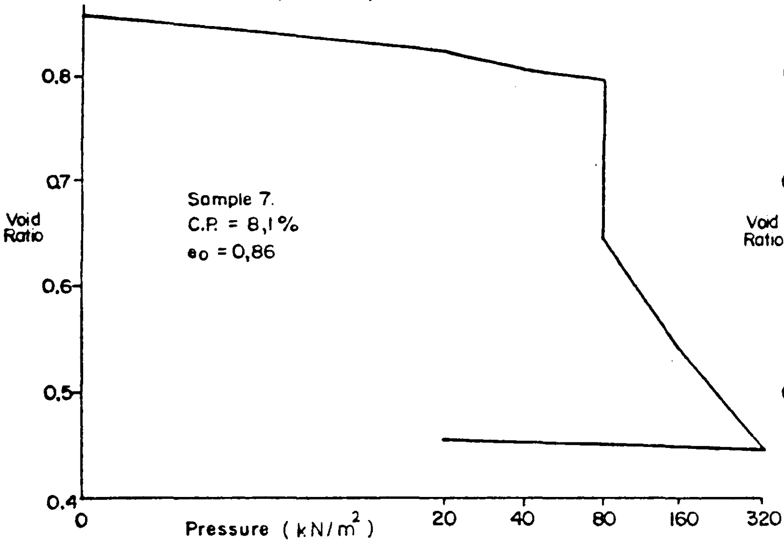

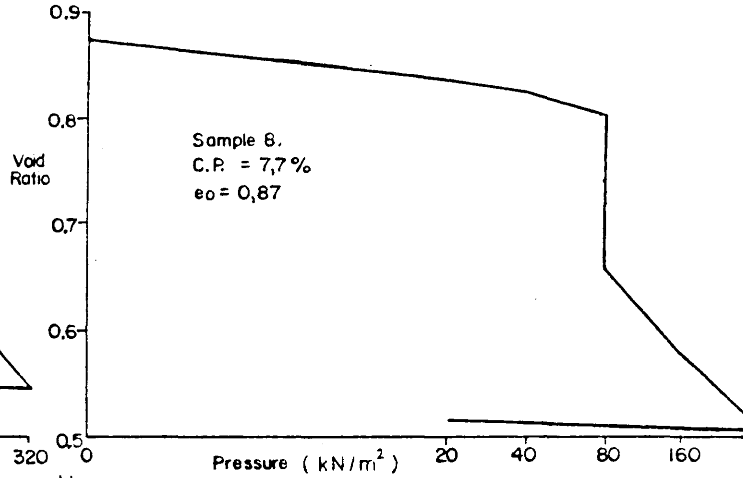

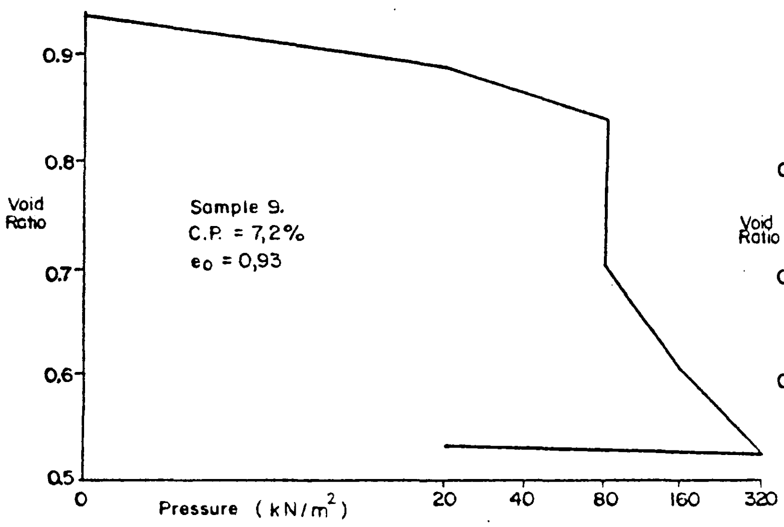

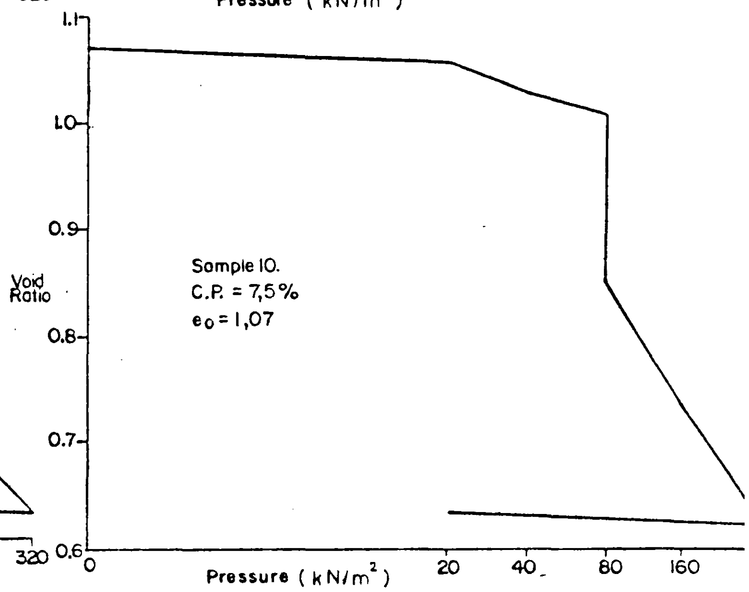

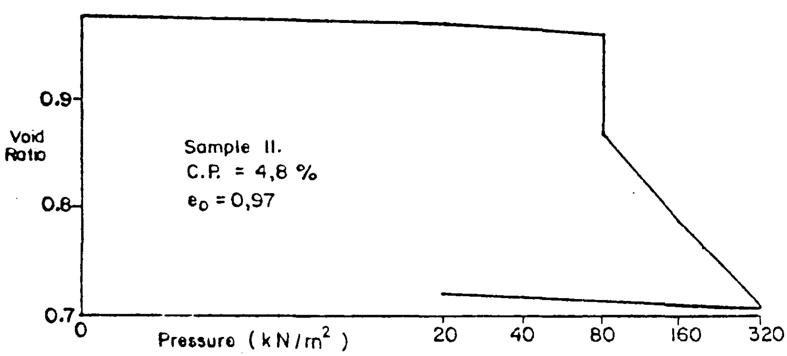

C.P. = Collapse Potential

e_0 = Initial Void Ratio

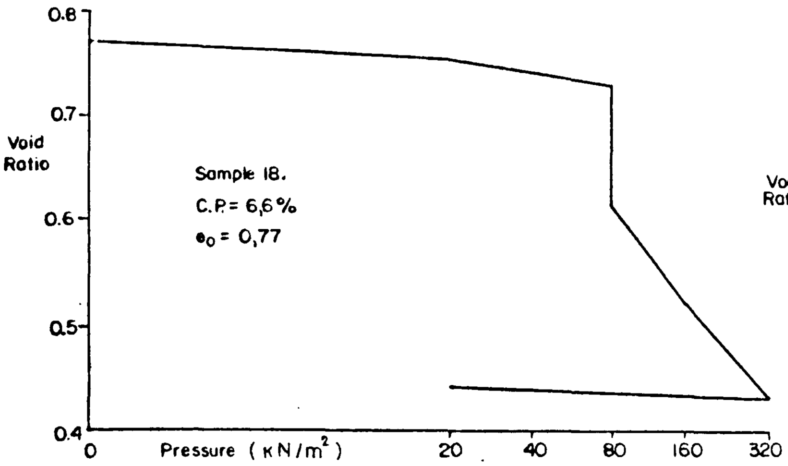

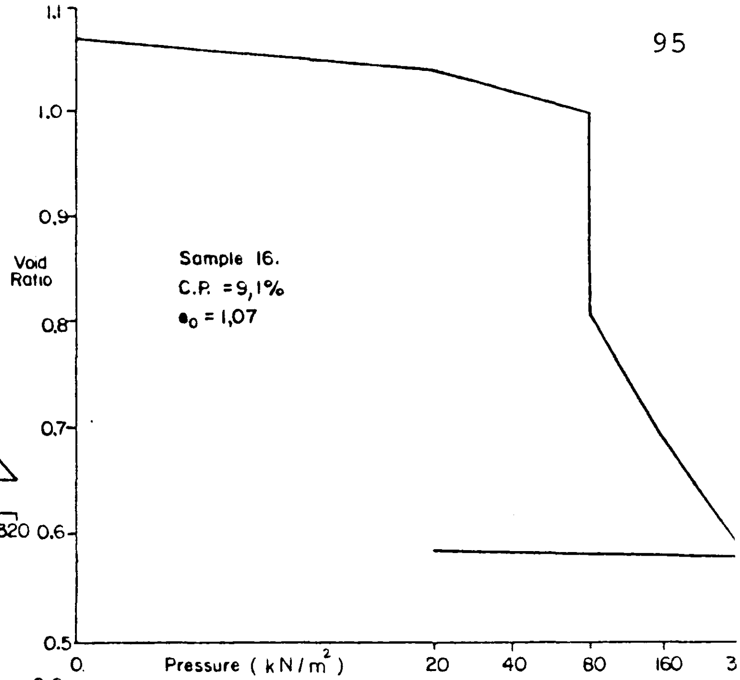

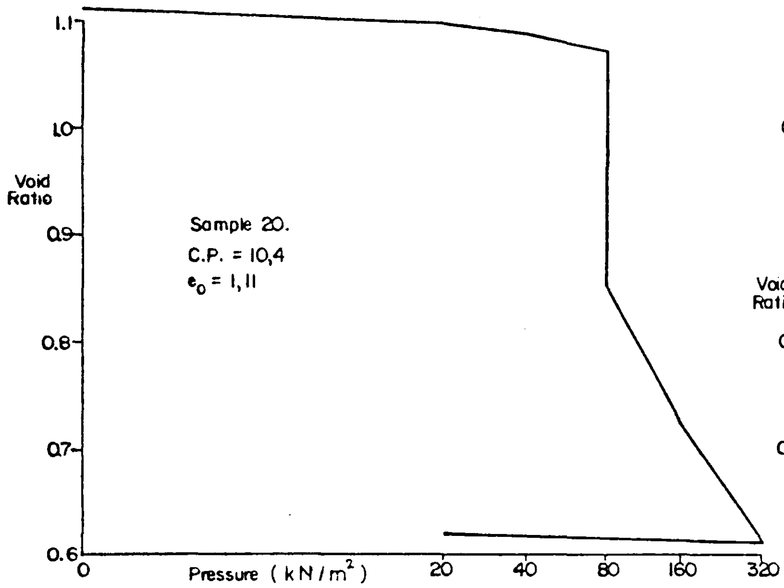

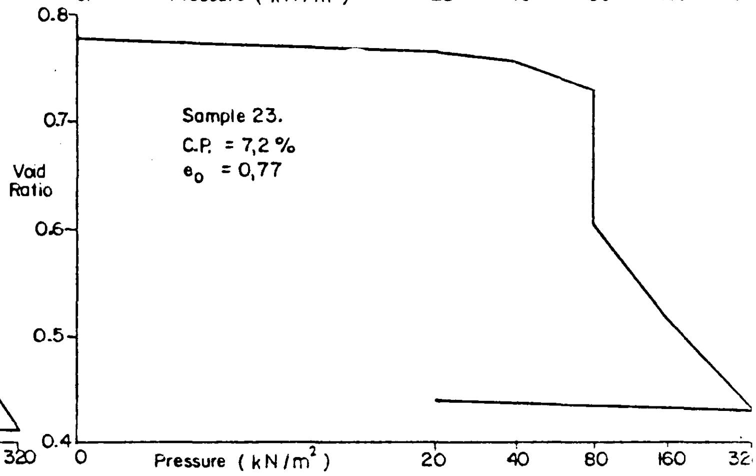

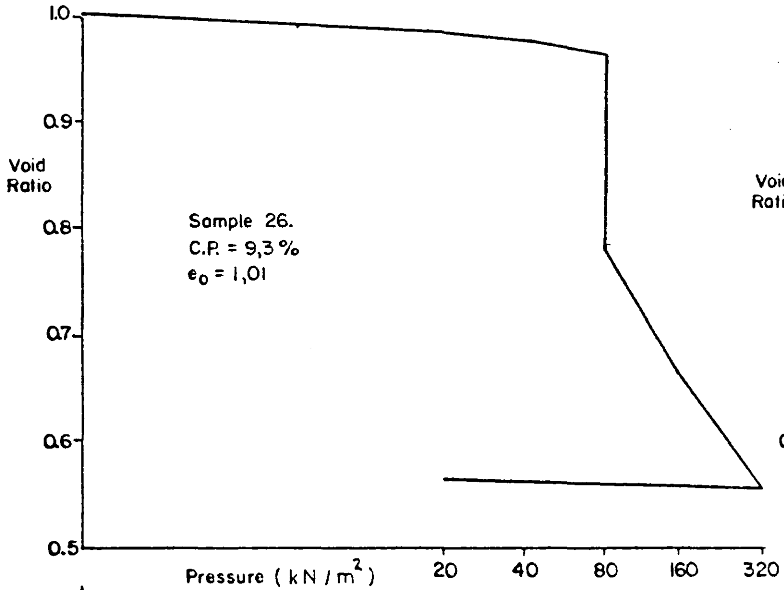

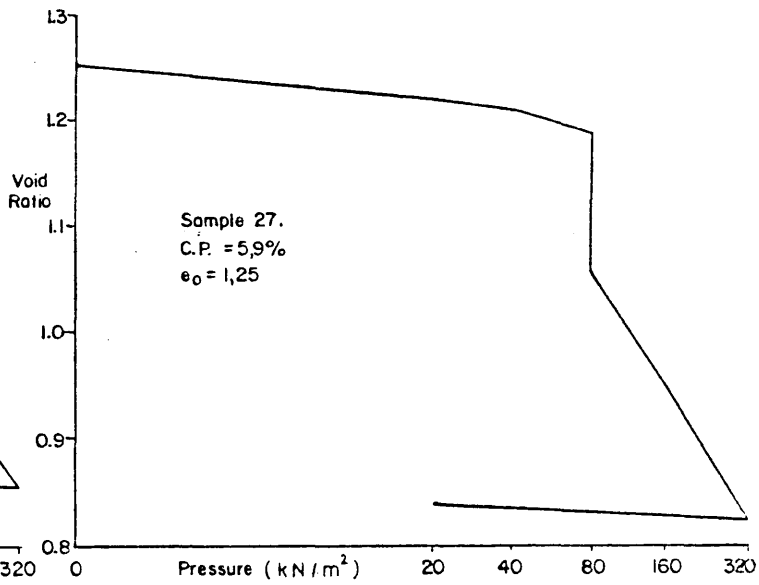

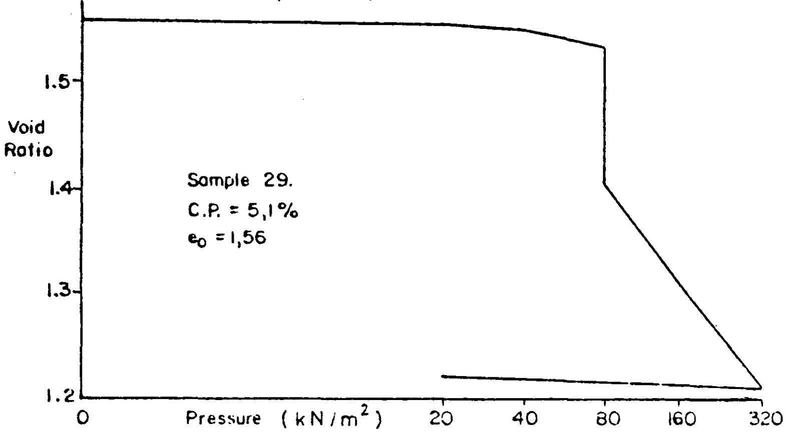

C.P. = Collapse Potential

e_o = Initial Void Ratio

Appendix 6. Single consolidometer test results for the sandy silt (Saturated at an applied load of 80 kN/m^2).

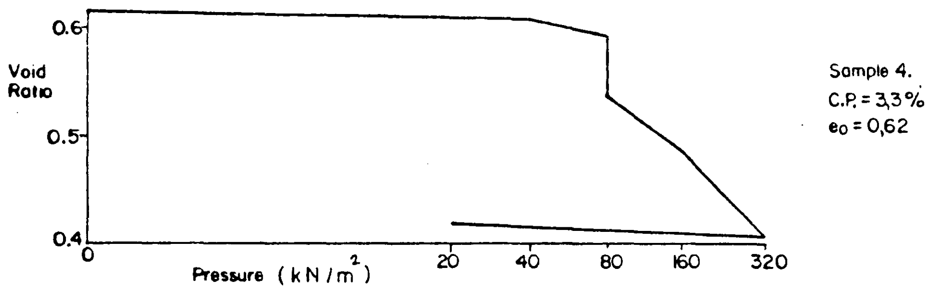

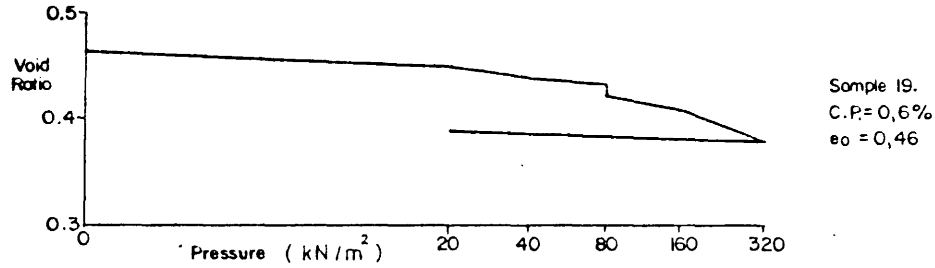

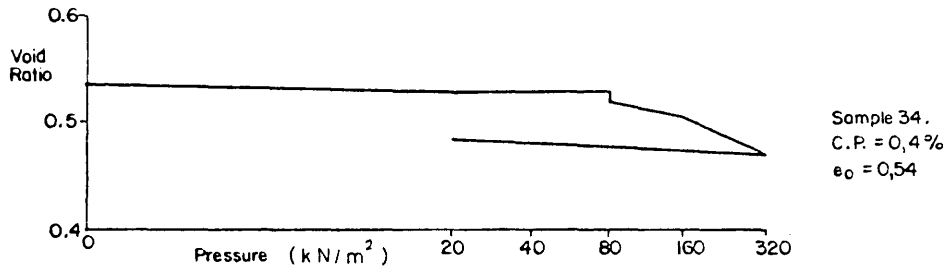

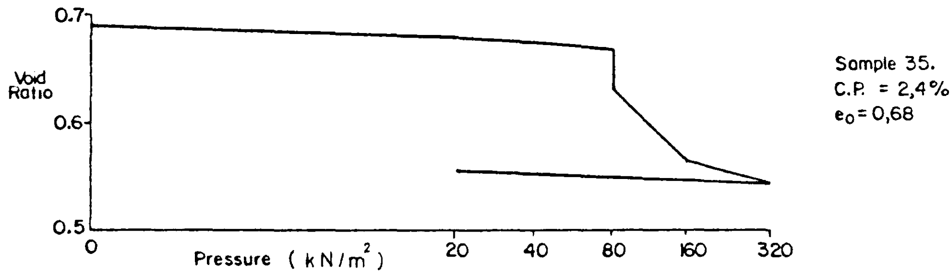

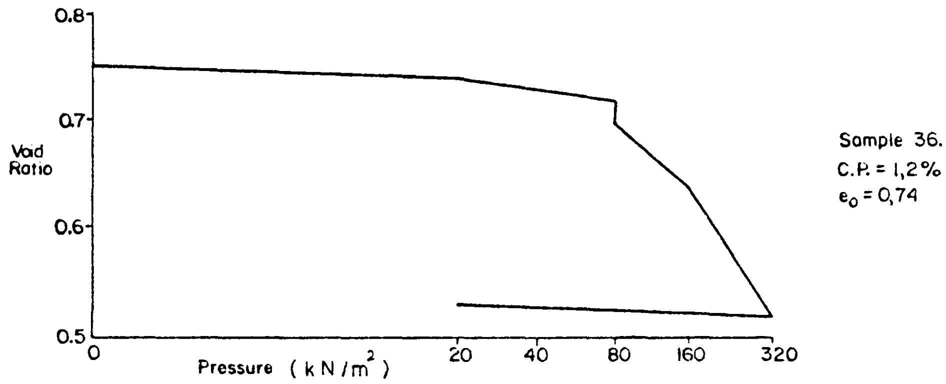

C.P. = Collapse Potential

e_0 = Initial Void Ratio

Appendix 7. Drained shear box test results for the clayey silt.

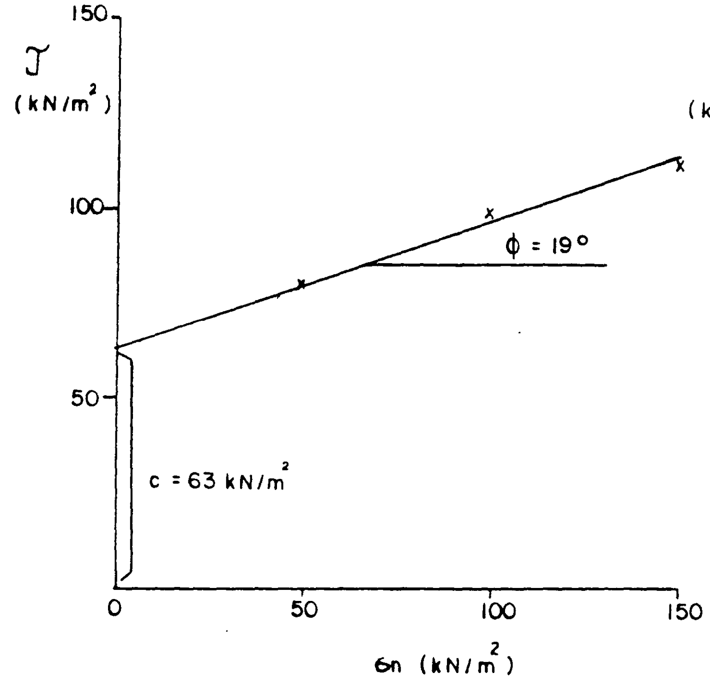

Sample 8. (2m)

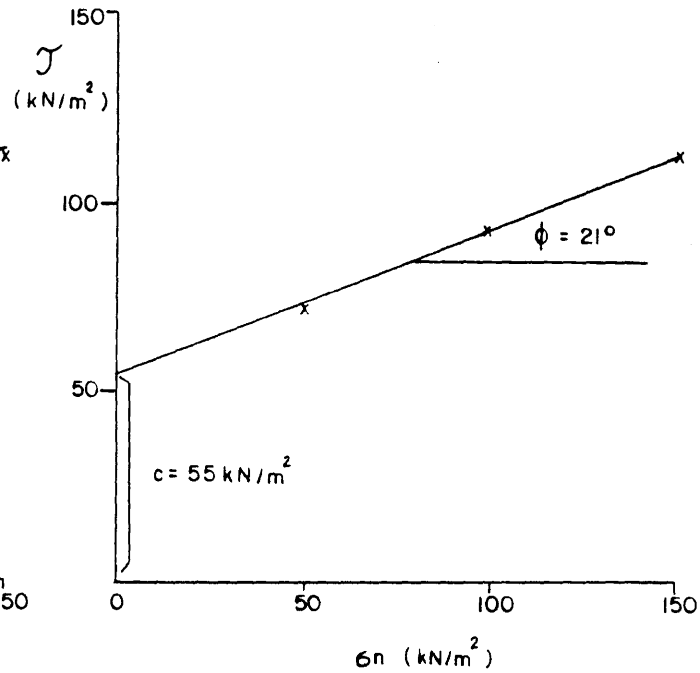

Sample 9. (2m)

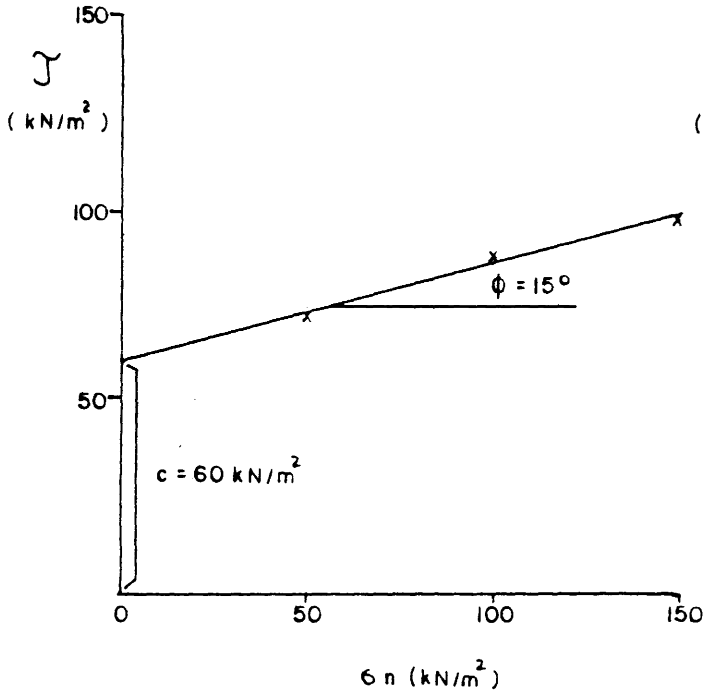

Sample 16. (2m)

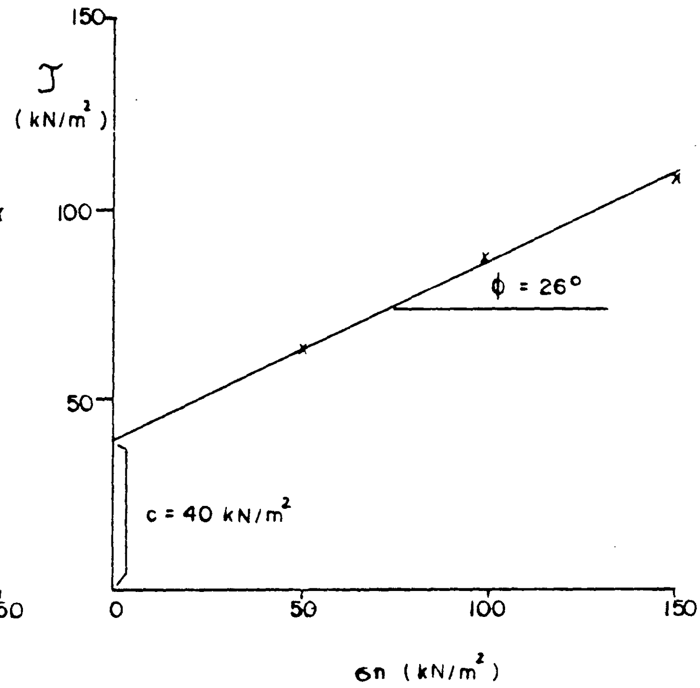

Sample 18. (2m)